The PHILOSOPHICAL MAGAZINE

FIRST PUBLISHED IN 1798

Vol. 44 SEVENTH SERIES No. 349 February 1953

A Journal of Theoretical Experimental and Applied Physics

PRICE 15s. 0d.
Annual Subscription £8 0s. 0d. payable in advance

AND PUBLISHED BY TAYLOR & FRANCIS LTD., RED LION COURT, FLEET ST., LONDON, E.C.4.

ADVANCES IN PHYSICS

A QUARTERLY SUPPLEMENT OF THE PHILOSOPHICAL MAGAZINE

On 1st January, 1952, the first number of this new Quarterly Supplement to the Philosophical Magazine was published. The aim of this Supplement will be to give those interested in physics comprehensive and authoritative accounts of recent important developments. It is felt by the Editor that in view of the rapid advances in many branches of physics, scientists will welcome a journal devoted to articles of this type.

VOLUME 2 JANUARY 1953 NUMBER 5

PRICE *per part* **15/-** *plus postage* **PRICE** *per annum* **£2 15s. 0d.** *post free*

Printed and Published by
TAYLOR & FRANCIS, LTD., RED LION COURT, FLEET ST., LONDON, E.C.4

XIV. *The Properties of* KH_2PO_4 *Below the Curie Point*

By H. M. Barkla and D. M. Finlayson*
Department of Natural Philosophy, University of St. Andrews†

[Received August 26, 1952]

Abstract

The study of the dielectric, piezoelectric and elastic properties of KH_2PO_4 has been extended into the ferroelectric range of temperatures, and should permit further theoretical consideration of the behaviour of this group of crystals. In addition to the main transition, the treatment of which is still inadequate, there is another transition for which no complete explanation can yet be given; this second characteristic temperature marks the onset of a steep rise of coercive field with decreasing temperature. A qualitative domain theory is presented to account for the main features of the ferroelectric state in KH_2PO_4.

§1. Introduction

More attention has been paid to the ferroelectric properties of Rochelle salt and barium titanate than to those of the group represented by potassium dihydrogen phosphate. Since cryogenic equipment is required to maintain crystals of the latter group in the ferroelectric state, they have found practical application only in virtue of the high susceptibility which they show even at room temperature; the Curie point of KH_2PO_4 is 122° K.

One unusual feature of the behaviour of the KH_2PO_4 group is that at a temperature some 60° below the Curie point the reversal of polarity starts abruptly to become increasingly difficult with decreasing temperature. It had been evident from electro-optical work (Zwicker and Scherrer 1944) and from dielectric measurements (Busch and Ganz 1942) that there could be such a discontinuity in the coercive field for individual specimens, but there was no published evidence that this occurred at a temperature which was a fundamental characteristic of the crystal rather than one determined, for example, by accidents of mechanical strain. This was therefore investigated.

The occurrence of spontaneous polarization in KH_2PO_4 may be accounted for by three theories, Slater (1941) treating the transition as a problem in statistical mechanics, Mason (1949) applying reaction-rate methods, while Mueller's phenomenological treatment of Rochelle salt (1940) may be applied to KH_2PO_4; when the results of this adaptation are discussed below, this is referred to simply as the Mueller theory.

* Now at the University of Aberdeen.
† Communicated by the Authors.

An extension of the electromechanical observations on KH_2PO_4 into the ferroelectric region was accordingly planned with a twofold object, firstly of looking for any change in other properties corresponding to the discontinuity in the coercive field, and secondly of providing more experimental material with which to test the existing theories.

§2. D. C. Dielectric Measurements*

The hydrogen gas cryostat employed was that used by Ganz and described by him (Busch and Ganz 1942). The apparatus was constructed to test, in the first place, whether in KH_2PO_4 there was true dipole extinction with decreasing temperature such as occurs in Rochelle salt. At that time no direct test of this had been made, although it was fairly clear that there was no lower Curie point, and that the diminution of the polarization reversal in a given a.c. field was simply the consequence of a rapidly increasing coercive field. A brief report has already been given (Barkla 1946), and better evidence is now added in confirmation. Although not ideal for the purpose, the apparatus was then employed in the investigation of the coercive field discontinuity. Observations of two main types were thus required. Firstly, maintaining a constant potential difference across the crystal, changes of polarization were recorded as the temperature was varied. Secondly, at constant temperature, the dielectric hysteresis loops were traced in a series of arbitrary steps ; as the cycle usually took from 3 to 5 minutes to complete, and as each change of polarization was normally given time to reach a steady value, these may be considered as ' static ' loops.

The circuit of fig. 1 was used for both purposes. A potential of up to $\pm 2\,000$ volts was applied to one face of the crystal, and could be varied by a controlling potentiometer and reversing switch. The crystal thickness was generally just over 1 mm, so that the maximum field was between 15 and 20 kv cm^{-1}. The other face of the crystal and one plate of a large compensating condenser were isolated from all but one grid of an electrometer triode bridge, and, by use of the bridge as a null detector, were kept at earth potential by small measured variations of potential on the other plate of the compensating condenser. These variations could be effected either by the manual compensating potentiometers, or by a similar string-operated potentiometer ; the latter was part of a controller-recorder unit by means of which hysteresis loops were traced directly onto paper.

The bridge was normally operated at two thirds of its maximum sensitivity of 590 cm $volt^{-1}$; this was obtained with an external-scale galvanometer of sensitivity of 17 cm $microamp^{-1}$. The growth or decay of polarization in a saturating field at the Curie point thus corresponded to a total change of deflection of about 200 cm with a crystal area of some

* This part of the investigation was carried out by the first author in the Royal Society Mond Laboratory in 1946 at the suggestion of D. Shoenberg. Assistance was received in the later stages from J. K. Hulm.

0·3 cm^2. The crystals had, however, an appreciable conductivity of some 10^{-11} to 10^{-12} ohm^{-1} cm^{-1}, even at low temperatures, and this gave a continuous drift to the potential of the free grid as long as the crystal was subject to a field. Moreover, other current leaks of comparable magnitude were found to occur in spite of considerable precautions to isolate the bridge circuit, and these were liable to change with any change in the ancillary electrical circuits such as that of the cryostat heater. The drift of the bridge could be eliminated at any instant by varying the 'earth' potential, and, although this balance seldom remained perfect throughout the period of observation of a hysteresis loop, the errors from this cause were much reduced. It became possible to obtain sensibly closed loops within the limit of accuracy of the recording device; in successive cycles the coefficient of variation of the total polarization reversal was about 4%. In the case of a crystal specimen showing abnormally high conductivity an equal and opposite leak through a high resistance could be introduced.

Fig. 1

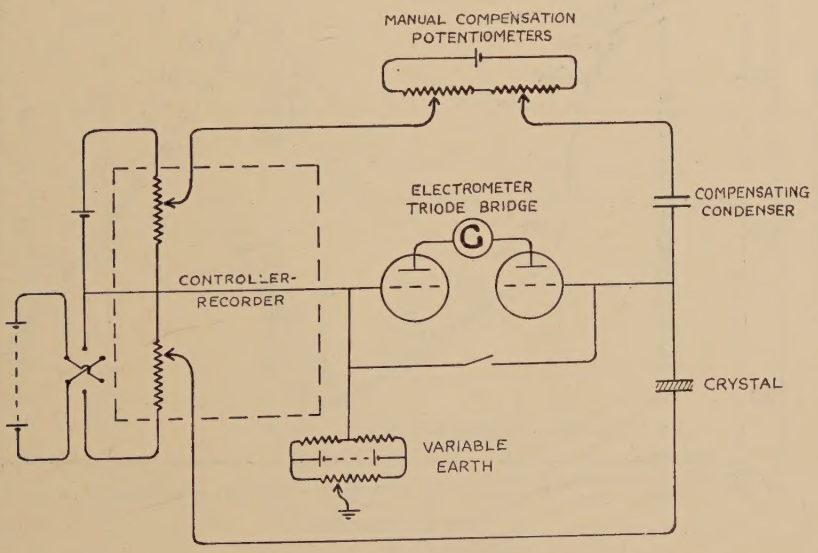

During measurements of the growth or decay of polarization with changing temperature in a constant field at the Curie point, it was considered preferable not to mask the current in the crystal by this artificial leak, but to make continuous observations of the manual compensation potentiometers; the record would then assume the form of fig. 2. As an alternative the expedient was sometimes employed of reducing the sensitivity of the bridge to one tenth of its normal figure and observing the deflection alone. This could be done with advantage only when the conductivity of the crystal was low or was fortuitously neutralized by incidental leaks. The observations already published furnish an example of the latter type.

The Constancy of the Saturation Polarization

Earlier work had shown the spontaneous polarization to grow to a constant value as the temperature was reduced by some 20° below the Curie point. With the apparatus described it was possible to observe this rise directly by applying a constant field sufficient to saturate the ferroelectric crystal, and the value obtained for the growth of the saturation polarization at the transition agreed to within a few per cent with that obtained from the hysteresis loops of the same specimen. (The term ' saturation ' is used here with reference to domain alignment, the field, that is, being adequate to bring the electric state of the crystal well onto the reversible tail of the hysteresis loop. But these tails had themselves an appreciable slope, and there was no sign of true saturation

Fig. 2

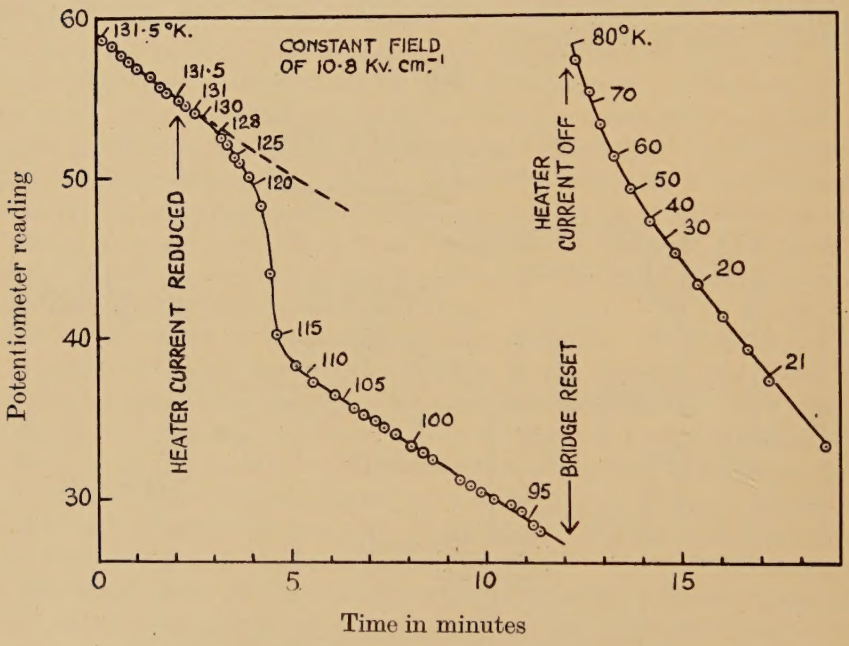

even at the highest fields employed, namely about 15 kv cm^{-1}.) Any abrupt change of saturation polarization at a lower temperature would thus be observable on warming or cooling if it exceeded 2 or 3%, although the chances of detection would diminish were the polarization change spread over a wider range of temperature.

Observations of the polarization of a crystal in a constant field were made on nine occasions while the temperature was raised or lowered through the range in which the ' lower Curie point ' was formerly believed to lie. Some were extended down to 20° K, and these tests gave no indication that the spontaneous polarization was anything but constant from 100° K downwards.

The case shown in fig. 2 represents a relatively slow cooling in two stages, in which the bridge was once reset ; such a resetting involves an abrupt change of potential across the compensating condenser, and the soaking-in effect of the dielectric, amounting to about 10% over a period of some two minutes, is clearly seen.

One significant feature of these observations is that the reduction of polarization with increasing temperature in a saturating field was no more abrupt than its growth at the Curie point with decreasing temperature.

The Relation of the Coercive Field to Temperature

It is well known that crystals of the KH_2PO_4 group, like Rochelle salt, show differences between successive slow cycles, even under the best conditions of temperature stability, so that their coercive field is not

Fig. 3

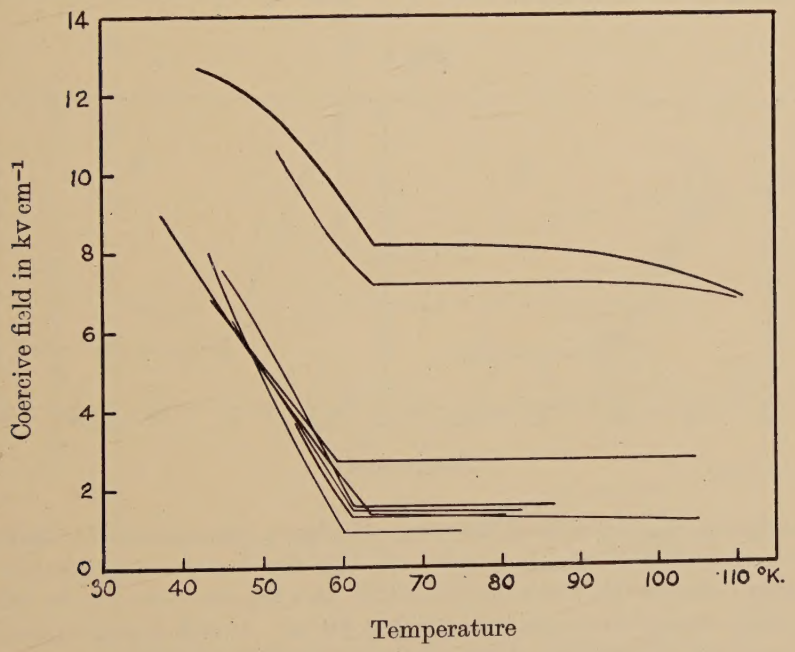

a quantity susceptible of very accurate treatment. The mechanical device used in these experiments was thus adequate for the study. It was found that the coefficient of variation of a single observation of the coercive field was of the order of 8%. Experiments were carried out using seven crystals, and nine temperature relations of the coercive field were obtained. Eight of these showed a marked similarity, and are presented in fig. 3. Two cases are shown in more detail in fig. 4. Within the limits of the experiment the very marked change of slope appears to be quite discontinuous in all eight cases. The manual control could with care be employed to maintain constancy of temperature

within $\pm\frac{1}{5}^\circ$ for the time required to record a loop, but $\pm\frac{1}{2}^\circ$ was the more usual standard. The discontinuities are seen to fall at very much the same temperature, although the value of the coercive field at any temperature may vary over a wide range. Even the same crystal may show a different value, though not, apparently a lower one, after being warmed to room temperature. The slight indication that the critical temperature is higher for specimens with a higher level of coercive field cannot be regarded as significant from these results. The critical temperature is not known with the same absolute accuracy, but may be said to lie within one or two degrees of 62° K. Below this, the coercive field rises with decreasing temperature at a rate which is very much the same for all specimens, namely $0{\cdot}30\pm0{\cdot}05$ kv cm^{-1} deg^{-1}. The experiment was repeated using a.c. by Hulm who has reported (1951) that his one specimen showed the same temperature for the discontinuity, the slope being some 60% higher than the average of the results now quoted.

Fig. 4

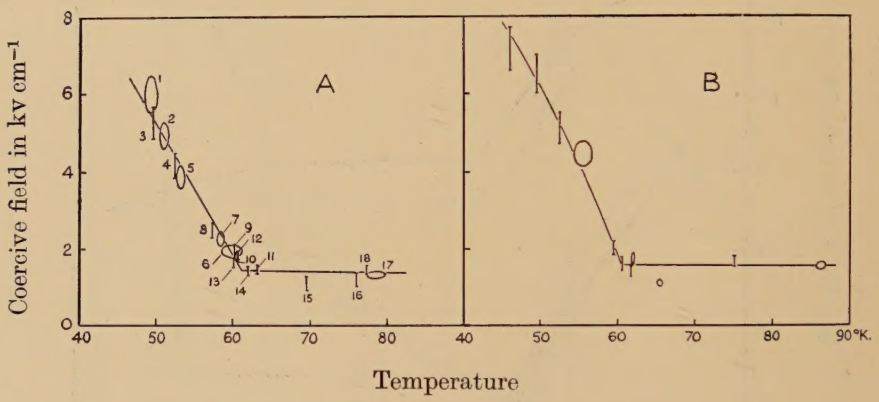

The one anomalous case of the nine, showing a more gradual transition from the sensibly constant coercive field of the higher temperatures to the rising value of the lower temperatures, was the one occasion on which the crystal was not first cooled well below 60° K. It still appears possible, then, that the occurrence of the sharp transition may depend to some extent on the previous treatment of the specimen. It is clear, however, from fig. 4 (*a*) in particular, that the discontinuity is reproducible, and that the coercive field is not itself subject to hysteresis.

§3. Dynamic Measurements*

Elastic Constants

It seemed reasonable to expect that the increased difficulty of reversing domains below 60° K might be associated with a change in the elastic constants of the crystal at this temperature.

* These measurements were made by the second author in St. Andrews.

In order to measure the initial values of the constants in the Curie region, field strengths of less than 10 v/cm were used for the elastic measurements. The elastic constants were evaluated from the resonant frequency of longitudinal and shear modes of vibration of various crystal cuts. Since KH_2PO_4 has six elastic constants, a minimum of six different cuts was required to evaluate the constants completely.

The constant s_{44} was found by measuring the resonant frequency of an X cut crystal with its length along the Z axis from the formula $s=1/(4b^2f^2\rho)$. Similarly, s_{66} was found from a Z cut crystal with its length

Fig. 5

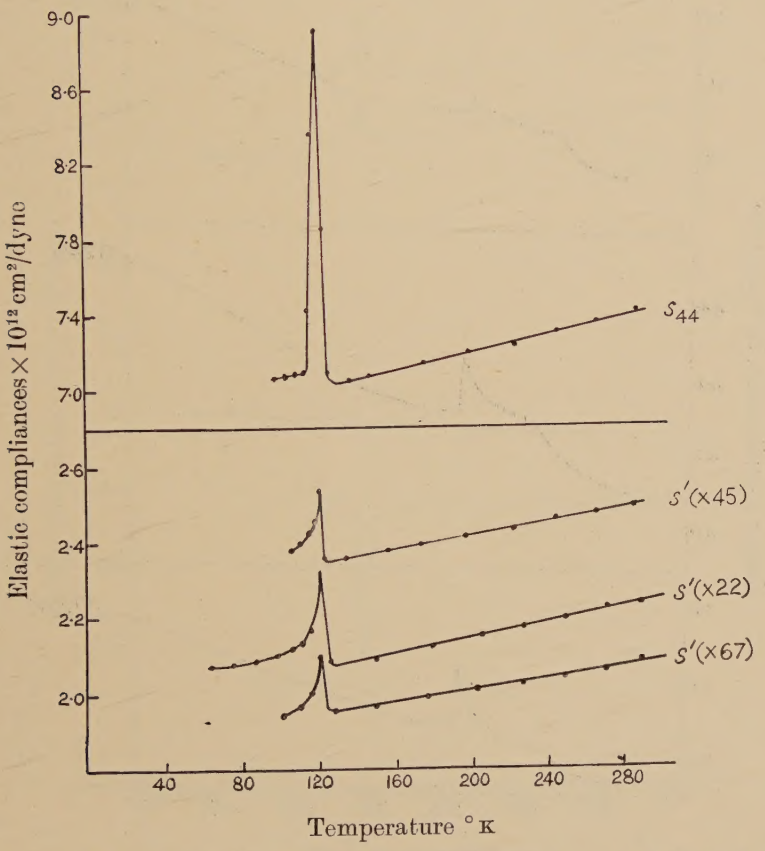

along the X axis. The formula is only correct for an infinitely long and narrow crystal but Atanasoff and Hart (1941) have shown that, when measuring a comparatively short specimen at high harmonics, it behaves as an infinitely long crystal.

Taking cuts at an angle to the crystal axes, bars vibrating in longitudinal modes were obtained. For an X cut the equation for rotated axes is

$$s'=s_{11}\cos^4\theta+(2s_{13}+s_{44})\sin^2\theta\cos^2\theta+s_{33}\sin^4\theta,$$

where θ is the angle between the length of the bar and the Z axis.

Three values of s' were obtained for $\theta=22\frac{1}{2}°$, 45° and $67\frac{1}{2}°$ and, solving these simultaneously, s_{11}, $(2s_{13}+s_{44})$ and s_{33} were obtained. s_{13} could then be calculated from the value of s_{44} previously found.

The equation for rotated axes for a Z cut is

$$s'=s_{11}(\sin^4\phi+\cos^4\phi)+(2s_{12}+s_{66})\sin^2\phi\cos^2\phi,$$

where ϕ is the angle between the length of the bar and the X axis. In a similar way, values of s_{11} and s_{13} were obtained.

Fig. 6

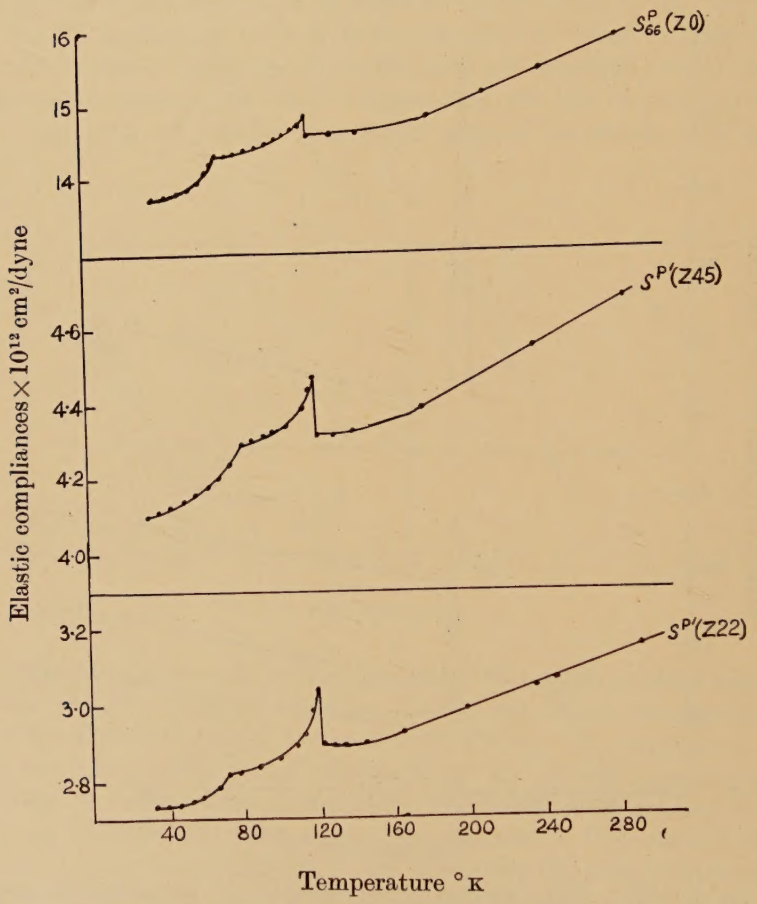

Mason (1946) has shown that, when the resonant frequency of a fully plated crystal is measured, the resonant frequency is governed by the compliance at constant field s^E. When the plating is removed and the frequency is measured in an air gap holder the elastic compliance at constant displacement s^D is obtained. This is numerically equal to the value of the compliance at constant polarization s^P within the limits of experimental error.

The values of s_{44} and s' for cuts perpendicular to the ferroelectric axis are shown in fig. 5. These all show anomalies at the Curie point larger than might be expected from the behaviour of Rochelle salt. They were measured with plated crystals but the difference between s^E and s^P for X cut crystals is very small since the piezoelectric coupling is small for these cuts.

In fig. 6 are shown the compliances for the Z cuts obtained from bare crystals. In addition to the anomaly at the Curie point, a change of gradient occurs between 75° and 80° K. The calculated values of s_{11},

Fig. 7

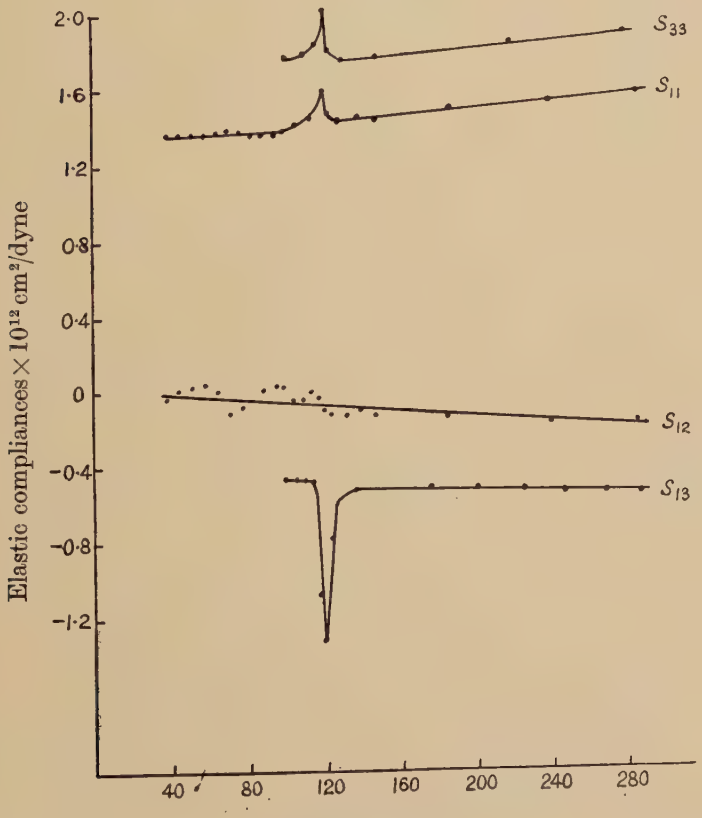

s_{12}, s_{13} and s_{33} are shown in fig. 7. No anomaly in any of the constants was observed below 70° K, thus ruling out the possibility of an explanation of the increase of coercive field at 60° K in terms of the elastic behaviour.

Measurements of the resonant frequency of fully plated Z cut crystals were found to be difficult near the Curie point, particularly in the case of shear modes and complete results were not obtained. The resonant

frequency of a plated $Z45$ cut was, however, measured over the complete range and the resulting compliance compared with that of the bare crystal in fig. 8. It will be seen that the compliance of the plated crystal undergoes a great change at the Curie point, while the unplated crystal shows only a small anomaly. This agrees with the findings of Mueller (1940) for Rochelle salt.

The measurements above the Curie point agree fairly well with those of Mason (1946).

Fig. 8

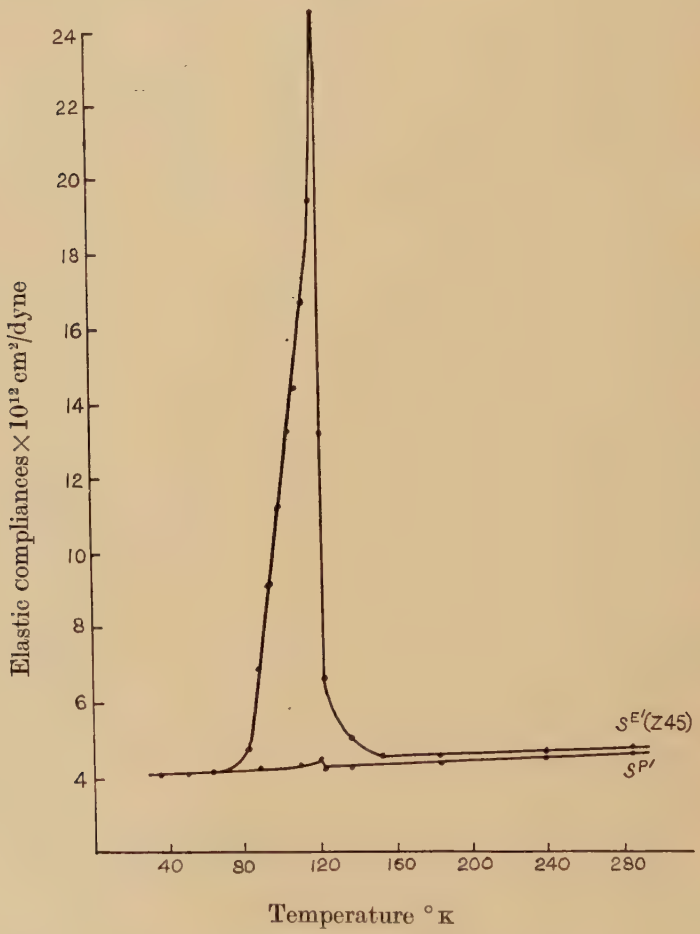

Dielectric Constants

The dielectric constant of a piezoelectric crystal which is free to deform differs appreciably from that of a crystal which is rigidly clamped on account of the piezoelectric contribution to the dielectric constant.

Measurements made at low frequencies yield the free dielectric constant. This was obtained by measuring the capacity of a crystal condenser at 2 000 cycles/sec by a bridge substitution method.

Rigid clamping of a crystal to prevent any mechanical distortion is impossible in practice. If, however, the applied frequency is raised to a sufficiently high value, the effect of the natural frequencies and their harmonics becomes negligible. For crystals of reasonable size the frequency should, according to Cady (1946, p. 328), be 10 Mc/s. An approximate value of the clamped dielectric constant was obtained in this way by measuring the capacity of a crystal condenser at 10 Mc/s by means of a *Q*-meter.

The free dielectric constant is shown in fig. 9. At the Curie point it rises to a value greater than 10^4, drops to about 3×10^3 at 100° K and then falls to a value of about 8 at 60° K, remaining constant below this temperature.

Fig. 9

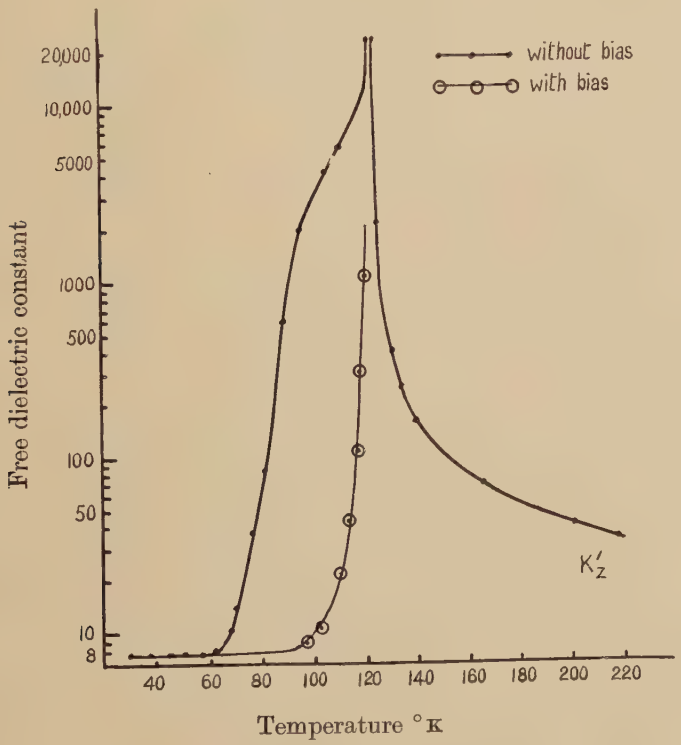

If, however, a biasing field of 3 kv cm^{-1} is applied during the measurements, the differential dielectric constant thus measured drops to this low value at about 100° K.

The clamped dielectric constant is shown in fig. 10. The anomaly at the Curie point, although still quite large, is much smaller than in the free case. The effect of a biasing field is similar to that in the low frequency case.

The dielectric constant at right angles to the ferroelectric axis at low frequency is shown in fig. 11. Little difference in behaviour is observed

between the clamped and free values, as might be expected from the small piezoelectric coupling of this direction. There is a marked contrast with the behaviour of Rochelle salt, which exhibits no maximum in the corresponding dielectric constant at the Curie point, whereas here κ_x falls off sharply below that temperature, reaching a constant value at about 60–70° K.

Fig. 10

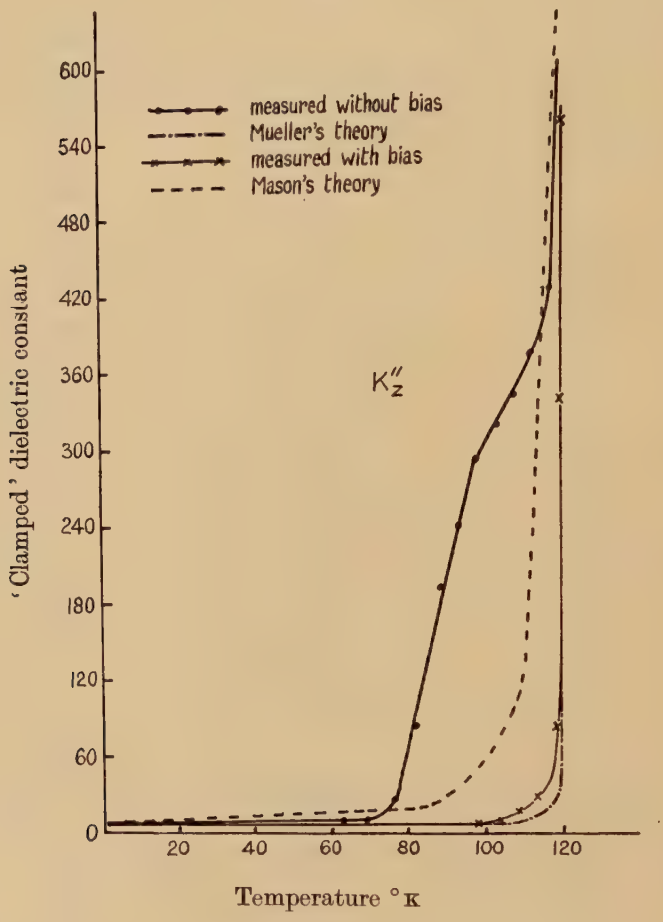

Piezoelectric Constants

In order to compare the behaviour of the 'polarization' and Voigt constants, as discussed in Cady (1946), Chap. XI, the piezoelectric coefficients were calculated from the following formulae :

$$b_{36}=\left[1-\left(\frac{f_P}{f_B}\right)^2\right]\frac{16\pi s^{E'}}{\kappa_z'} \qquad a_{36}=b_{36}c_{66}^{P}$$

$$e_{36}=a_{36}\frac{\kappa_z''}{4\pi} \qquad d_{36}=b_{36}\frac{\kappa_z'}{4\pi},$$

where f_P and f_B are the resonant frequencies of a $Z45$ crystal when plated and bare.

To eliminate errors caused by uncertainty in the angle of cut, the same crystal was used for the plated and bare measurements. Only a minimum of plating was used as excess lowers the crystal frequency.

Fig. 11

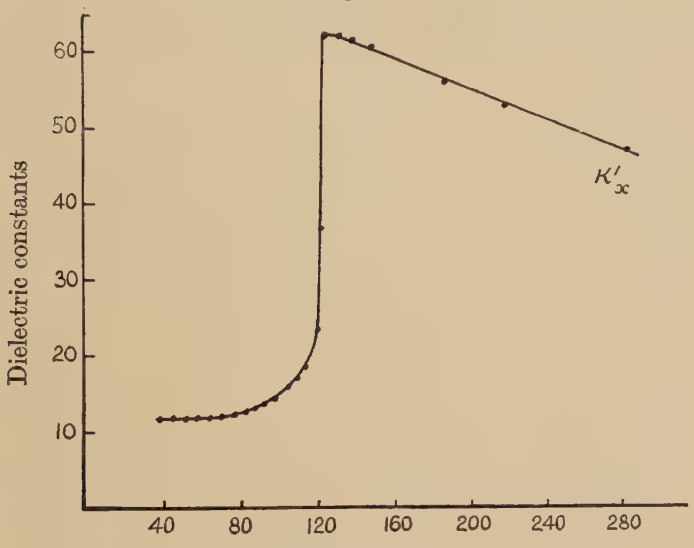

The temperature dependence of the piezoelectric constants calculated from the compliances and dielectric constant is shown in figs. 12 and 13. In fig. 12 the Voigt coefficient d_{36} is compared with the polarization theory coefficient b_{36} and in fig. 13 e_{36} and a_{36} are compared. Again, as in the elastic measurements, the ' polarization ' constants show an almost normal temperature variation, while the Voigt constants give a large anomaly at the Curie point.

§4. Discussion

Comparison with Theories for Single Domain Crystals

Mueller's (1940) form of interaction theory, while unsatisfactory in the sense that is is entirely phenomenological, nevertheless gives very good agreement with experiment for Rochelle salt. The principal features to be explained are that the elastic compliances measured at constant polarization show only a normal variation with temperature, as do the piezoelectric constants a_{36} and b_{36}, while both the clamped and free dielectric constants show a large anomaly at the Curie point.

That this last is true for KH_2PO_4 was first indicated by Mason's (1946) measurements, and is confirmed by the more complete measurements presented above.

Fig. 12

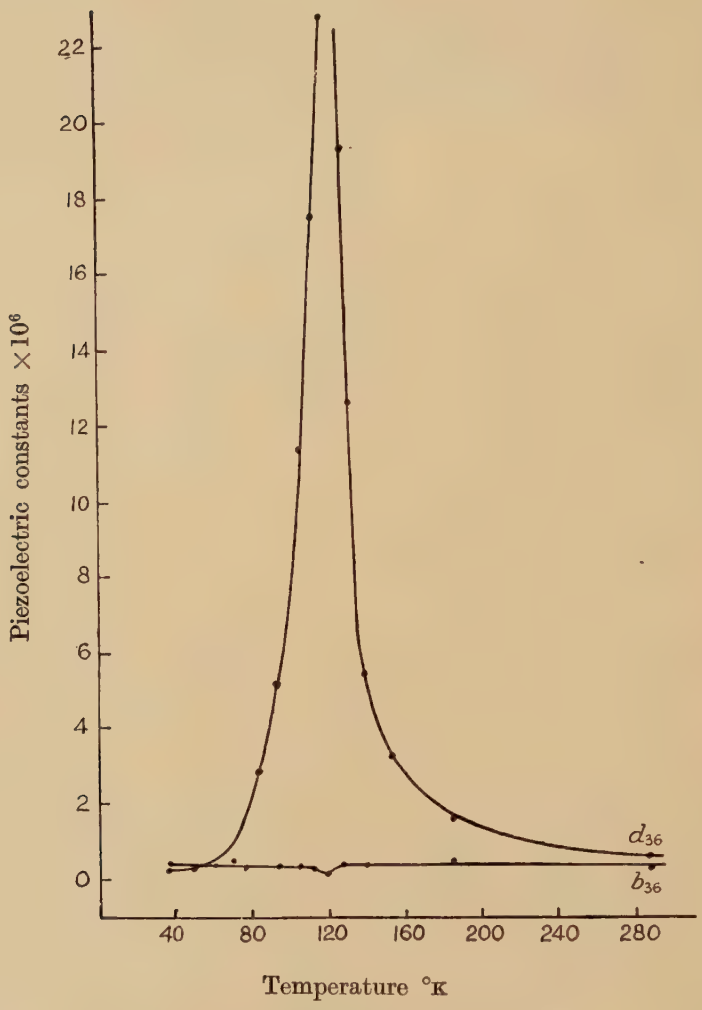

Mueller's next step was to introduce a term in P^3 to account for the non-linearity of E in terms of P so that $E=\chi' P+BP^3$ where B is a constant which can be determined as follows:

$$1=\frac{\partial P}{\partial E}(\chi'+3BP^2),$$

$$\text{but} \quad \frac{\partial P}{\partial E}=\eta \quad \text{and} \quad \chi'=\frac{1}{\eta_0},$$

$$\text{so} \quad \frac{1}{\eta_E}=\frac{1}{\eta_0}+3BP^2.$$

Writing

$$X=\frac{\eta_0-\eta_E}{\eta_0\eta_E}$$

we get

$$\frac{E}{X^{1/2}} = \frac{\chi'}{(3B)^{1/2}} + \frac{X}{3(3B)^{1/2}}.$$

Plotting $E/X^{1/2}$ against X for any given temperature should yield a straight line, from the gradient of which B can be calculated.

The field dependence of the dielectric constant has been measured by Baumgartner (1949). From his results $E/X^{1/2}$ was plotted against X for several temperatures, and the gradients of the approximately parallel curves gave $B = 2{\cdot}5 \times 10^{-9} \pm 12\%$.

Fig. 13

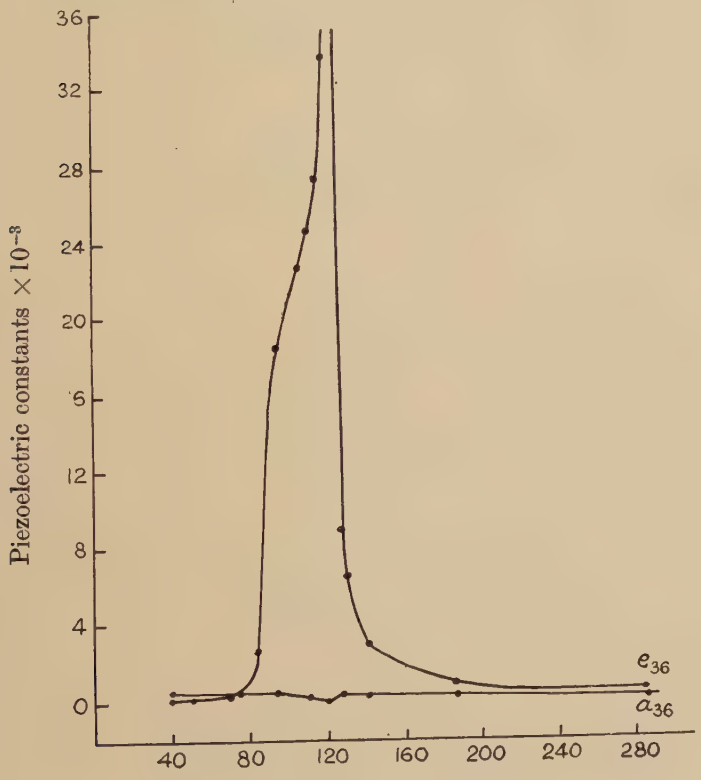

In a manner similar to Cady's (1946, Chap. 23) treatment of Mueller's interaction theory, it can be shown that the following relations hold:

$$\chi_s' = 2BP_0^2,$$

where χ_s' is the free reciprocal susceptibility measured below the Curie point;

$$\chi_s'' = \frac{4\pi}{\kappa_s'' - 1} = 2BP_0^2 + a_{36}b_{36}, \quad \ldots\ldots \quad (1)$$

where χ_s'', κ_s'' are the clamped reciprocal susceptibility and dielectric constant, a_{36} and b_{36} are the piezoelectric constants;

$$E_c = -\frac{2BP_0^2}{3\sqrt{3}}, \quad \ldots\ldots\ldots \quad (2)$$

where E_c is the coercive field for a single domain.

We may now use these equations to check the interaction theory for KH_2PO_4.

From eqn. (1) we can calculate the value of the clamped dielectric constant using the values of B, a_{36}, b_{36} already determined and the values of the spontaneous polarization measured by Arx and Bantle (1943). The result is shown in fig. 10 and compared with the experimental curves and a curve calculated from Mason's (1950) theory. The

Fig. 14

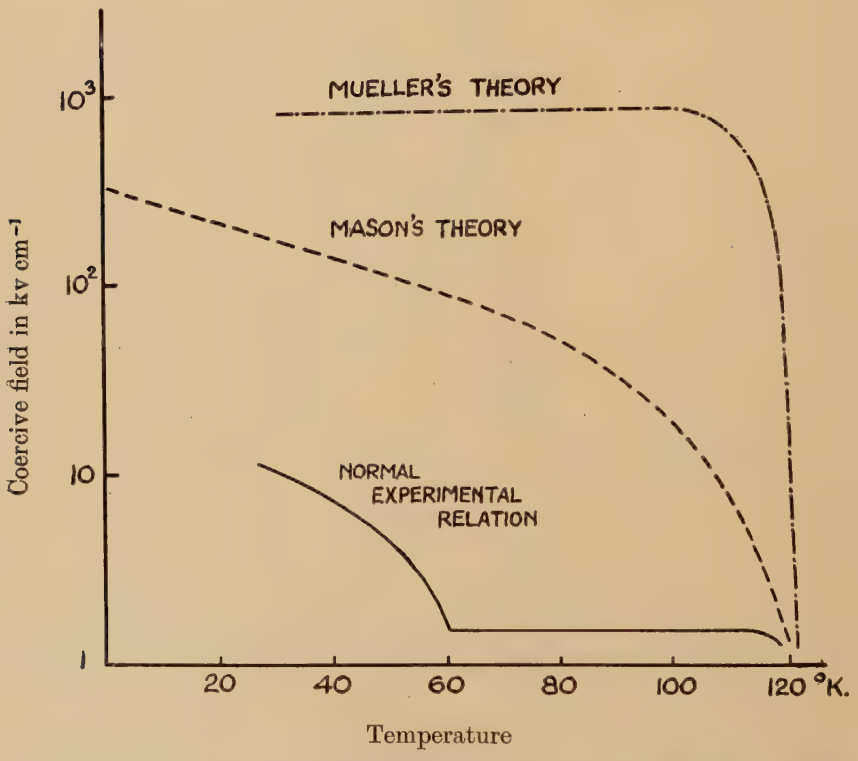

experimental curve obtained by measurement of κ_z'' at high frequency without biasing field gives no agreement with that calculated from either theory, but we see also from fig. 10 that the 'biased' dielectric constant gives much better agreement with theory, and particularly with the Mueller rather than the Mason form.

The coercive field for a single domain may be obtained from eqn. (2) using the measured value of the spontaneous polarization, and this again will be referred to as the 'Mueller theory'. The curve is shown in fig. 14.

The corresponding expression from Mason's theory has not been given explicitly by Mason, but he quotes his own treatment of Rochelle salt as implying that the coercive field becomes very high at low temperatures; in fact the approximation necessary for the case of Rochelle salt is not even valid for KH_2PO_4, since it presumes a low degree of alignment of dipoles, whereas the solution for the coercive field of the latter is really much simpler; on the basis of a constant dipole we may start from Mason's basic eqn. (11.23)

$$\frac{P_d}{N\mu}=\tanh A\left(\frac{E}{\beta N\mu}+\frac{P_d}{N\mu}\right),$$

where P_d is dipole polarization, N the dipole density, μ their strength, β the Lorentz factor and $A=T_0/T$.

Taking the coercive field as the value of E for which $\partial E/\partial P=0$, this being the condition for instability, we get

$$\frac{N\mu}{A}\,\frac{1}{1-(P_d/N\mu)^2}\,\frac{1}{N\mu}-1=\frac{1}{\beta}\,\frac{\partial E}{\partial P_d}=0,$$

giving

$$\frac{P_d}{N\mu}=\sqrt{\frac{A-1}{A}}.$$

Hence

$$E_c=\beta N\mu\left[\frac{1}{A}\tanh^{-1}\sqrt{\frac{A-1}{A}}-\sqrt{\frac{A-1}{A}}\right].$$

This is the function shown in fig. 14 as 'Mason theory'; it will be observed that on this theory also E_c reaches a finite limit at $T=0$, but neither of the two theoretical curves shows any relation to those observed experimentally.

It is seen, then, that theories developed on the basis of single-domain crystals, though throwing some light on the processes involved in the phenomenon of ferro-electricity, do not give an adequate representation of the properties of KH_2PO_4 in the ferroelectric range.

Interpretation in Terms of Domain Theory

No direct observations have been made of the domains of KH_2PO_4, and the x-ray evidence of Ubbelohde and Woodward (1947) is that the crystal is composed of sub-crystalline units of side not greater than 5×10^{-3} cm. Until the theory of the balance of energy in the domains is developed, only a tentative explanation can be attempted.

From the Curie point down to about 90° K the disorder within the domains is only gradually being eliminated. Previous indications of this were available in the spontaneous polarization from a.c. dielectric measurements, in x-ray measurements of shear (de Quervain 1944), and particularly, as de Quervain pointed out, in the close correspondence of the two as they grow from 122° K down to a steady value at under 100° K; since the x-ray analysis was made on a neutral crystal, in which

comparable volumes are sheared in opposite directions, whereas the dielectric measurements require a saturating field, this effect of slow growth of polarization cannot be simply a manifestation of domain interaction. Conclusive evidence is afforded by the observations reported in § 2. If between 100° and 120° K the domains were each fully polarized, but were not themselves fully aligned by an alternating field, as is suggested by Yomosa and Nagamiya (1949), then on applying a constant saturating field at a temperature below 100° K and warming the crystal to above the Curie point, the disappearance of the spontaneous polarization should show itself by an abrupt flow of current from the plates of the crystal; this would have been clearly seen and there was no such effect.

The existence in the range 100° to 120° K of appreciable numbers of dipoles along, say, the negative *c*-axis in a domain principally polarized along the positive *c*-axis would also account for the clamped and free dielectric constants, measured in the presence of a superposed constant field, being quite high in this range, and only reaching a level of the order of 10 below 100° K; these observations are shown as 'measured with bias' in figs. 9 and 10. Furthermore, when the biasing field is removed, the dielectric constant returns to the high value which it has in the neutral crystal at that temperature. Now the remanence of these crystals is high, so that the removal of a saturating field still leaves the majority of the domains polarized in the same sense; if the reversible movement of domain walls made the major contribution to the high susceptibility in this range, then this would be expected to alter after the application and removal of a strong field. It seems then that the high susceptibility arises mainly from the presence of a considerable degree of disorder in domains, so that quite a small field along the $+c$ direction may alter appreciably the proportions of dipoles along the $+c$ and $-c$ directions. Even a biasing field that suffices to align all the domains is evidently far from sufficient to effect the complete ordering of dipoles, which is presumed to reach its limit only when the temperature has fallen nearly 30° below the Curie point. Similarly a number of dipoles along the $\pm a$ and $\pm b$ directions in this temperature range would give the strongly polar value to the dielectric constant perpendicular to the ferroelectric axis which is observed, as is seen in fig. 11.

Below 90° K, however, reversible domain wall movement almost certainly makes the major contribution to the low-field susceptibility, which is independent of frequency up to at least 10^4 c/s. If the asymmetric hydrogen bond, as suggested by Slater, is accepted as at least a characteristic, if not the cause, of the ferro-electric state in KH_2PO_4, there is one very simple form for the boundary between oppositely polarized domains, consisting of a single layer of PO_4 groups in an *ac* or *bc* plane. For any such layer there are two possible configurations which preserve completely the assignment of two and only two protons as close neighbours to each PO_4 group. These are illustrated schematically in

fig. 15, following the representation employed by de Quervain (1944), but with the elementary cell in accordance with that of West (1930); only the hydrogen atoms and the outlines of the PO_4 tetrahedra are shown, and the numbers on the tetrahedra represent the coordinates of their centres as fractions of the lattice spacing along the positive *c*-axis; the structure is viewed along the positive *c*-axis, so that the diagonals

Fig. 15

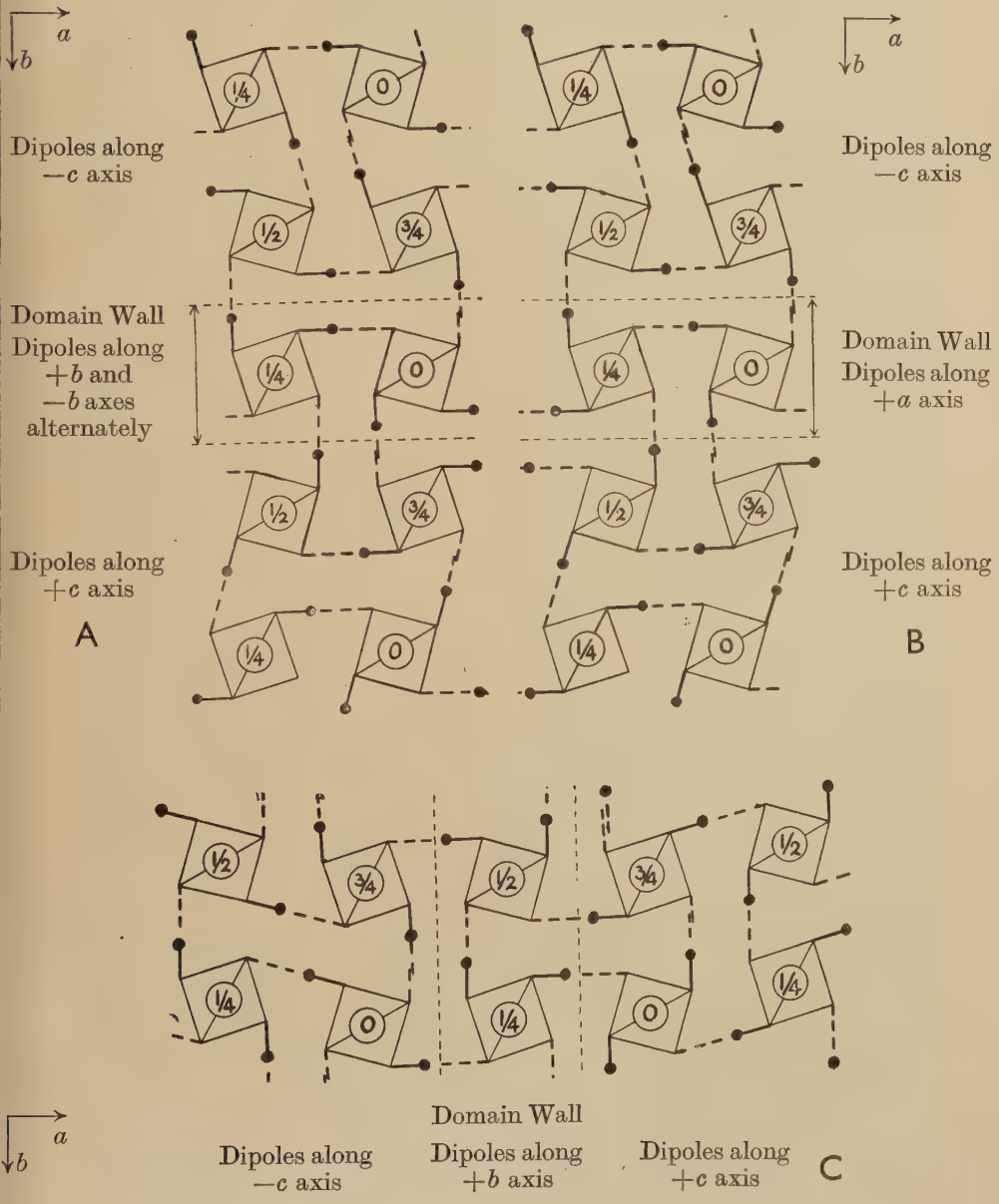

mark the line joining the two nearer oxygen atoms, that is the lower of the two pairs. The tetrahedra have been taken to be regular, as has been demonstrated by Frazer and Pepinski (1952). The shear of the lattice and the asymmetry of the O–H· ·O bond are both greatly exaggerated. As suggested by Mason (1950, p. 258), the H_2PO_4 unit has been treated as constituting a dipole with its negative end towards the pair of oxygens which have the hydrogen atoms closer to them. The details of the polarization induced in the PO_4 group do not appear to have been worked out, but this assumption, although at variance with what is known of molecular dipoles in solution, in which the hydrogens would form the positive end, does resolve one curious difficulty; the reversal of polarity in the ordered, ferroelectric state requires the movement of the hydrogens along the bonds throughout a domain, and the O–H· ·O bonds, though nearly perpendicular to the *c*-axis, still have a small *c*-component; then, if the pair of oxygens with the close hydrogens were the positive ends of the dipoles, the hydrogen nuclei would be required to move to a position of higher electrostatic energy in the applied field. The determination of the polarity is not, in fact, essential to the argument here, but it is of interest that it is a misconception of the process of reversal that has led to the use of the term ' freezing-in of the dipoles ' as an explanation of the rising coercive field at low temperatures.

In one of the configurations shown in fig. 15, the dipoles in the wall layer alternate in direction, lying almost normal to the wall, which is thus electrically neutral, as in fig. 15 (*a*). In the other, the dipoles are all aligned parallel to each other in the plane of the wall; this latter configuration corresponds to the Bloch wall in ferromagnetic materials, the polarization in this case being reversed in but two stages; if the domain boundary is in an *ac* plane, the dipole vector rotates with a left-hand screw motion, as in fig. 15 (*b*); if it is in a *bc* plane, the screw motion is right-handed, as in fig. 15 (*c*). Without a more detailed theoretical analysis it is impossible to say whether the neutral or the polarized wall is the more likely. In either case the layer forms a twinning plane, which may be assumed to move on the application of even the smallest field along the *c* axis. The extent to which the favourably oriented domain grows at the expense of its twin would be determined by the equilibrium with the elastic energy stored. The relation is particularly simple for ferroelectrics like KH_2PO_4, which exhibit spontaneous polarization along one axis only, and in which oppositely polarized domains have opposite shear. (This is in contrast with ferromagnetic materials, in which the strain due to magnetostriction is unaffected by a reversal of magnetization.) The sharp fall of the dielectric constant from 1000 at 90° to 8 at 60° K suggests that such wall movement is becoming impossible, and it would seem that in this range it is becoming energetically more favourable to have a boundary with irregular bond arrangements, so that it becomes a crystallite boundary, rather than to have one that preserves the continuity of the crystal but requires the presence of dipoles lying along the *a* or *b* axis, and having

therefore a high anisotropy energy. From 60° K downwards, then, the material would be composed almost entirely of single domain crystallites.

It is clear that the reversible movement of twinning planes within crystallites, however important for the low-field susceptibility, can never contribute a large portion to the reversal of the crystal as a whole, for even at 90° K a field of 10^{-4} of the coercive field can reverse only some 2×10^{-6} of the neutral crystal, while at 60° K this has fallen by a further factor of 10^2. Furthermore, in the case of ferromagnetic materials there is a strong inverse correlation between the coercive field and the initial susceptibility, and, although the latter requires only reversible changes while the former involves irreversible movements of domain walls, the processes are basically the same, and depend on the compressibility and magnetostriction of the material. Now it has been seen that there is no abnormality in the elastic properties or in the spontaneous polarization of KH_2PO_4 at 60° K, and as, in addition, de Quervain could observe no structural change in KD_2PO_4 at the corresponding temperature of 135° K, it appears necessary to seek another source for the 60° K anomaly. On both counts we are driven to assume that there is an additional, quite different process contributing to the reversal of the crystal. Such a process might be the irreversible transfer of whole layers or parts of layers of dipoles across a boundary between oppositely polarized crystallites, and this may be presumed to require fields of the order of 1 kv cm^{-1}. This process will be referred to as ' layer transfer '. The interpretation of plastic deformation in crystals in terms of the migration of dislocations provides a close analogy, and the behaviour of the coercive field may then be explained on the basis of the following model.

Both the Mueller and Mason theories predict a coercive field of the order of 10^2 to 10^3 kv cm^{-1}, which is much higher than that observed. Even if such a field were, in fact, required to reverse an unconstrained domain, the necessary field would be much reduced by a favourable strain. Suppose, now, that the growth of favourably oriented crystallites, starting perhaps from a very small nucleus of twinned crystallites, might proceed at the expense of oppositely polarized neighbours by this suggested irreversible mechanism of layer transfer until a fraction of the order of half the crystal had been reversed. The mean favourable strain in domains would be that of the crystal as a whole, and though at first only a few would, through local concentrations of strain, have their coercive field so lowered as to be reversed directly by the applied field, the process would thereafter accelerate rapidly. The protracted reversal at constant field observed on the steep portions of many of the d.c. hysteresis loops, extending over periods of the order of a minute, is an indication that some of the reversal is triggered by a mechanical process which may be quite slow if the applied force is only just adequate.

Furthermore, if a decrease in temperature effected a gradual decrease in the number of inter-crystallite boundaries at which layer transfer could take place, the coercive field of the crystal as a whole might well

start to rise quite abruptly when the reversal possible by layer transfer began to fall short of some critical fraction necessary to trigger the bulk reversal of the remainder. On the other hand the number of crystallite boundaries having less than a certain degree of dislocation, for example, would be expected to vary from specimen to specimen, and it is hard to see why there should be some characteristic temperature, such as there appears to be at 60° K, unless there was a second, still undetected, structural change at that temperature, which was too small to affect the principal electrical and mechanical properties, and was yet sufficient to accentuate the dislocations at crystallite boundaries, and so to raise the potential energy required for layer transfer.

References

Arx and Bantle, 1943, *Helv. Phys. Acta*, **16,** 211.
Atanasoff and Hart, 1941, *Phys. Rev.*, **59,** 85.
Barkla, 1946, *Nature, Lond.*, **158,** 340.
Baumgartner, 1949, *Helv. Phys. Acta*, **22,** 400.
Busch and Ganz, 1942, *Helv. Phys. Acta*, **15,** 501.
Cady, 1946, *Piezoelectricity* (New York : McGraw Hill Book Company).
Frazer and Pepinski, 1952, *Phys. Rev.*, **85,** 479.
Hulm, 1951, *Proc. Phys. Soc.* A, **63,** 1184.
Mason, 1946, *Phys. Rev.*, **69,** 173 ; 1950, *Piezoelectric Crystals* (New York: Van Nostrand).
Mueller, 1940, *Phys. Rev.*, **57,** 829.
de Quervain, 1944, *Helv. Phys. Acta*, **17,** 509.
Slater, 1941, *J. Chem. Phys.*, **9,** 1633.
Ubbelohde and Woodward, 1947, *Proc. Roy. Soc.* A, **188,** 358.
West, 1930, *Zeit. Kristallogr.*, **74,** 306.
Yomosa and Nagamiya, 1949, *Progr. Theor. Phys.*, **4,** 263.
Zwicker and Scherrer, 1944, *Helv. Phys. Acta*, **17,** 346.

XV. *Instability and Melting of the Alkali Halides*

By J. H. C. Thompson
Wadham College, Oxford*

[Received in final form October 19, 1952]

Summary

A condition for instability of the thermal vibrations of an expanded lattice of the NaCl type is established. It is found that the instability occurs when the increase of interionic distance, as compared with that at 0° K under no stress, is between 6% and 7%. The thermal expansion to the melting point is computed for five alkali halides and found to be some 5%. The type of instability and its relation to melting are discussed.

§ 1. Introduction

The melting of solids has been the subject of several investigations. Born (1939), who gives references to previous literature, worked from the standpoint that the resistance to elastic shearing vanishes when the solid melts, so that for a cubic crystal the elastic modulus c_{44} would vanish. Though this is a property of the liquid it is not necessarily a property of the solid at the melting point, and Hunter and Siegel (1942) found experimentally that c_{44} does not vanish in the case of NaCl. They also found that NaCl behaved as an elastic solid right up to the melting point. Born developed a thermodynamical theory to give the elastic constants as functions of temperature, and returned to the problem (Born 1943) considering the stability in a more general way. Unfortunately the theory becomes extremely complicated in its application.

When a cubic crystal expands on increase of temperature the expansion is a simple dilatation. The amplitude of the thermal vibrations of the atoms or ions will increase as the thermal energy increases, and the forces determining the vibration about the lattice points will change as the lattice expands. It seems that the melting point must be that point where the perfect lattice breaks up as a result of the thermal motion of the atoms or ions: lattice imperfections, which may exist at lower temperatures, can hardly explain the sudden change. The instability of the thermal vibrations may result, either from the size of the vibrations or from the instability of the harmonic vibrations (i.e. neglecting the effects of size). According to the theory of Lindemann (1910) the mean amplitude of vibration at the melting point is 0·075 times the interatomic distance. But the mean amplitude is also a measure of the expansion of the solid, and Grüneisen (1910) noted that the cubical expansion from

* Communicated by the Author.

the absolute zero to the melting point is approximately 15% for several substances. Fürth (1941) has discussed the experimental evidence of melting under pressure. He found that the condition that the volume at the melting point should be independent of pressure was approximately though not accurately satisfied. The results of Lindemann and Grüneisen are of surprising generality, but neither result is more than approximately satisfied and results expressed in terms of interatomic distance are sometimes rather insensitive to assumptions made about the interatomic forces.

The object of the present investigation is to determine the degree of expansion which causes instability of the thermal vibrations of an alkali halide of the NaCl type lattice, and to determine the nature of the instability. Though the ionic lattice is not typical of all crystals there is the advantage that we know rather more about the forces than in other cases. The assumption of central forces in itself demands the satisfaction of Cauchy's relations for the elastic constants at 0° K (though not at higher temperatures as is sometimes assumed). These relations do not hold for most metals, but in the case of the alkali halides the agreement is satisfactory. We shall assume that the interionic forces are the Coulomb electrostatic forces, together with a repulsive force between nearest neighbours only. This has been shown by Born and Göppert-Mayer (1933) and Wasastjerna (1935) to give satisfactory results in the calculation of physical properties of the crystals.

The first step is to consider the stability of the harmonic vibrations, for even if the instability is due to the amplitude the type of vibration which will first cause instability is likely to be indicated in this way. A full investigation of the stability of the expanded lattice requires the determination of the spectrum of the normal frequencies for that lattice. The harmonic vibrations will be unstable only if a normal frequency (ω) is imaginary. The character of the normal modes of vibration of the alkali halides is known. The problem was worked out first by Born and v. Kármán (1912) for a model, the device of the cyclic lattice being used to deal with boundary conditions. The difficulties associated with the Coulomb forces can be overcome (Born and Thompson 1934, Thompson 1935); and Kellerman (1940) has set up the frequency equation for NaCl for the unexpanded lattice, and has obtained numerical solutions to determine the spectrum. But the problem of finding the expansion which would cause any root of the resulting frequency equation to be imaginary is difficult. Born (1940) and Power (1942) have attempted to find under what conditions the stability of the acoustic vibrations ensures the stability of all vibrations of the lattice: they have proved that this is so in special cases using models with quasi-elastic bindings. Though the result has not been proved in general it is the instability of the acoustic vibrations which I investigate here. This will give a sufficient condition for the instability of the lattice, and the best condition for the instability of the acoustic modes.

We consider an infinite crystal. In the expanded lattice the lattice points are positions of equilibrium of the ions, whether the expansion is due to increase of temperature or the application of a dilatational tension. The ions are not, of course at rest, but are vibrating about the lattice points; and the amplitude of vibration will be greater when the expansion is due to increase of temperature than when it is due to a mechanical tension. By taking the thermal expansion as a fact, the question of stability is reduced largely to a mechanical problem, simpler than the thermodynamical problem. Though its solution can only deal with stability in terms of expansion, and not in terms of temperature, it can give just as much information about the manner in which a solid breaks up at the melting point.

§ 2. Instability of the Expanded Lattice

In an expanded lattice of the NaCl type the equilibrium positions of the ions are at $\mathbf{x}^l = \mathbf{l}a$, where $\mathbf{l} \equiv l_1, l_2, l_3$ (integers). The ion is positive or negative according as $l_1+l_2+l_3$ is even or odd. The unit cell has sides $(0, a, a)$ etc. and is of volume $2a^3$; and the positive ion at $(0, 0, 0)$ and the negative ion at (a, a, a) are contained in a cell.

Using the method of the cyclic lattice, we consider the vibrations of the ions in a block of N^3 cells, and suppose that this forms part of an infinite lattice built up from similar blocks, in which the displacements of corresponding ions at any instant are identical. To consider an infinite crystal we make $N \to \infty$. The wave-like character of the displacement of positive ions, or of negative ions, follows immediately from consideration of the cyclic lattice condition. Further properties of the normal modes are explained most easily in terms of the one-dimensional model with alternate particles of different masses (see Born and Göppert-Mayer 1933, p. 640). For the long waves it is readily seen that the displacement of the different particles are in phase; and in the acoustic modes the ratio of the amplitudes differs from 1 by $O(1/N^2)$, which $\to 0$ as $N \to \infty$. This is true, not only with quasi-elastic bindings between neighbours only, but also for a more general force system provided that the system of forces acting on a particle of one kind is the same as that acting on a particle of the second kind. The character of the normal modes in the real three-dimensional lattice can be considered in the same way: and it is found that the wave-like expressions for the displacement are of the same amplitude and phase for the positive and negative ions provided that the force system acting on the positive ion is the same as that acting on the negative ion. Now this is true of the force system we are considering (Coulomb electrostatic forces together with repulsive forces between first neighbours only), but it would not be true if there were repulsive forces between positive ions at distance $a\sqrt{2}$, and different repulsive forces between negative ions at the same distance.

The displacement of an ion in an acoustic normal mode is thus of the type

$$\mathbf{u}^l = \mathbf{u}(t) \sin [(\mathbf{x}^l \,.\, \mathbf{b}) + \epsilon],$$

where $\mathbf{b}$ is a vector of $O(1/Na)$, so chosen that the cyclic lattice condition is satisfied. We find that

$$\mathbf{b} = \frac{\pi}{Na}(r, s, t),$$

where r, s, t are integers, all even or all odd and small compared with N. This displacement can be considered as a strain (and rotation), where the strain tensor $\mathbf{e}$ is given by

$$\left.\begin{aligned} \mathbf{e} &= \mathbf{e}^0 \cos [(\mathbf{x} \,.\, \mathbf{b}) + \epsilon], \\ \text{and} \qquad e_{11}{}^0 &= u_1 b_1, \text{ etc.} \\ e_{23}{}^0 &= \tfrac{1}{2}(u_2 b_3 + u_3 b_2), \text{ etc.} \end{aligned}\right\} \quad \ldots\ldots \quad (1)$$

As $\mathbf{b}$ is $O(1/Na)$ the strain approximates to a uniform homogeneous strain for distances small compared with Na. With N large this is true for a distance $a\sqrt{N}$, which itself tends to infinity as $N \to \infty$. Thus in finding the forces acting on an ion in its displaced position in an acoustic normal mode we can consider the lattice to be subject only to a uniform strain; but in calculating the energy of the block we must remember that the strain is periodic in the block, so that the mean value of a strain component vanishes and the mean value of the product of two strain components is one-half the greatest value of the product in the block. The strain tensor $\mathbf{e}^0$, given by (1), is not the most general form of strain tensor, as the determinant of its components vanishes. This is the only restriction on it.

We calculate the potential energy of the force bonds per cell when the lattice is in a state of homogeneous strain. We then obtain the potential energy per cell averaged over the whole block in the displacement appropriate to an acoustic normal mode. If this is less than the potential energy when the ions are in their equilibrium positions the motion in the normal mode will be unstable. The calculations in the first stage follow methods already used in the determination of the elastic constants (see Born and Göppert-Mayer 1933, p. 738), and are given in outline only. They are not identical with previous calculations, which do not apply to the expanded lattice.

The displacement $\mathbf{u}^l$ of the lth ion is determined by

$$u_i{}^l = e_{ik} x_k{}^l,$$

where the suffixes i, k denote axial directions and a repeated suffix indicates summation over the values 1, 2, 3 of that suffix, and e_{ik} are the components of the strain tensor.

Not only the force bonds but also the geometrical displacement of the rest of the lattice is the same in relation to the ion at (0, 0, 0) as to that at (a, a, a). Thus, denoting the whole potential of a force bond by $\phi(r)$, the energy per cell is

$$U = \sum_l \phi(|\mathbf{x}^l + \mathbf{u}^l|),$$

where the summation extends over all positive and negative integral values of l_1, l_2, l_3 excluding (0, 0, 0).

Using Taylor's theorem to expand ϕ, we obtain

$$U=\sum_{l}\{\phi(r^l)+P(r^l)x_i{}^l x_k{}^l e_{ik} + \tfrac{1}{2}[\delta_{ij}P(r^l)+x_i{}^l x_j{}^l Q(r^l)]x_k{}^l x_m{}^l e_{ik}e_{jm}+\text{higher powers of } e_{ik}\},$$

where $$r^l=|\mathbf{x}^l|=a(l_1{}^2+l_2{}^2+l_3{}^2)^{1/2}=al$$

and $$P(r)=D\phi(r), \qquad Q(r)=D^2\phi(r), \qquad D\equiv\frac{1}{r}\frac{d}{dr}.$$

For the Coulomb electrostatic forces

$$\phi(r^l)=\frac{e^2}{r^l}(-1)^{l_1+l_2+l_3},$$

when e denotes the electronic charge. Hence to the second order in the strain components

$$U_{el}=\frac{e^2}{a}\sum_{l}(-1)^{l_1+l_2+l_3}\left\{\frac{1}{l}-\frac{l_i l_k}{l^3}e_{ik}+\tfrac{1}{2}\left(-\frac{\delta_{ij}}{l^3}+\frac{3l_i l_j}{l^5}\right)l_k l_m e_{ik}e_{jm}\right\}. \quad . \quad (2)$$

The repulsive forces, of potential $\psi(r)$, between first neighbours contribute only to the $(\pm1, 0, 0)$ and similar terms, and we obtain

$$U_{re}=6\psi(a)+2a\psi'(a)[\Sigma e_{11}+\Sigma e_{23}{}^2]+a^2\psi''(a)\Sigma e_{11}{}^2. \quad . \quad . \quad . \quad (3)$$

In (2) the sums of terms involving l_1, l_2, l_3 vanish whenever there is an odd power of l_1, l_2 or l_3; and simple symmetry relations enable other sums to be expressed in terms of

$$\sum_{l}(-1)^{l_1+l_2+l_3}\frac{1}{l}=-S_0(1) \qquad \text{(Madelung's constant)}$$

and $$\sum_{l}(-1)^{l_1+l_2+l_3}\frac{l_1{}^4}{l}=-\tfrac{1}{3}S_1(1).$$

The numerical values of $S_0(1)$ and $S_1(1)$ (see Born and Göppert-Mayer 1933) are

$$S_0(1)=1{\cdot}7476, \qquad S_1(1)=3{\cdot}226. \quad . \quad . \quad . \quad . \quad . \quad (4)$$

After making these simplifications we obtain

$$U=U_{el}+U_{re} = \left\{-\frac{e^2}{a}S_0(1)+6\psi(a)\right\}+\left\{\frac{e^2}{3a}S_0(1)+2a\psi'(a)\right\}\Sigma e_{11} + \tfrac{1}{2}\{A\Sigma e_{11}{}^2+2B\Sigma e_{22}e_{33}+4C\Sigma e_{23}{}^2\}, \quad . \quad . \quad (5)$$

where

$$\left.\begin{aligned} A&=[\tfrac{1}{3}S_0(1)-S_1(1)]\frac{e^2}{a}+2a^2\psi''(a)=-2{\cdot}643\frac{e^2}{a}+2a^2\psi''(a),\\ B&=\tfrac{1}{2}[S_1(1)-S_0(1)]\frac{e^2}{a}=0{\cdot}7392\frac{e^2}{a},\\ C&=B+\frac{e^2S_0(1)}{6a}+a\psi'(a). \end{aligned}\right\} \quad . \quad . \quad (6)$$

The energy per cell averaged over the block is thus

$$\overline{U}=\left\{-\frac{e^2}{a}S_0(1)+6\psi(a)\right\}+\tfrac{1}{4}\{A\Sigma(e_{11}{}^0)^2+2B\Sigma e_{22}{}^0e_{33}{}^0+4C\Sigma(e_{23}{}^0)^2\}$$
$$=\text{constant}+\tfrac{1}{4}B(\Sigma e_{11}{}^0)^2+\tfrac{1}{4}(A-B)\Sigma(e_{11}{}^0)^2+C\Sigma(e_{23}{}^0)^2, \quad . \quad . \quad . \quad (7)$$

when the strain components are now the greatest values of the strain components in the block.

When the ions are at rest, which is approximately true at 0° K, the potential energy per cell, $-e^2S_0(1)/a+6\psi(a)$, must be a minimum, so that

$$\frac{e^2S_0(1)}{a_0{}^2}+6\psi'(a_0)=0. \quad . \quad . \quad . \quad . \quad . \quad . \quad . \quad (8)$$

Thus when $a=a_0$, $C=B$. We assume that $-\psi'(a)$ decreases more rapidly with increasing a than does $1/a^2$. It follows that, when $a>a_0$, $C>B$. From (6) we see that, though B decreases with increasing a, it is always positive; and it follows that C is always positive when $a>a_0$.

The condition that the motion in the normal mode should be unstable is that the quadratic function in (7) should be negative, and this can be true only if $A<B$, $\Sigma e_{11}{}^0=0$, $e_{23}{}^0=e_{31}{}^0=e_{12}{}^0=0$. . . . (9)

There is also the condition that the determinant of the strain components is zero, so that one at least of $e_{11}{}^0$, $e_{22}{}^0$, $e_{33}{}^0$ must vanish. Hence the value of $\mathbf{e}^0$ in an unstable acoustic normal mode must be of the type

$$e_{11}{}^0=e^0, \quad e_{22}{}^0=-e^0, \quad \text{all other components}=0. \quad . \quad . \quad (10)$$

We return to the discussion of this motion in the next section. Using (6), the conditions $A<B$ gives

$$\psi''(a)<1{\cdot}692\,\frac{e^2}{a^3}. \quad . \quad . \quad . \quad . \quad . \quad . \quad . \quad (11)$$

Combining this with (8), we obtain

$$-\frac{a^3\psi''(a)}{a_0{}^2\psi''(a_0)}<5{\cdot}81. \quad . \quad . \quad . \quad . \quad . \quad . \quad . \quad (12)$$

In order to determine the value of a for which this condition is satisfied it is necessary to make some assumption about the potential $\psi(r)$ of the repulsive force. The form r^{-n} has been assumed most often, but has no theoretical basis. The value of n can be obtained in several ways, and values obtained are tabulated by Born and Göppert-Mayer (1933, p. 720). Values obtained by different methods vary considerably: for instance, in the case of NaCl they range from 7·8 to 11·3. The difficulty here is that these determinations of n all amount to the evaluation of the ratio of derivatives of ψ with a value a_0 for the distance. This cannot tell us much about the value of $\psi''(a)$. The most useful determination to use here is that made by Slater (1924) as his method involved the third derivative of ψ, and this might be expected to give a reasonable estimate for the second derivative $\psi''(a)$ by extrapolation.

If we assume $\psi(r) \propto r^{-n}$, the condition (12) for instability becomes

$$\frac{a}{a_0}>\left(\frac{n+1}{5{\cdot}81}\right)^{\frac{1}{n-1}}. \quad . \quad . \quad . \quad . \quad . \quad . \quad . \quad (13)$$

It follows immediately that if $1<n<4{\cdot}81$, the lattice is unstable when $a=a_0$. The critical value of a/a_0 varies with n. It increases from 1 to 1·076 approximately as n increases from 4·81 to 13, and decreases to 1 as $n\to\infty$. The values for different n are

$$\left.\begin{array}{lccccccc} n= & 6 & 7 & 8 & 9 & 10 & 11 & 12 \\ a/a_0> & 1{\cdot}038 & 1{\cdot}054 & 1{\cdot}065 & 1{\cdot}070 & 1{\cdot}074 & 1{\cdot}075 & 1{\cdot}076 \end{array}\right\}. \quad (14)$$

Except for the lithium halides values of n obtained by various methods lie within the range 7·8 to 12·3, which makes the critical value of a/a_0 lie within the range 1·062 to 1·076. Lower values of n have been obtained for the lithium halides, the smallest always being for LiF, for which Slater (1924) obtained $n=5{\cdot}9$. The corresponding critical value of a/a_0 is 1·036, but this must be regarded with suspicion. The values of n for the lithium halides are not as well substantiated as for the other alkali halides; and the assumption that the repulsive forces between closest negative ions can be neglected, which has been made here, may be too crude an approximation for the lithium halides.

Other forms of the repulsive potential have been suggested: that obtained by Wasastjerna (1935) seems to be on the best foundation. He attempted to find an expression which takes account of the additive property of the ionic radii, and the form which is to be expected from wave mechanics. He finds that

$$\psi(r)=9{\cdot}2\times10^5\,\frac{e^2}{\rho_1+\rho_2}\,\frac{b+\xi^7}{b+46}\exp(-10\xi) \quad . \; . \; . \quad (15)$$

explains with reasonable accuracy the measurable properties of all the alkali halides except the lithium halides, which he does not consider. Here $b=b_1+b_2$, and the suffixes on b and ρ indicate the alkali and halide ions respectively. The radii ρ_1, ρ_2 are basic radii (not the Goldschmidt radii obtained from closest packing), and $\xi=r/(\rho_1+\rho_2)$. At 0° C, $\xi=1{\cdot}87$ for the NaCl type lattice, and 1·63 for the CsCl type. At 0° K we take $\xi=1{\cdot}85$ for the NaCl type. Here we are interested in the behaviour of ψ in the region 1·85 to 2 for ξ. The expression for ψ has not been subject to any independent check for the larger values of ξ, but it can be used with more confidence than can r^{-n} as the form of the function has some theoretical basis.

The use of (15) in (12) leads to complicated formulae. Writing $\xi=\xi_0(1+\eta)$, so that $\eta=(a/a_0)-1$, we finally obtain for the critical value of η

$$\exp(-10\xi_0\eta)=\frac{5{\cdot}81(11{\cdot}5+10b/\xi_0{}^6)}{125+111\eta+342\eta^2+100b/\xi^5}\,\frac{1}{(1+\eta)^8}, \quad . \; . \quad (16)$$

in which form the equation can be solved by successive approximation. The value obtained for η is not very sensitive to the value of b, and for $b=0$ we find

$$\eta=0{\cdot}064(5), \quad \text{or} \quad a/a_0=1{\cdot}064(5). \; . \; . \; . \; . \; . \quad (17)$$

Using the values of b given by Wasastjerna the following results are obtained :

	KCl	KBr	KI	NaCl
b	−1·5	−0·5	2·0	−8·0
η	0·064	0·064	0·065	0·062

. . (18)

These values for the critical linear expansion are surprisingly close to the values obtained in (14). We see that the harmonic thermal vibrations of all the alkali halides (except possibly for the lithium halides) become unstable when the expansion of the lattice from its state under no stress at 0° K is between 6% and 7%.

§ 3. Melting

It is of interest to compare the thermal expansion up to the melting point with the expansion necessary to cause the instability discussed in § 2.

The expansion of the alkali halides from −184° C to 0° C has been determined by Henglein (1925). Eucken and Dannöhl (1934) have determined the coefficient of expansion of five alkali halides from 20° C to within 70° of their melting points, and find that the coefficient of expansion can be represented by an expression $\alpha=a+bt+ct^2$, the appropriate values of a, b, c being determined for each substance. It is not clear whether they define α as $\frac{1}{l}\frac{dt}{dl}$, $\frac{1}{l_{20}}\frac{dl}{dt}$, or $\frac{1}{l_0}\frac{dl}{dt}$ (the suffixes referring to temperatures in ° C). I have assumed the last, and the uncertainty here would not cause an error exceeding 0·001 in the value of a_T/a_0.* Some experiments have shown differences between the expansion determined by x-ray measurements and that determined by macroscopic measurements ; but the most recent investigation by Connell and Martin (1951) show no substantial deviation from the results of Eucken and Dannöhl in the range they examined. I do not know of any experimental check of the expansion for high temperatures. The main possibility of error in the determination of α lies in the extrapolation from the highest temperature of the experiments to the melting point. The coefficient of expansion is about twice its value at 0° C, and the formula has no theoretical basis. On the other hand, no abnormal effects are to be expected provided the lattice structure persists, for according to Grüneisen's formula the increase in α at these temperatures is mainly due to the increase in the compressibility. The extrapolation at the lower end of the temperature range is not important. The value of α

* In *Landolt Bornsteins Tables* (Erg. Bd. III. 3, p. 2226) a formula is given for the linear extension which seems to assume that $\alpha=(l-l_0)/l_0$. This would make an important difference, giving $a_T/a_0=1{\cdot}07$ instead of 1·05 approximately. I can find no justification for this in Eucken and Dannöhl's paper.

at 89° K can be determined approximately from Henglein's results (it is of the order 3×10^{-5}) : we know that in the range 0° K to 89° K $\alpha \propto C_v$ approximately, and again we know roughly the form of C_v. I have taken the linear expansion from 0° K to 89° K as 0·001 in all cases. The melting point has been taken as an average, when experimental values differ without known reason. The results are set out in the table below :

Crystal	Melting temperature T in ° C	Total linear expansion $(a_T/a_0)-1$	Value from § 2 of $(a/a_0)-1$
LiF	840	0·050	?0·036
KCl	770	0·045	0·064
KBr	748	0·049	0·064
KI	678	0·044	0·065
NaCl	800	0·052	0·062

. . (19)

Except for LiF the values of $(a/a_0)-1$ in the last column are the values calculated, using Wasastjerna's form for the repulsive potential, and set out in (18). In the case of LiF the only expression for the repulsive potential which has been obtained is r^{-n}, and we take $n=5{\cdot}9$ as determined by Slater. As previously stated in § 2 the resulting value of a/a_0 cannot be considered to be well founded. For the other substances, however, it has been seen that the figures are much more reliable.

The results show that the expansion necessary to cause instability of the harmonic normal vibrations of the acoustic type is of the same order of magnitude but greater than the thermal expansion at the melting point.

We now examine the nature of the motion in the normal mode which becomes unstable. Solving the eqns. (1) for the components of the strain $\mathbf{e}^0$ for the strain given by (10), we find

$$u_3=b_3=0\ ;$$

and either $\quad b_1=b_2, \qquad u_1=-u_2,$

or $\quad b_1=-b_2, \qquad u_1=u_2.$

Thus the strain at any point of the lattice is given by

$$\mathbf{e}=\mathbf{e}^0\cos\left[b(x_1\pm x_2)+\epsilon\right], \qquad . \ . \ . \ . \ . \ (20)$$

where $e_{11}{}^0=-e_{22}{}^0$, all other components=0. The relative displacement of adjacent ions at any instant is determined by the strain : this varies slowly and periodically through the lattice and has its numerically greatest values (of alternate sign) on planes parallel to the planes (1, 1, 0) and (1, −1, 0). The relative displacement of the ions on either side of a plane of the first type is a simple shear in the direction (1, −1, 0) or its reverse. A similar result holds for planes of the second type and other planes obtained by rotation of the axes.

Strictly any theory of small vibrations breaks down when the vibrations become large : but it is reasonable to suppose that, if the

forces controlling the thermal vibrations are such as to place little restraint on the increase in size of a vibration when it is small, it will in fact become large if the energy of the motion is fixed. This is the case here as the total energy in a normal mode is kT, and we should expect a large shear across any of the planes of the six types (1, 1, 0) etc. occurring periodically through the crystal for an expansion close to but not equal to the critical expansion. It is to be expected that this large shearing displacement of one part of the crystal against the other in a normal mode would split up the crystal into smaller pieces, having for surfaces the planes of this type.

Now, if the crystal breaks up, not because the vibrations are essentially unstable but because they are large, as is suggested by the numerical results, it is possible that a break of this kind is achieved only by a change of some kinetic (thermal) energy into an increase of potential energy, and the process of creating further breaks in the crystal would follow only through the supply of further kinetic energy in the form of heat. This would supply a qualitative explanation of the latent heat of fusion essentially the same as that already suggested by Mackenzie and Mott (1950), who consider the liquid as the limiting form of a polycrystalline solid when the crystal size becomes very small, and ascribe the latent heat of fusion to the energy of misfit of the crystalline boundaries.

References

Born, M., 1939, *J. Chem. Phys.*, **7,** 591 ; 1940, *Proc. Camb. Phil. Soc.*, **36,** 160 ; 1943, *Ibid.*, **39,** 100.

Born, M., and Göppert-Mayer, M., 1933, *Hand. d. Phys.* XXIV (2), Ch. IV, (Springer).

Born, M., and Thompson, J. H. C., 1934, *Proc. Roy. Soc.* A, **147,** 594.

Born, M., and v. Kármán, Th., 1912, *Phys. Zeits.*, **13,** 297.

Connell, L. F., and Martin, H. C., 1951, *Acta Crystrallogr.*, **4,** 75.

Eucken, A., and Dannöhl, W., 1934, *Zeits. Elch.*, **40,** 814.

Fürth, R., 1941, *Proc. Camb. Phil. Soc.*, **37,** 34.

Grüneisen, E., 1910, *Ann. Phys., Lpz.*, **33,** 33.

Henglein, F. A., 1925, *Zeits. f. phys. Chem.*, **115,** 91 ; **117,** 285.

Hunter, L., and Siegel, S., 1942, *Phys. Rev.*, **61,** 84.

Kellermann, E. W., 1940, *Phil. Trans. Roy. Soc.* A, **238,** 513.

Lindemann, F. A., 1910, *Phys. Zeits.*, **11,** 609.

Mackenzie, J. K., and Mott, N. F., 1950, *Proc. Phys. Soc.* A, **63,** 411.

Power, S. C., 1942, *Proc. Camb. Phil. Soc.*, **38,** 61.

Slater, J. C., 1924, *Phys. Rev.*, **23,** 488.

Thompson, J. H. C., 1935, *Proc. Roy. Soc.* A, **149,** 487.

Wasastjerna, J. A., 1935, *Comm. Phys-Math., Soc. Scient. Fennica*, **8,** nos. 9, 20, 21.

XVI. *Helium 3 Reactions in Nuclear Photographic Emulsions*

By J. H. Fremlin
Department of Physics, University of Birmingham*

[Received August 30, 1952]

Abstract

An attempt has been made to learn something of the kinds of nuclear reaction undergone by Helium 3 in the range of energy from 0 to 29 mev, by examining individual reactions taking place in nuclear emulsions. About 130 000 tracks produced by 30 mev ^{3}He ions accelerated by the Birmingham University cyclotron were examined. Apart from deflections due to collisions with silver and bromine nuclei, 231 nuclear reactions were observed. Half of these represented close elastic collisions with light nuclei, including 102 with hydrogen nuclei. Among the others, reactions of the types (^{3}He, n), (^{3}He, α), (^{3}He, d), (^{3}He, t), (^{3}He, 2p), (^{3}He, pn) and (^{3}He, αp) were definitely identified, while (^{3}He, 2p2α) and (^{3}He, αpn) were almost certainly so.

§ 1. Introduction

Owing to the rarity of the light isotope of helium, less is known of its reactions than is known of those of other light nuclei. It was believed that a useful survey of the commoner types could be obtained by studying individual reactions occurring in nuclear emulsions bombarded by ^{3}He ions of known energy. A similar investigation has already been carried out by Lukirsky, Mescheryakov and Khrenina (1947), but they were able to use ions of only 5·7 mev energy, and observed two nuclear reactions only in 100 000 tracks.

§ 2. Experimental Method

Helium 3 ions were accelerated in the Birmingham University cyclotron by running this at its normal frequency but with three-quarters of the normal magnetic field used for accelerating deuterons. In the work to be described here, ordinary atmospheric helium—containing 1·3 parts per million of ^{3}He—was fed into the arc source. Beams of ^{3}He ions were obtained; some experiments on the production of ^{11}C and ^{13}N from carbon by the internal beam at 20 in. radius (18·5 mev) have already been described (Fremlin 1952). Beyond 20 in. all but about 1 in 10^3 of the particles are lost from the internal beam owing to unsuitable shimming at the reduced field.

* Communicated by the Author.

Those which survive, however, can be deflected into an external beam in the usual way, the deflector voltage also being three-quarters of the deuteron value, and an external beam of the order of 10^{-9} of the alpha-particle beam can be obtained. This still represents a few thousand ions per second, which is quite sufficient for nuclear emulsion work.

The use of the extracted beam avoids confusion with undesired particles such as $^{14}N^{+++}$ and HD^{+}, which are accelerated in nearly the same resonance conditions but with lower angular velocities.

§ 3. Exposure of the Nuclear Plates

Ilford C2 plates with emulsion thicknesses first of 200 μ and later of 400 μ were exposed in vacuum to the extracted beam without the interposition of any absorber between the plates and the main vacuum tank. In order to avoid delay due to the 'degassing' of the plates, these were vacuum dried for a few hours before exposure.

The plates were exposed at 10° to the beam for about 5 minutes, during which time the magnet current was varied continuously over a range of $\pm\frac{1}{2}\%$ since the beam of ions could not be monitored and small variations in oscillator-frequency and dee-position were liable to occur between runs. To check the exposure, a test strip with a much thinner C2 emulsion was exposed on the same target by the side of each main plate. By using suitable warm solutions the test emulsion could be made ready for microscopic examination ten minutes or less after removal from the vacuum.

Besides the C2 plates, one electron-sensitive G5 plate was also exposed but, although a number of events were found in this, no advantage was gained. The cyclotron tank has now a very considerable γ-ray activity and the background of electron tracks was too great for any such tracks following a nuclear reaction to be identified.

In all cases a certain amount of surface blackening was produced by light from the interior of the machine ; removal of this entailed the loss of the first part of each track, so that the useful energy was 28–29 Mev.

3.1. *General Results*

An area of 9 cm^2 containing some 130 000 ^{3}He tracks has been searched for nuclear reactions. The finding and measuring of the events to be described took about four months of actual microscope work by a skilled observer. Later check measurements by a second observer, of all the events discussed quantitatively below, took a further month. Considerable resources would therefore be needed if the number of each type of event were to be much increased for statistical purposes.

A total of 231 events have been found so far, apart from simple deflections without change of charge and without visible recoil. Examples of several types are shown in fig. 1 (figs. 1 *a–g*, Plates 3 and 4). From the known composition of the emulsion, shown in table 1, the nuclei may be

divided into three main groups: hydrogen; other 'light' nuclei (C, N, O); and 'heavy' nuclei (Br, Ag). These three groups of nuclei have been found to give events of characteristically different appearances:

Table 1

Element	Atomic Weight	Number of atoms per c.c. of dry C2 emulsion
Hydrogen	1·0080	$3{\cdot}35\times10^{22}$
Carbon	12·010	1·35
Nitrogen	14·008	0·29
Oxygen	16·000	1·02
Sulphur	32·06	0·02
Bromine	79·916	1·01
Silver	107·880	1·03
Iodine	126·92	0·02

The events may be classified as follows:

(^{3}He, xn) reaction	1
Scattering of ^{3}He ions by hydrogen atoms	102
Scattering of ^{3}He ions by carbon, nitrogen and oxygen	14
Reactions giving one singly-charged particle:	
Heavy nuclei	20
Light nuclei	16
Other two-pronged stars	5
Three-pronged stars	60
Four-pronged stars	10
Five-pronged stars	3
	231

Besides these, 134 simple deflections were examined as described in §5.1, but this figure must not be compared with the others in considering cross-sections, as during much of the search for events such simple deflections were ignored.

§4. Methods of Analysis

In analysing individual events of the types shown in the photographs, the first problem is to identify the light nuclei emitted. When tracks more than 20–30 μ long are involved, singly or doubly charged particles can at once be distinguished by eye unless they dip very steeply. The separation of particles of the same charge and different mass is, however, more difficult. Some guidance as to whether a proton or a deuteron was

more probable was provided by grain counts,* but certainty was never achieved (see fig. 2).

No useful distinction between ^{3}He and α tracks has yet been found and, though light recoil nuclei from boron to flourine can readily be separated from either helium nucleus when their tracks are more than a few microns long, it has not proved possible to distinguish them from one another.

When the nature of a singly or doubly charged particle has been established, its energy and momentum can be found with considerable accuracy, so long as its range lies wholly within the emulsion, by using the

Fig. 2

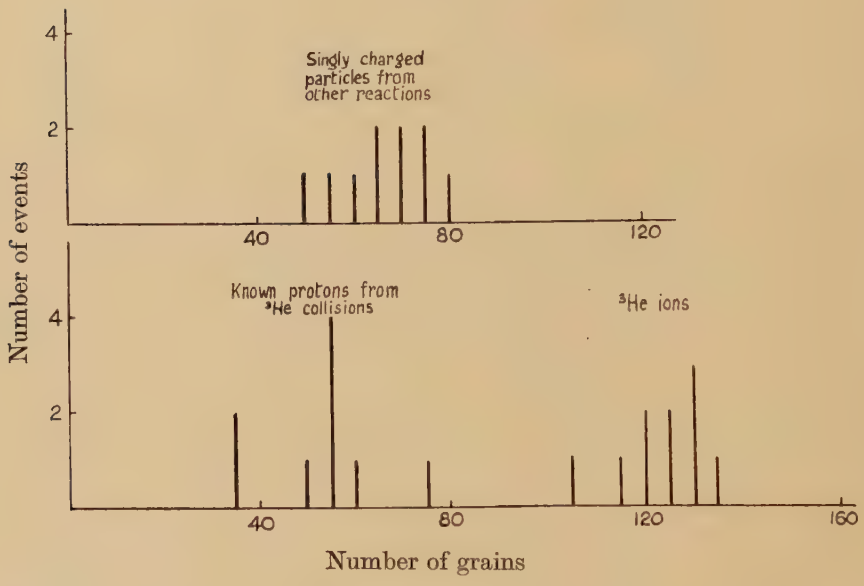

Number of grains between 200 μ and 300 μ from the stopping end of a track for various particles (plate 407). Doubly-charged particles are clearly distinguished, but there is only a suggestion of the presence of anything other than protons among singly-charged particles. (§ 4.)

range–energy relations for C2 plates given by Rotblat *et al.* (1951). The probable error for the energy, mainly due to straggling, is in the region of 1% for ^{3}He ions of full energy. The range–energy relations for nuclei more highly-charged than alpha-particles were obtained from A.E.R.E. Report No. G/R 664 by J. J. Wilkins (1951).

* The best discrimination was found by counting the grains, in a given plate, between 200 μ and 300 μ residual range. This work was carried out by Mr. R. G. Freemantle.

§ 5. Detailed Results

The different kinds of reaction observed will now be discussed in more detail.

5.1. *Simple Deflection Corresponding to Large-angle Scattering or to* (^{3}He, α) *reactions*

Thirty-four tracks showing a deflection of 60° or more were recorded and examined. Of these none showed a significant increase in total range, but three showed a loss of range well beyond that to be expected by chance. These could correspond to inelastic collisions involving a loss of 8·1, 9·3 and 14·2 Mev respectively, but could also represent reactions of the form $X(^3\mathrm{He}, yn+\alpha)Y$, where X represents a silver or bromine nucleus and y is 1, 2 or 3.

Fig. 3

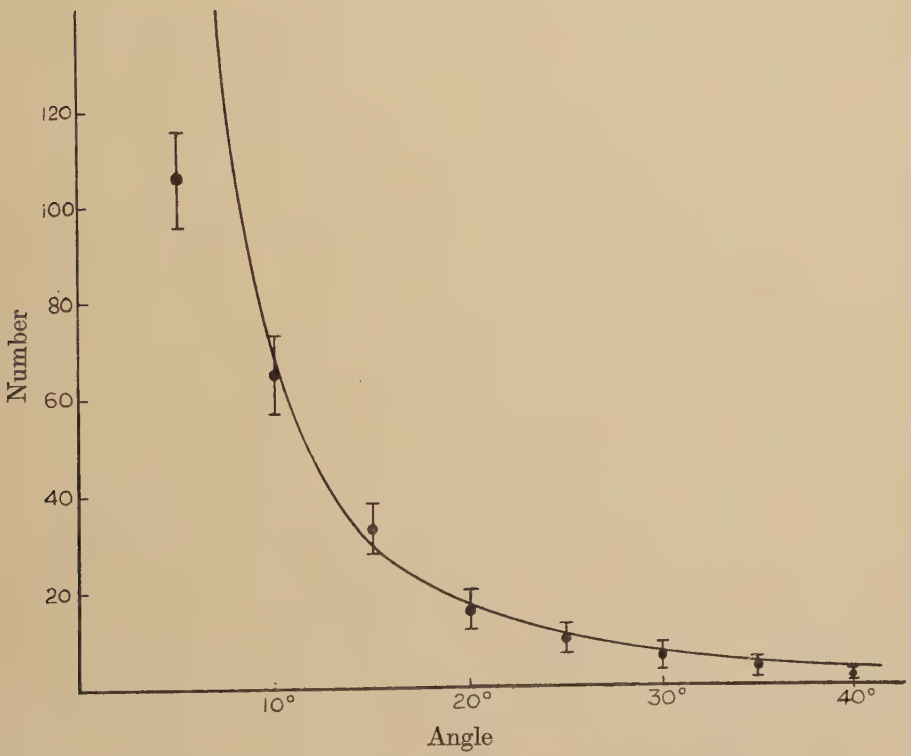

An area containing 3 700 ^{3}He tracks was searched for deflections above 5° at energies above 16 Mev. The points show the observed numbers with deflections *greater* than the angles against which they are plotted. The curve shows the absolute numbers to be expected on the basis of Coulomb scattering. (§ 5.1.)

An examination of a further 100 tracks which showed a deflection of more than 5° at an energy above 16 Mev was also made. Not one of these

showed a length greater than that which might be shown by a scattered particle, though five showed reductions in total range which were probably significant.

The distribution of number against angle is shown in fig. 3. It seems clear that some of those with less than 10° deflection were missed, as would be expected if their projected angles were small. The curve shows the number to be expected from pure Coulomb scattering averaged over the same energy range for the same number, 3 700, of particles.

5.2. (^{3}He, xn) *Reactions*

Only one event which might be interpreted this way has been observed. It is to be noted, however, that such reactions would be extremely easy to miss in searching, as no secondary charged particle would be emitted and in the reactions with heavy nuclei not even a recoil would be visible.

In the particular case observed, a short recoil is visible and the momentum and energy requirements would be fitted reasonably well by the assumption of one neutron of 16 to 25 Mev in the appropriate direction, but no confirmatory data are available.

5.3. *Scattering of* ^{3}He *Ions by Hydrogen Atoms in the Emulsion.* (102 *events observed*)

See fig. 1 (*a*), (Plate 3). This is easily the commonest type of event. In all cases the three tracks were coplanar within the (rather large) limits of observation.

Examination of these collisions has been very useful in determining the reliability with which the momentum and energy of a single particle can be found. For each event for which complete data are available, the ' expectation of range ', at impact, of the ^{3}He ion was calculated, from the mean range of particles in the same region of the plate. This was compared with the range to be expected for an ion with energy equal to the total measured energy following the collision. The standard deviation for all events was 9·8 μ, in good agreement with that to be expected from the variations of normal ^{3}He track lengths. This gives a standard deviation in energy at the mean range for collision (about 160 μ) of 0·6 Mev or $3\frac{1}{2}$%. The errors in momentum would then be expected to be under 2%. The angles between the tracks of particles are, however, much more difficult to measure than the ranges, owing to finite grain size and the scattering of the particles concerned.

Figure 4 shows the errors observed for 30 cases. The calculated momenta in a horizontal plane, in units of (Energy in Mev $\times$ mass in atomic units)$^{1/2}$, are plotted, and it will be seen that the probable error is in the region of 0·1 in these units. In a typical case this is about 10% for the sideways momentum, but is about 2% as expected for the longitudinal component which necessarily is always several times as great as the sideways one. The earlier measurements of vertical momenta were very much worse and even in the latest examples show more than twice the error, owing to difficulty in observing, and allowing for, vertical scattering

through moderate angles soon after leaving the point at which collision took place. (Vertical angles are found by measuring the change in depth over a finite length of track, usually 25 μ.) Part of the error in the horizontal momenta calculated must be regarded as a second-order effect of these vertical errors. It will be seen, however, that the accuracy achieved is sufficient for quite a useful check to be made of the identification of the reaction concerned.

In fig. 5 is shown a distribution of a number of collisions with protons observed against ^{3}He particle range. There is a suggestion of non-uniformity, but this is not statistically significant. The apparent drop above 320 μ is due to loss of the earlier part of tracks in most plates due to surface damage as mentioned earlier.

Fig. 4

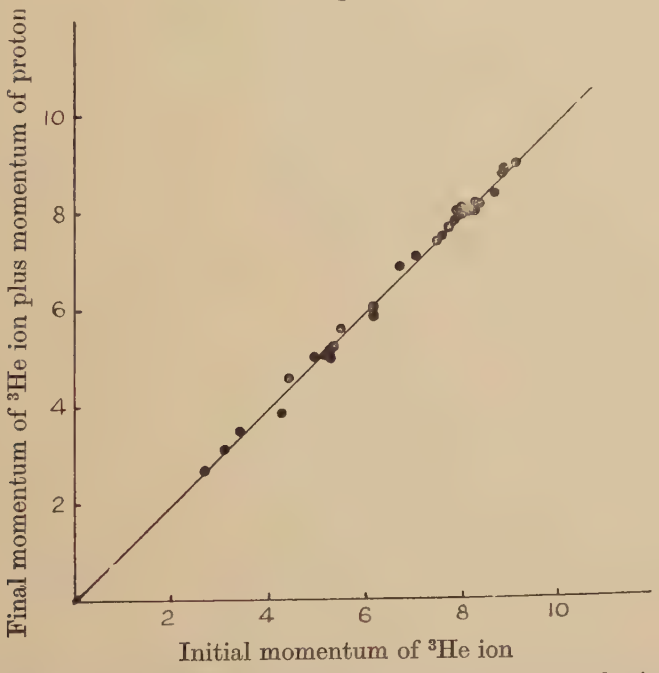

Momenta along the projected initial path of the ^{3}He ion on a horizontal plane. The abscissae represent momenta calculated from the initial energy and the ordinates represent momenta calculated from the energies and directions of particles after the collision. Deviations from the straight line show experimental errors. (§ 5.3.)

The average cross-section for collisions transferring over 1 MeV over the whole range is $0{\cdot}50 \pm 0{\cdot}2$ barns, which is about the geometrical cross-section to be expected. The purely Coulomb total cross-section corresponding to the collisions observed would be 0·02 barns.

A noticeable feature of these events is the rarity of low-energy proton tracks. Only three have less energy than 0·8 MeV (10 μ) although the plates were quite free from neutron recoils or other distracting features,

and tracks down to $3\,\mu$ (0·3 MeV) would be easy to see and should not often have been missed. Not too much weight can be attached to this observation as yet, however, since it is very difficult to devise an objective test to find the proportion of any kind of event which a particular observer will miss.

5.4. *Scattering of* ^{3}He *Ions by Carbon, Nitrogen and Oxygen.* (14 *events observed*)

See fig. 1 (*b*), (Plate 3). As was indicated at the end of § 3, this cannot always be distinguished from a reaction of the (^{3}He, α) type. In five of the events the secondary doubly-charged particle leaves the emulsion. The energies and momenta for seven more fit well the assumption that they represent elastic scattering of ^{3}He from one of the light nuclei, and the

Fig. 5

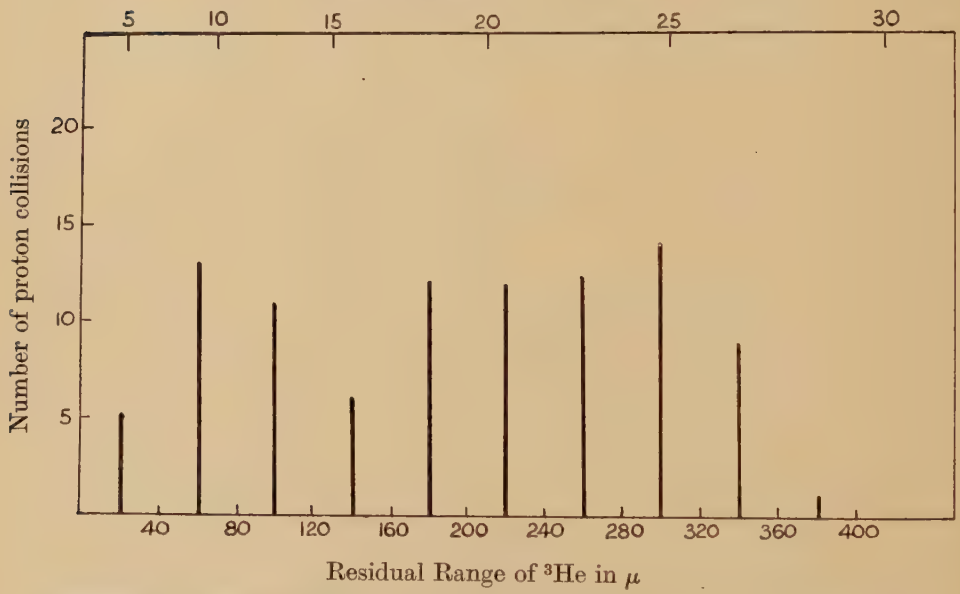

Histogram showing variation of cross-section for proton collisions with ^{3}He energy. (§ 5.3.)

results would be difficult to fit with the reaction $X^A(^3\mathrm{He}, \alpha)X^{A-1}$. The average cross-section for events of this appearance was found to be only $0{\cdot}08\pi R^2$, but recoil nuclei with less than about $\frac{1}{2}$ MeV would probably not be observed. The events would then be confused with the very common deflections from silver or bromine nuclei.

Of the two remaining events, one agrees excellently, both from energy and momentum considerations, with the reaction

$$^{12}\mathrm{C}\ (^3\mathrm{He}, \alpha)\ ^{11}\mathrm{C}\ .$$

The production of ^{11}C from carbon bombarded by ^{3}He has already been reported (Fremlin 1952).

The other does not give a reasonable momentum balance for any simple assumption and it is possible that one of the heavy nuclei was involved, a short-range (5 μ) α-particle having been mistaken for a heavier recoil nucleus.

In fig. 6 (5.4) is shown a distribution of numbers of events against ^{3}He particle range. There is no indication of any significant variation of cross-section with energy.

5.5. *Reactions giving One Singly-charged Particle*

5.5.1. *Heavy nuclei* (20 *events observed without visible recoil*).—An example is shown in fig. 1 (*c*), (Plate 3). The distribution of number of observed events with particle range, fig. 6 (5.5.1), shows only one case below 16·9 MeV and this is a special case, as will be seen below. The evidence is thus strong that in the rest of the cases the nuclei of silver and bromine are involved. (The Coulomb barrier height for bromine is 16 MeV for a doubly-charged particle.) Where the whole of the range occurs in the emulsion, the energy of the secondary particle could be determined for each assumption as to its identity. The fact that a heavy nucleus (silver or bromine) was involved is confirmed by the large amount of momentum missing without any visible recoil nucleus. The possible reactions, which might involve the emission of a singly-charged particle alone, are as follows :

Table 2

Target Nucleus	No. of nuclei per c.c. of emulsion	*Q*-value for type of reaction involved		
		(^{3}He, p)	(^{3}He, d)	(^{3}He, t)
^{79}Br	$0{\cdot}51 \times 10^{22}$	+8·6 MeV	+3·2 MeV	−1·1 MeV
^{81}Br	0·50 ,,	+8·9 ,,	+4·2 ,,	−0·8 ,,
^{107}Ag	0·53 ..	+7·3 ,,	+1·7 ,,	−2 ,,
^{109}Ag	0·50 ,,	+7·5 ,,	+1·8 ,,	−1 ,,

The last set of values are derived from the β-particle energies of the unstable product-nuclei, where these are known. In all other cases the values are obtained from the tables of empirical masses given by Metropolis and Reitweisner (1950). Comparison of mass differences in similar known cases suggests that these should not be in error by more than about 1 MeV.

In the majority of cases the grain density suggests that the secondary particle was a proton, and in the large majority of cases the amount of energy missing, whatever the secondary particle might have been, was so great that at least one neutron must have been emitted as well.

The cases in which there is no such evidence of neutron emission are shown in table 3 below.

Table 3

Event Number	Approx. energy of ^{3}He on impact MEV	Range of singly charged particle μ	Energy of singly charged particle			Energy of recoil nucleus MEV	Reaction giving best fit	Energy error MEV
			If p MEV	If d MEV	If t MEV			
34	17·7±0·5	972	13·9	**18·6**	22·0	0·7	Ag (^{3}He, d) Cd	0·1
49	21·4 ,,	850	12·9	17·2	**20·3**	0·1	^{79}Br (^{3}He, t) ^{79}Kr	0·1
166	21·3 ,,	766	12·1	16·2	**19·1**	0·3	^{107}Ag (^{3}He, t) ^{107}Cd	0
234	18·6 ,,	1410	17·1	**23·1**	27·6	0·02	^{81}Br (^{3}He, d) ^{82}Kr	0·3

Fig. 6

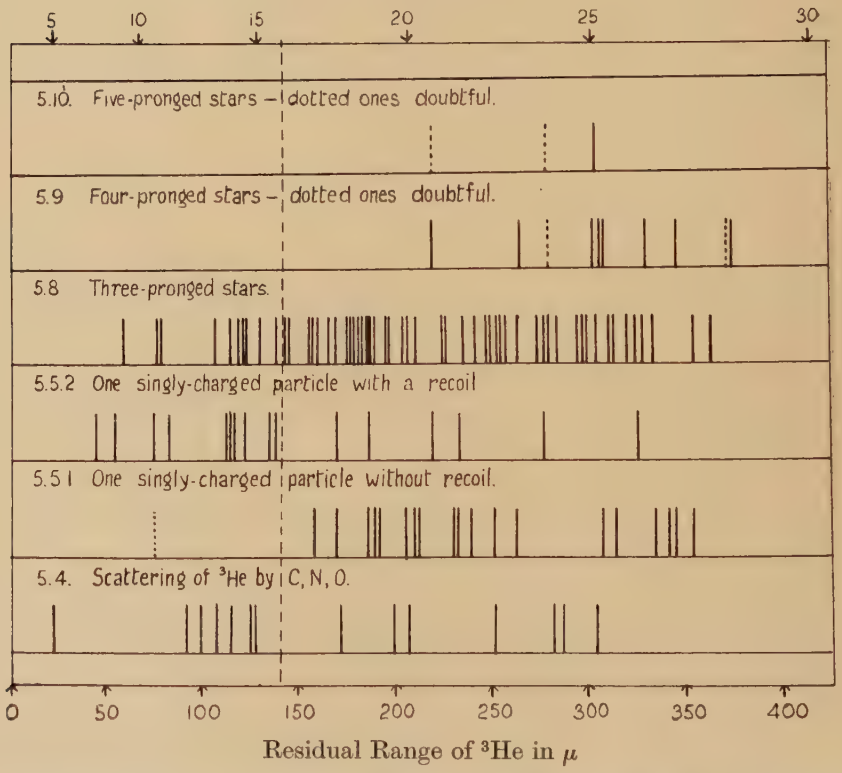

Distribution chart showing energies at which reactions occurred. This gives, very roughly, the apparent excitation functions for each of the different forms of event observed. (§ 5.4 to 5.10.)

The energy carried away by the heavy recoil nucleus is always small, but can be calculated from the momenta of the other particles for any reaction that may be assumed. It is seen that two reactions almost certainly represent deuteron production, and two triton production.

It will be noticed that in all four cases the energy of the secondary particle is quite close to that of the primary one. The mean range for these four cases is 997 μ. For the remaining eleven cases in which the secondary particle range ends in the emulsion the ranges are as follows :

522, 511, 459, 454, 438, 434, 420, 397, 344, 128, 96 μ.

There is a strong suggestion of a well-defined group, with mean range of $442 \pm 12\,\mu$. The mean energy of this group, if they are supposed to be protons, is 8·8 MeV$\pm$0·15. The mean energy of the initial ^{3}He ions is 24·1 MeV$\pm$0·6. The mean *velocities* are thus almost equal. This may of course be a coincidence, but it is a striking one. Inside the group there is no individual correlation between initial energy and secondary energy, although the total range of initial velocity is about equal to the range of secondary velocity. The initial energy of the two ^{3}He ions giving short-range particles are 18·9 and 16·9 MeV respectively.

The one event (No. 124) with initial energy 10·7 MeV, mentioned at the beginning of the section, may be explained by the fact that the secondary particle travels on a path which is amost a continuation of the original one. If it is a triton, it has almost exactly the initial momentum. Hence no momentum is available for the other nucleus involved and this will show no recoil even if it is one of the light group. It will be assumed that this is a correct explanation of this event, which will therefore be added to those of the next section.

5.5.2. *Light nuclei* (16 *events observed*).—These are distinguished from the events of 5.5.1 simply by the presence of a visible recoil track which would not be given by the heavier nuclei. They include, however, the single event No. 124 mentioned above for the reasons there indicated. The distribution with incident energy shown in fig. 6 shows reactions taking place with much lower energy than in 5.5.1, which is consistent with the interpretation. The possible reactions, neglecting isotopes less abundant in the emulsion than 0·2% of the ^{12}C abundance, are as follows :

Table 4

Target Nucleus	No. of nuclei per c.c. of emulsion	*Q* value for type of reaction involved		
		(^{3}He, p)	(^{3}He, d)	(^{3}He, t)
^{12}C	$1{\cdot}3\times10^{22}$	4·8 MeV	−3·55 MeV	−18 MeV
^{13}C	$0{\cdot}015\times10^{22}$	10·7 ,,	+2·0 ,,	−2·2 ,,
^{14}N	$0{\cdot}29\times10^{22}$	15·2 ,,	+1·9 ,,	(−2·8)
^{16}O	$1{\cdot}02\times10^{22}$	2·2 ,,	−4·9 ,,	(−16)

In these reactions we have more data as the range and direction of the residual nucleus can be observed. These data are not very accurate, however, as the range is usually 5 μ or less and the range–energy relations for these particles are not very precisely known.

As in the previous section there are several cases in which one or more neutrons must have been emitted besides the observed particles. In table 5 are shown the results of analysis of those events for which reasonably unambiguous results can be obtained.

Table 5

Event No.	Initial ^{3}He energy (Mev)	Energy of singly-charged particles			Recoil		Reaction giving best fit	Neutron energy (Mev)	Energy error (Mev)
		If p (Mev)	If d (Mev)	If t (Mev)	Range (μ)	Energy (Mev)			
45	18·7	7·1	9·3	10·9	6·5	10	^{14}N (^{3}He, d) ^{15}O	—	~1
49	15·6	6·9	9·1	10·7	3·3	2·0	^{16}O (^{3}He, d) ^{17}F	—	0·4
64	20·6	14·3	19·1	22·6	3·6	3·1	^{14}N (^{3}He, pn) ^{15}O	3·1±0·5	0
94	14·0	6·1	7·9	9·3	2·2	1·3	^{12}C (^{3}He, pn) ^{13}N	0·5±0·3	0
							or		
							^{16}O (^{3}He, p) ^{18}F	—	−8·8
124	10·7	6·3	8·3	9·6	0	0	^{13}C (^{3}He, t) ^{13}N		1·1
154	11·4	8·5	11·2	13·1	1·9	1·0	^{14}N (^{3}He, pn) ^{15}O	2·8±0·5	1·2±0·5
168	13·8	5·3	7·0	8·1	0·5	1·2	^{32}S (^{3}He, pn) ^{33}Cl	9·1±1	—
262	8·8	4·6	6·1	7·0	2·2	1·3	^{14}N (^{3}He, pn) ^{15}O	5·2±1	2½±1

The production of ^{13}N from carbon bombarded by ^{3}He ions has already been reported (Fremlin 1952).

It will be seen that two events may be attributed with some confidence to (^{3}He, d) reactions and one to a (^{3}He, t) reaction. In two cases, and perhaps a third, momentum considerations give an energy for an assumed neutron which agrees well with the possible reaction shown, and rule out conclusively any simpler reactions. In reaction 94, in which the neutron momentum would be small, a perfect momentum fit can also be obtained by postulating a heavier recoil nucleus, ^{18}F, in an excited state 8·8±0·6 Mev above the ground state, and it is not possible to determine which reaction is correct.

5.6. *Two-pronged Stars in which Both Prongs are Singly-charged.* (4 *events*)

None occur below 17·7 Mev initial energy. Three of these certainly represent the reaction (^{3}He, 2p) with heavy nuclei. In two cases, unfortunately, one of the long-range protons has left the emulsion.

From the empirical mass tables, the Q values for this reaction with silver or bromine are all between −1·3 and −0·2, while the first three apparent Q values are −2·0, $>+1$ and $>-5·5$ Mev. The only other reaction which needs to be considered is the simple dissociation (^{3}He, pd)

for which the Q is $-5{\cdot}5$ MeV. If the shorter range particle in each case were supposed to be a deuteron, the three observed Q values would be $-0{\cdot}3$, $>+4{\cdot}5$, $>-2{\cdot}7$, which rules out this reaction. The fourth gives an apparent Q for a (^{3}He, 2p) reaction of $-13{\cdot}4$ MeV, or for (^{3}He, pd) of $-12{\cdot}7$ MeV. Either, therefore, the final nucleus is left in a highly excited state or a neutron must have been liberated.

Reactions such as (^{3}He, 2d) or (^{3}He, pt) have very large negative Q values; none of these appear to fit this last case.

5.7. *Other Two-pronged Stars.* (5 *events observed*)

One of these occurs at 18·1 MeV, three more very close to 27 MeV initial energy. In each case there is a short-range track under 30 μ long, probably due to an α-particle, and a longer (80–700 μ) track due to a singly-charged particle. In each case, on any assumption, much energy and momentum is missing and they probably represent reactions of the form (^{3}He, αpn) with silver or bromine. The fifth has an initial energy of only 13·9 MeV and shows what may be a very short ($\frac{1}{2}\mu$) recoil. A good deal of momentum is missing, but hardly enough energy to allow for an additional neutron. It is easiest to suppose that one of the sulphur isotopes is involved, but one track emerges from the emulsion so that no comparison of observed with calculated Q values can be made.

5.8. *Three-pronged Stars.* (60 *events observed*)

An example is shown in fig. 1 (*d*), (Plate 4). Events of this form may represent a number of different types of reaction. In all but two cases a recoil nucleus heavier than an α-particle is observed, so that most, if not all, involve one of the lighter nuclei in the plate. This is also shown by the distribution shown in fig. 6 (5.8).

No events have been observed with an initial ^{3}He energy below $8{\cdot}8 \pm 1$ MeV, but above this energy there is no statistically significant variation in cross-section. This could not be the case if the high Coulomb barriers of the heavier nuclei were involved in any great number of cases.

It is not practicable to analyse in detail every one of the events for each possible interpretation in the same way as for the simpler reactions mentioned above. This is partly because of the large numbers and partly because, in many cases, at least one of the tracks beside the recoil is so short that it cannot be stated with certainty whether it is singly or doubly charged. Thus the number of possible reactions to be considered becomes very large. In every case in which tracks are long enough to be identified, at least one is singly charged.

5.8.1.—The commonest case, with 17 completely measurable events, appears to give rise to one singly and one doubly charged particle with a recoil nucleus. The Q values of the possible reactions are given below for the three commonest light nuclei in the emulsion.

In fig. 7 (5.8.1) are shown the apparent Q's of the 17 events. It can be seen that, to the accuracy expected, the whole of the events can be attributed to ^{12}C (^3He, αp) ^{10}B and ^{16}O (^3He, αp) ^{14}N, the final nucleus sometimes perhaps being excited, while at the most two could be attributed to ^{14}N (^3He, αd) ^{12}C. The lack of any observed case of ^{14}N (^3He, αp) ^{12}C $+8{\cdot}1$ MeV might be attributed to the very high probability of yet another heavy particle being emitted, with so large a liberation of energy.

Table 6

Initial Nucleus	Energy liberated (Q)	
	^3He, αp	^3He, αd
^{12}C	$-6{\cdot}8$	$-13{\cdot}1$
^{14}N	$+8{\cdot}1$	$-8{\cdot}4$
^{16}O	$-2{\cdot}4$	$-10{\cdot}7$

Half a dozen cases analysed in detail gave a satisfactory momentum balance. The two possible (^3He, αd) reactions were among the half dozen. In each the momentum balance was better on the assumption of the αp reaction, though in one case both reactions fitted within the limit of error.

5.8.2.—Fourteen completely measurable events gave rise each to two singly charged tracks besides the recoil. (Figure 1 (*e*), Plate 3.) In three cases these could with some confidence be ascribed to protons, but in most cases the mass could not be determined. As before, the Q values for the reasonably probable reactions with the three commonest light nuclei are given below, the product being assumed to be left in the ground state.

Table 7

Initial Nucleus	Energy liberated (Q) in MeV				
	(^3He, 2p)	^3He, pd	^3He, 2pn	^3He pt	^3He, 2d
^{12}C	$-2{\cdot}77$	$-5{\cdot}49$	$-7{\cdot}72$	$-17{\cdot}95$	$-21{\cdot}98$
^{14}N	$+3{\cdot}12$	$-5{\cdot}49$	$-7{\cdot}72$	$-9{\cdot}78$	$-13{\cdot}81$
^{16}O	$-3{\cdot}58$	$-5{\cdot}49$	$-7{\cdot}72$	$-14{\cdot}83$	$-18{\cdot}86$

In fig. 7 (5.8.2) are shown the apparent Q's. It can be seen that one group of three agrees well with the reaction ^{1}C (^3He, 2p) ^{13}C and three more could represent ^{16}O (^3He, 2p) ^{17}O, the ^{17}O being left either in the ground or in an excited state. These cases could, as far as the energy goes, be due to (^3He, dp). The remaining group, however, does not readily fit any of the reactions above. This can be explained on the supposition that

^{13}C is left in the 5·4 MeV excited state or ^{17}O in the 4·5 MeV excited state. The numbers involved are too small for the non-appearance of other excited states to be worth discussion in relation to their spins and parities.

5.8.3.—Seven three-pronged stars remain which do not fall into any of the cases dealt with in the last two sections. In four a high-energy ^{3}He ion gives rise to three short tracks, with a large energy and momentum

Fig. 7

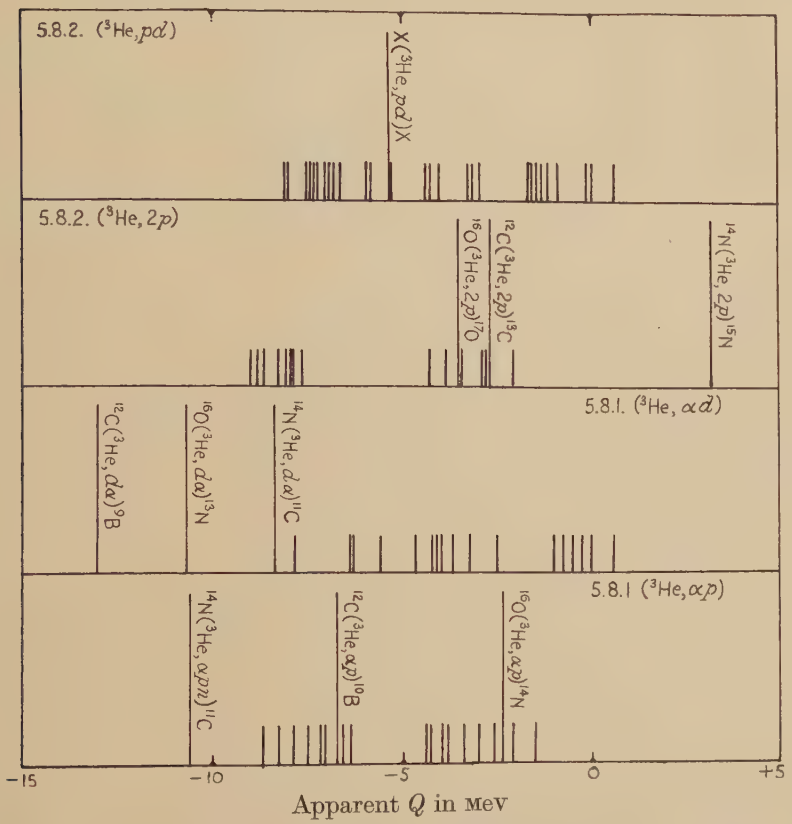

Apparent Q values for three-pronged stars. The values in the lower two charts are both taken from the same set of 17 analysable events treated in § 5.8.1, first on the assumption that the singly-charged particle is a proton and second that it is a deuteron.

The upper two charts are similarly calculated for the same set of 14 events treated in § 5.8.2. Each event gives two lines in the top diagram as either of the particles may be taken as a deuteron.

loss suggesting a reaction with silver or bromine, possibly involving the emission of one or more neutrons as well as the observed particles, most of which appear to be doubly charged though several are too short for this to be certain. In two more a high-energy primary gives rise in each case to two short tracks and one singly-charged track about 100 μ long. The same explanation would seem to hold. In the seventh, however, the

initial energy is only 11 MeV and there is little energy loss ; this might represent a reaction with a light nucleus giving itself too small a recoil for observation—for example ^{14}N (^3He, p2α) ^8Be or ^{14}N (^3He, α2p) ^{11}B. There is in fact a very large grain at the reaction centre which might represent this recoil.

The remainder of the three-pronged stars appear to be mostly (^3He, αp), with some (^3He, 2p), but have one or both long tracks leaving the emulsion and cannot usefully be examined.

5.9. *Four-pronged Stars.* (*8 events plus two doubtful.* See fig. 1 (*f*), Plate 4)

These again clearly belong to more than one type. Some show two long-range singly-charged particles, while in some not even one of the four secondary tracks is long enough to be sure of its charge. In two only there are short tracks which from their directions might be recoils, but in most there is no evidence of any. Indeed, after such a reaction with a light nucleus, little would be left to recoil. In fig. 6 (5.9) is shown the distribution of number as a function of energy. The fact that none has an initial energy below 21 MeV suggests strongly that the heavier nuclei in the plate are involved. Reactions of the form (^3He, 2p 2α), (^3He, p 3α) or (^3He, 4α) do not involve large negative Q values in either bromine or silver. The reaction (fig. 1 (*f*), Plate 4) shows two singly and two doubly charged tracks, and the energy loss agrees to 0·1 MeV with that calculated from the empirical mass tables for the reaction

$$^{107}Ag_{47}\ (^3He,\ 2p\ 2\alpha)\ ^{100}Tc_{43}—5{\cdot}8\ \text{MeV}.$$

The corresponding reaction with ^{109}Ag is also possible but no bromine reaction could be made to fit.

One more event appears to be the same, while one could be attributed to a similar bromine reaction. In one more so much energy is lost that at least one neutron must also have been liberated. The remaining four events cannot be analysed, as one or more tracks leave the emulsion almost at once. One of these, however, shows a distinct indication of a ' hammer ' track. If this were genuine it would be most interesting as the energy available is quite inadequate to give ^8Li or ^8B by any possible process. Unless further examples can be found, however, the chance of its being an alpha particle which suffers a large-angle deflection from carbon seems to be more likely.

5.10. *Five-pronged Stars.* (*One event plus two possible.* See fig. 1 (*g*), Plate 4)

In the event figured the initial energy of the ^3He was 25 MeV, and the combined energies of the other visible tracks, assuming the singly-charged particle to be a proton and the rest α-particles, was 26·5 MeV. The apparent Q is then about $+1{\cdot}5\pm1{\cdot}2$ MeV. According to the empirical tables, the most favourable heavy-nucleus reaction,

$$^{107}Ag_{47}\ (^3He,\ p\ 4\alpha)\ ^{93}Zr_{40},$$

would have a Q of $-4{\cdot}0$ MeV.

On the other hand the light nucleus reaction

$$^3\mathrm{He}+^{14}\mathrm{N}\rightarrow\mathrm{p}+4\alpha$$

gives a Q of $+0{\cdot}8$ MEV, well within the probable error limits. A detailed momentum analysis, assuming this reaction to be correct, is given in the caption to fig. 1 (*g*).

The momentum balance lies well within the probable error limits found in § 5.1, remembering that five secondary tracks had to be measured rather than two. The identity of the reaction may be regarded as established.

Two other events of this form may have been observed, but took place so close below the emulsion surface that some tracks left the emulsion after a few microns ; in each case one appeared to come straight out but was so short that its very existence was not certain, and analysis was not worth while.

§ 6. Discussion

The most striking general result, and one which does not depend in any way on interpretation, is the very large proportion of reactions showing the emission of more than one charged particle, with quite moderate bombarding energies. This is made more striking by the small proportion in which a neutron is emitted as well. Both effects may be regarded as consequences of the fact that ^{3}He, alone among stable compound nuclei, has itself an excess of protons over neutrons, and of the fact that it has a low binding energy.

It is interesting to compare the present results with those obtained by Gardner and Peterson (1949) for stars produced in emulsions by high energy deuterons, and by Gardner (1949) for stars produced by α-particles. Both with 35 MEV deuterons and with 50 MEV α-particles it was found that the majority of stars had three prongs. This is also the case for the ^{3}He results given above if we neglect those two-prong stars found to be due to scattering. In the Berkeley work, however, protons of more than 10 MEV might have been missed, which might reduce the apparent average number of prongs.

Owing to the probability of neutron emission no attempt was made to identify individual reactions as has been done in this paper. The average cross-section for all atoms of 0·08 barns found by Gardner for 50 MEV α-particles is rather smaller than most of those found in the present work, but this is not of great significance in view of the probable errors involved.

Though the detailed interpretation of the results is not always certain, there is good evidence for the occurrence of

(^{3}He, α), (^{3}He, n), (^{3}He, d,) (^{3}He, t), (^{3}He, 2p), (^{3}He, pn), (^{3}He, αp),

and fair evidence for

(^{3}He, 2 α2p), (^{3}He, αpn),

of which most are new reactions. The last two types are essentially similar to spallation reactions, as of course is the particular reaction in which a nitrogen nucleus is knocked to pieces.

We shall now examine the different mechanisms by which reactions can occur with ^{3}He nuclei up to 30 MeV.

(*a*) *Elastic scattering.* This may involve either Coulomb or nuclear force interactions. The excess of the scattering by hydrogen over the calculated Coulomb effect is of course due to specifically nuclear interactions. The smaller apparent cross-sections for scattering by carbon, nitrogen and oxygen, however, must not be taken seriously owing to the large risk of missing such events. The total cross-section for silver bromide can be seen from fig. 3 to agree well with pure Coulomb scattering for moderate deflections, as would be expected.

(*b*) *Compound nucleus formation.* In this type of interaction the initial ^{3}He energy is supposed to be distributed between all the nucleons. This is likely to represent the state of affairs only for heavy nuclei. Then the nuclear temperature is low, which would favour neutron evaporation, but the proton-excess of ^{3}He may result in competition from proton or alpha emission. It would still be expected in general that only one charged particle would be emitted, and it is difficult to see how such reactions as (^{3}He, 2p, 2α) could occur with the high Coulomb barriers involved, but as indicated in § 5.9 it is also difficult to explain some of the four-pronged stars on the basis of the lighter nuclei. It is just possible that ^{32}S is the nucleus concerned, but the energies do not fit very well and the concentration of sulphur is low. An independent method of investigation is badly needed here.

(*c*) ' *Stripping* ' *type reactions.* Reactions of this type are now familiar in deuteron bombardments. In the case of ^{3}He one or more nucleons of the incident particle may be absorbed into the bombarded nucleus without the necessity for complete penetration. This leads to a ' stripped ' particle and an excited residual nucleus, which may have sufficient energy to emit a further heavy particle by the evaporation process. Such reactions as the (^{3}He, αp) type might similarly be looked at as a combination of a splitting of the ^{3}He nucleus followed by one of the well-known forms of reaction, in this case the (d, α) reaction.

The best evidence for these ' stripping ' reactions is probably that given in § 5.5.1, where the reactions (^{3}He, d) and (^{3}He, pn) with heavy nuclei are shown often to give secondary particles with very nearly the same velocity as the original ^{3}He. It is possibly significant that of the nine events described which show secondary proton-velocities near to the original ^{3}He velocities, six show the proton moving within 40° of the original direction of the ^{3}He ion, and only one over 90° from the original direction. There is, however, a much increased chance of emerging from the emulsion of the particles leaving at large angles to the initial direction, when the events will evade analysis. It is for this reason also that in most kinds of reaction no mention has been made of angular distribution.

Further investigations of the energy- and angular-distributions seem highly desirable, to distinguish between compound nucleus and ' stripping ' reactions. Such an investigation of the (^{3}He, 2p) reaction would be particularly interesting as, if this represents the stripping off of a neutron, some evidence might be obtained of the initial state of interaction of the two protons.

(*d*) *Reactions with light nuclei.* In these there is probably little true compound-nucleus formation due to the large energy per nucleon involved, and no thermal equilibrium could be expected before any particles escaped. ' Stripping ' reactions may again be important, often followed by the decay of a very short-lived compound nucleus in a very wide particle-unstable state. Thus, in events of the type (^{3}He, αp), treated in § 5.8.1, there is some evidence that the proton is emitted first ; of 19 cases 17 showed a proton energy above that required to surmount the Coulomb barrier, while in the same 19 cases ten alpha-particle energies were well below the necessary value, several being between $2\frac{1}{2}$ and 3 Mev. No obvious proton energy-groups were observed, but it is reasonable to expect a larger spread of energy and angle of the escaping particle after a ' stripping ' reaction with a small nucleus. The light nuclei were responsible for the great majority of the stars observed, as would be expected from their low barriers, which are of greater importance in controlling the escape of secondary particles than in preventing the initial ^{3}He approach to the nuclear surface.

(*e*) (^{3}He, t) *reactions.* These can occur by an evaporation process from a heavy nucleus but there is also the possibility of a charge-exchange with the target nucleus. This may be more likely in the case of the emission of tritons of energy around 20 Mev, examples of which are observed.

It is hoped in future experiments to extract the initial beam to a sufficient distance from the cyclotron to enable reasonably well screened electron-sensitive plates to be used. A good deal of useful information about unstable product-nuclei might then be obtained, by observing the emission of β-particles and, for the heavier nuclei, of conversion electrons whose ranges might enable the actual levels of excitation involved to be found.

Acknowledgments

The author wishes to express particular appreciation of the help of Mrs. E. Munday, who not only found and measured nearly all of the events described and did the processing of the plates, but also made a number of useful practical suggestions in both fields. The large amount of numerical work involved was only made possible by Mrs. Reinet Fremlin, who constructed properly smoothed range-energy tables with 1μ intervals, based on Rotblat's experimental results, for all of the particles which were or might be involved.

It is a pleasure also to thank Professor P. B. Moon for his advice and help and for making the necessary facilities available, Professor W. E. Burcham for many useful discussions, and Mr. W. Hardy for his help with the cyclotron bombardments.

References

Fremlin, J. H., 1952, *Proc. Phys. Soc.* A, **65,** 762.
Gardner, E., 1949, *Phys. Rev.*, **75,** 379.
Gardner, E., and Peterson, V., 1949, *Phys. Rev.*, **75,** 364.
Lukirsky, P. I., Mescheryakov, M. E., and Khrenina, T. I., 1947, *C. R. Acad. Sci., U.R.S.S.*, **55,** 117.
Metropolis, N., and Reitweisner, G., 1950, *U.S. Atomic Energy Commission Report*, N.P. 1980.
Rotblat, J., Catala, J., and Gibson, W. M., 1951, *Nature, Lond.*, **167,** 550.
Wilkins, J. J., 1951, *A.E.R.E. Report* G/R 664.

XVII. *Commutation Relations in Lagrangian Quantum Mechanics*

By W. K. Burton and B. F. Touschek
Department of Natural Philosophy, University of Glasgow*

[Received September 29, 1952]

Abstract

Schwinger's method for deriving commutation relations is shown to fail in the case of first order equations of motion. A new method, adapted from some recent work of Peierls is discussed in connection with two examples of first order equations in point mechanics.

§1. Introduction

In a recent paper Schwinger (1951) has presented a comprehensive scheme of Lagrangian field dynamics, in which the commutation relations of the field variables are deducible from a variation principle together with a postulate of time symmetry. Translating Schwinger's method into point mechanics his published results are that the canonical commutation rules are

$$[q_r p_s]_{\mp} = i\delta_{rs}, \qquad (1)$$

where the minus sign applies to a scalar Lagrangian and the plus sign to a pseudoscalar Lagrangian under the transformation $t \to -t$. In the present paper we want to discuss two examples, both representing systems which correspond classically to a harmonic oscillator for which an uncritical application of eqn. (1) leads to a contradiction. It will be shown that the quantized equations of motion derived from the variation principle differ from those obtained by evaluating by means of (1) the time derivatives as commutators with the energy operator H. It will further be shown that the argument leading to (1) breaks down when the equations of motion are of the first order.

In §2 we shall give a brief account of Schwinger's method; §3 contains a discussion of two examples for which a straightforward application of Schwinger's method is impossible. Both examples lead to the same equations of motion but to different commutation relations owing to different Lagrangians. A method based on recent work of Peierls (1952) enables us to find the commutation rules for these two examples. The correct commutation relations derived by this method differ from eqn. (1) by the occurrence of a factor $\frac{1}{2}$ on the right-hand side. The general theory will be developed in §4, its application to the two examples in §5. Finally a general class of first order Lagrangians admitting an explicit determination of the canonical commutation relations is studied in §6.

* Communicated by the Authors.

§ 2.

The basic quantity in Schwinger's formulation of quantum theory is the transition amplitude

$$(a't_1 \mid a''t_2), \qquad \ldots\ldots\ldots \quad (2)$$

the square of whose modulus gives the probability of finding the system in a state specified by the eigenvalues a' of a complete commuting set of operators a at the time t_1 provided that the system has been found in the state specified by a'' at the previous time t_2. A linear unitary transformation U leads from the set of operators a to a new set $\bar{a}=UaU^{-1}$, the eigenstates of which are $\bar{\psi}(a')=U\psi(a')$.

Infinitesimal changes in the results of measurements carried out at times t_1 and t_2 may be brought about in two ways: (i) by a change of the measuring apparatus, which corresponds to infinitesimal unitary transformations of the operators a at times t_1 and t_2 and (ii) by a change of the parameters of the system. Both types of change are expressed by infinitesimal variations $\delta(a't_1 \mid a''t_2)$ of the transition amplitude (2). The variation $\delta(a't_1 \mid a''t_2)$ represents an antihermitian matrix $i\delta W_{12}$ for which the composition law of unitary transformations gives

$$\delta W_{13}=\delta W_{12}+\delta W_{23}.$$

Putting

$$\delta(a't_1 \mid a''t_2)=i(a't_1 \mid \delta W_{12} \mid a''t_2)=i(a't_1 \mid \delta \int_{t_2}^{t_1} L\,dt \mid a''t_2), \quad \ldots \quad (3)$$

where L is a function of the coordinates of the system and their derivatives $L=L[q]$ we find that (3) expresses the quantum analogue of Hamilton's principle. For, by integrating L over the time interval t_1t_2 we find that δW_{12} must be of the form

$$\delta W_{12}=F(t_1)-F(t_2), \qquad \ldots\ldots\ldots \quad (4)$$

provided that the parameters of the system are not altered. In (4) $F(t_1)$ and $F(t_2)$ only contain operators defined at the times t_1 and t_2 respectively. They are Hermitian and induce the transformation

$$\delta(a't_1 \mid = i(a't_1 \mid F(t_1) \qquad \delta \mid a''t_2)=-iF(t_2) \mid a''t_2), \quad \ldots \quad (5)$$

in the eigenfunctions $(a't_1 \mid$ and $\mid a''t_2)$. Equation (4) with the subsequent interpretation of the F is the quantum analogue of Hamilton's principle. The operator transformation corresponding to (5) is

$$a-\bar{a}=\delta a(t_i)=i[F(t_i)a(t_i)]_-; \qquad i=1, 2. \quad \ldots\ldots \quad (6)$$

The commutation relations are now obtained in the following manner. Consider a change δq of the coordinates of the system at times t_1 and t_2. This change will induce a corresponding change $\delta W_{12}=p_s\delta q_s$ (summation convention) in the action integral, the functions p being completely defined if the commutation properties of the δq_s with all the other variables are known. If one chooses $\delta q(t_2)=0$ then from (6)

$$\delta q_r=i[p_s\delta q_s, q_r]_-; \qquad 0=i[p_s\delta q_s, p_r]_-. \quad \ldots\ldots \quad (7)$$

Provided the variations involved in (7) are independent and $\neq 0$ the

commutation relations for p, q and p, p respectively can be obtained by comparing coefficients of the δq_s on both sides of (7). (The remaining q, q-commutation rules are obtained by considering variation of p.) This can only be done by bringing all the δq_s to one side, say the right of eqn. (7). This again involves the commutation properties of the δq. These are obtained from a consideration of the time symmetry of the Lagrangian. Schwinger's result is that if the Lagrangian is a scalar under time reflection the δq should commute with all the q and if the Lagrangian is pseudoscalar the δq should anticommute. In this manner one obtains from eqn. (7)

$$\pm i[p_s q_r]_{\mp}\delta q_s=\delta q_r, \quad . \quad . \quad . \quad . \quad . \quad . \quad . \quad . \quad (8)$$

according to whether the Lagrangian is a scalar or a pseudoscalar. (8) reduces to (1) if the δq are independent.

§ 3.

In this section we shall discuss two examples taken from particle mechanics. Let us consider the two Lagrangians

$$L_s=iq_s\beta_{sr}\dot{q}_r+\omega q_r q_r=iq\beta\dot{q}+\omega qq, \quad . \quad . \quad . \quad . \quad . \quad . \quad (9)$$

and

$$L_p=iq\dot{q}+\omega q\beta q. \quad . \quad . \quad . \quad . \quad . \quad . \quad . \quad . \quad (10)$$

q is a vector with two Hermitian components, ω a real parameter and β a 2×2 Hermitian matrix with the properties

$$\beta^2=1\,; \qquad \beta^T=-\beta. \quad . \quad . \quad . \quad . \quad . \quad . \quad . \quad (11)$$

Both Lagrangians lead to the same equation of motion, namely

$$i\dot{q}+\omega\beta q=0. \quad . \quad . \quad . \quad . \quad . \quad . \quad . \quad . \quad (12)$$

These equations of motion are invariant under time reflection, if $t\rightarrow -t$ induces

$$q\rightarrow \bar{q}=\alpha q, \qquad \alpha^2=1, \qquad \beta\alpha+\alpha\beta=0. \quad . \quad . \quad . \quad . \quad . \quad (13)$$

The second of these equations follows from $t\rightarrow -t$ being an involution. We see that under the transformation (13)

$$L_s\rightarrow -iq\alpha^T\beta\alpha\dot{q}+\omega q\alpha^T\alpha q=L_s,$$
$$L_p\rightarrow -iq\alpha^T\alpha\dot{q}+\omega q\alpha^T\beta\alpha q=-L_p$$

if $\alpha^T\alpha=1$. That this is indeed the case follows from the fact that only one of the Pauli spin matrices, namely β, can be antisymmetric: the others are symmetric.

At this stage it is perhaps worth stressing that these examples demonstrate that the statistics are not so much determined by the equations of motion, as by the Lagrangian from which they are derived. For according to Schwinger we should expect Bose statistics for the Lagrangian (9) and Fermi statistics for (10). Yet both lead to the same equation of motion. The field theoretical generalization of (10) leads to Majorana's (1937) neutrino theory. There is no generalization of (9) leading to

Dirac's equations; the reason for this is to be found in the transposition properties of the Dirac γ-matrices.

In the following we shall restrict our attention to the case (10), quoting only the final results for the case (9).

To apply Schwinger's formalism we start from the variation of the action integral, which in the pseudoscalar case gives

$$\delta W_{12}=\int_{t_2}^{t_1}\{\delta q(i\dot{q}+\omega\beta q)+(-i\dot{q}+\omega\beta^T)\delta q\}\,dt+[iq\delta q+L\delta t]_{t_2}^{t_1}. \quad (14)$$

We see that the condition $\beta^T=-\beta$ ensures that the right and left factors of δq differ only in sign, permitting the use of the condition $[q_r\delta q_s]_+=0$. The use of (7), with $F(t_1)=iq(t_1)\delta q(t_1)$ then gives

$$[q_rq_s]_+=\delta_{rs}, \quad (15)$$

provided that $\delta q(t_2)=0$ does not imply $\delta q(t_1)=0$. In fact the derivation of (15) fails just at this point, since $F(t_1)\equiv F(t_2)$, because the general solution of our two component equations of motion involves only two arbitrary constants, the equation being only of the first order. For equations of higher order than the first this difficulty would not occur. The analogue of (15) for the case (9) is

$$[q_sq_t]=\beta_{st}. \quad (16)$$

The use of (15) and (16) leads to a contradiction. If for example in case (10) we put $\delta q(t_2)=\delta t_2=0$, $\delta q(t_1)=-\dot{q}(t_1)\delta t_1$ then

$$-\dot{q}(t_1)\delta t_1=i[\delta_{t_1}W_{12}, q]_-, \quad (17)$$

where δ_{t_1} denotes changes induced by a translation δt_1 along the trajectory and

$$\delta_{t_1}W_{12}=-H\delta t_1=\omega q\beta q\delta t_1, \quad (18)$$

which because of (15) yields

$$\dot{q}+2\omega\beta q=0, \quad (19)$$

in contrast to eqn. (12).

§ 4.

In view of the difficulty encountered in applying Schwinger's method to the two examples discussed in the previous section, we conclude that it is necessary to consider a more general variation of the action integral than we have hitherto employed.

For the purpose of defining his covariant bracket expressions in classical relativistic field dynamics Peierls (1952) has introduced a variation which appears to be suitable for the purpose of deriving commutation relations in the Lagrangian formalism. The Peierls brackets reduce to the Poisson brackets whenever the latter are applicable. Peierls uses them to derive covariant commutation rules in quantum field theory by an extension of the usual method based on the correspondence principle. The same goal can be achieved immediately in the context of Schwinger's theory. The canonical commutation rules obtained in

this way for the two examples (9) and (10) are consistent with the rest of the formalism.

Consider the effect on the transition amplitude of changing L into

$$L'=L+\delta(t-t_0)\lambda_s q_s, \qquad (20)$$

where the additional term is Hermitian and is of the same parity as L under time reflections. The additional term may be symmetrized in the scalar case and antisymmetrized in the pseudoscalar case; thus

$$L'=L+\tfrac{1}{2}\delta(t-t_0)(\lambda_s q_s \pm q_s \lambda_s). \qquad (21)$$

We shall consider the λ_s as small variations of some dynamical quantity, so that Schwinger's identity rule (stating the equality of terms differing only in the position of variants) can be applied. This rule will certainly be satisfied if

$$[\lambda_s q_t]_{\mp}=0, \qquad (22)$$

the minus and plus signs applying to the scalar and pseudoscalar case respectively. A physical interpretation of the λ can be given by considering them as functions of the coordinates Q of a second system coupled instantaneously to the first at the time $t=t_0$. For instance in the case of the example (10) discussed in the previous section we could choose

$$\lambda_s=\epsilon Q_t \beta_{ts},$$

with ϵ an infinitesimal parameter. Instead of (21) we should then start from the Lagrangian

$$L'[q,\ \lambda(Q)]+L[Q],$$

in which for example $L[Q]$ is of the same analytical form as $L[q]$, but with different parameters.

If we now consider the λ as infinitesimal operators Schwinger's basic dynamical principle (*loc. cit.* (2.14)) gives

$$\begin{aligned}\delta(a't_1 \mid a''t_2)&=i(a't_1 \mid \lambda_s q_s(t_0) \mid a''t_2) \text{ for } t_1<t_0<t_2\\ &=0 \text{ otherwise.}\end{aligned} \qquad (23)$$

This equation may be interpreted in two ways: the change in the transition amplitude $(a't_1 \mid a''t_2)$ may be brought about by an infinitesimal transformation on the variables at $t=t_1$, or by an infinitesimal transformation at t_2. Since $\delta W_{12}=F(t_1)-F(t_2)$, where the F are the infinitesimal generators of the variations at t_1 and t_2 respectively, we have $F(t_1)=\delta W_{12}$ in the first case and $F(t_2)=-\delta W_{12}$ in the second. The two interpretations give rise to retarded and advanced variations of the q's, namely

$$\begin{aligned}\overset{R}{\delta} q_r(t)&=i[\lambda_s q_s(t_0)\,;\ q_r(t)]_- \text{ for } t>t_0\\ &=0 \text{ otherwise,}\end{aligned} \qquad (24)$$

if $F(t_2)=0$ and

$$\begin{aligned}\overset{A}{\delta} q_r(t)&=-i[\lambda_s q_s(t_0)\,;\ q_r(t)]_- \text{ for } t<t_0\\ &=0 \text{ otherwise,}\end{aligned} \qquad (25)$$

if $F(t_1)=0$. The indices R and A indicate 'retarded' and 'advanced' respectively.

Equations (24) and (25) present relations between the δq and the λ involving the commutation properties of the variables q. We now proceed to determine the δq as functions of λ from the equations of motion. Comparing the resulting eqns. (30) with (25) and (24) will then lead to the covariant commutation relations.

Let $q'(t)$ be a solution of the equations of motion resulting from the variation of the modified Lagrangian (21). In particular let us call $\overset{R}{q'}(t)$ that solution which coincides with $q(t)$ for $t<t_0$, and $\overset{A}{q'}(t)$ the solution which coincides with $q(t)$ for $t>t_0$. Considering the perturbation term occurring in (21) as infinitesimal, we may write

$$\overset{R,A}{q'}(t)=q(t)-\delta^{R,A}q(t). \quad . \quad . \quad . \quad . \quad . \quad . \quad . \quad . \quad (26)$$

Denoting by $L_r[q]$ the functional derivative of $\int L\,dt$ with respect to q_r, we may write for the equations of motion

$$L_r[q]=0\,; \qquad L_r[q']+\lambda_r\delta(t-t_0)=0. \quad . \quad . \quad . \quad . \quad (27)$$

The definition of $L_r[q]$ is: $\delta\int L\,dt=\int L_r[q]\delta q_r\,dt$, where the δq_r are taken to the right using the commutation properties of the δq. The difference between the two eqns. (26) and (27) gives a differential equation which is linear in δq. Putting

$$L_r[q-\delta q]=L_r[q]-F_{rs}\delta q_s, \quad . \quad . \quad . \quad . \quad . \quad . \quad . \quad (28)$$

where F_{rs} is a function of the q and the operators d/dt, we may write for this linear equation

$$F_{rs}\delta q_s-\lambda_r\delta(t-t_0)=0. \quad . \quad . \quad . \quad . \quad . \quad . \quad . \quad . \quad (29)$$

The advanced and retarded solutions of (29) can be written

$$\left.\begin{aligned}\delta^R q_s&=-G^R_{st}\lambda_t\\ \delta^A q_s&=-G^A_{st}\lambda_t\end{aligned}\right\} \text{ where } \begin{cases}G^R_{st}(tt_0)=0 \text{ for } t<t_0\\ G^A_{st}(tt_0)=0 \text{ for } t>t_0\end{cases} \quad . \quad . \quad (30)$$

The G satisfy the equation

$$F_{rs}G^{R,A}_{st}+\delta_{rt}\delta(t-t_0)=0. \quad . \quad . \quad . \quad . \quad . \quad . \quad . \quad (31)$$

Comparing these results with eqns. (24) and (25) we obtain

$$\begin{aligned}&[\lambda_t q_t(t_0)\,;\ q_s(t)]_-=iG^R_{st}(tt_0)\lambda_t \text{ for } t>t_0,\\ &[\lambda_t q_t(t_0)\,;\ q_s(t)]_-=-iG^A_{st}(tt_0)\lambda_t \text{ for } t<t_0, \quad . \quad . \quad . \quad . \quad . \quad (32)\end{aligned}$$

which because of (14) leads to the covariant commutation relations

$$[q_t(t_0)q_s(t)]_{\mp}=iG_{st} \text{ for } t\neq t_0, \quad . \quad . \quad . \quad . \quad . \quad . \quad . \quad (33)$$

where

$$G_{st}(tt_0)=G^R_{st}-G^A_{st} \quad . \quad . \quad . \quad . \quad . \quad . \quad . \quad . \quad (34)$$

is a solution of $F_{rs}G_{st}=0$. An elementary continuity argument shows that (33) hold also for $t=t_0$. In the derivation of (34) we have made use of the commutation or anticommutation of $\lambda(t_0)$ with $q(t)$, whereas (22) only involves $q(t_0)$. To derive the stronger result $[\lambda(t_0)q(t)]$ for all t

we may assume that the parameters in the Q-system can be chosen in such a way that its total energy may be made arbitrarily small.

The solutions of eqn. (31) are not in general c-numbers, and a general solution of this equation appears hard to obtain even for the limit $t=t_0\pm 0$.

§ 5.

In this section we shall determine the commutation relations for the two examples discussed in §3. We introduce D for the operator d/dt. For L we obtain by using the commutation relations for the δq

$$L_r[q]=(2(i\beta D+\omega)q)_r, \quad \ldots\ldots\ldots \quad (35)$$

for the Lagrangian (9) and

$$L_r[q]=-(2(iD+\omega\beta)q)_r, \quad \ldots\ldots\ldots \quad (36)$$

for the Lagrangian (10). Hence the operators F_{rs} defined in eqn. (28) are

$$F=2(i\beta D+\omega); \qquad F=-2(iD+\omega\beta), \quad \ldots\ldots \quad (37)$$

respectively. From eqn. (31) we now obtain

$$(i\beta D+\omega)G^{R,A}+\tfrac{1}{2}\delta(t-t_0)=0, \quad \ldots\ldots\ldots \quad (38)$$

$$-(iD+\omega\beta)G^{RA}+\tfrac{1}{2}\delta(t-t_0)=0. \quad \ldots\ldots\ldots \quad (39)$$

The canonical commutation relations are obtained by considering the case $t\to t_0\pm 0$. For by integrating the eqns. (38), (39) from t_0-0 to t_0+0 we have

$$\lim_{t\to t_0+0} G^R=\frac{i}{2}\beta \qquad \lim_{t\to t_0-0} G^A=-\frac{i}{2}\beta, \quad \ldots\ldots \quad (40)$$

and

$$\lim_{t\to t_0+0} G^R=-\frac{i}{2}; \qquad \lim_{t\to t_0-0} G^A=+\frac{i}{2}, \quad \ldots\ldots \quad (41)$$

therefore $G=\frac{1}{2}i\beta$ or $G=-\frac{1}{2}i$ respectively. Using eqn. (33) we find

$$[q_s q_t]_-=\tfrac{1}{2}\beta_{st}, \quad \ldots\ldots\ldots \quad (42)$$

$$[q_s q_t]_+=\tfrac{1}{2}\delta_{st}, \quad \ldots\ldots\ldots \quad (43)$$

and these are the correct commutation relations; the contradiction mentioned in §3 now no longer occurs.

The explicit form of G is determined from

$$(D^2+\omega^2)G=0, \quad \ldots\ldots\ldots \quad (44)$$

obtained by iteration. Its general solution is

$$G=A\cos\omega t+B\sin\omega t, \quad \ldots\ldots\ldots \quad (45)$$

where $\tau=t-t_0$. (40) and (41) now show that

$$B=i\beta A, \quad \ldots\ldots\ldots \quad (46)$$

and therefore

$$G=\frac{i}{2}\beta\cos\omega\tau-\tfrac{1}{2}\sin\omega\tau=\frac{i\beta}{2}\exp(i\beta\omega\tau), \quad \ldots \quad (47)$$

$$G=-\frac{i}{2}\cos\omega\tau+\tfrac{1}{2}\beta\sin\omega\tau=-\frac{i}{2}\exp(i\beta\omega\tau). \quad \ldots \quad (48)$$

§6.

Finally we shall discuss a more general class of Lagrangians, to which the two previous examples belong and for which the canonical commutation relations can be obtained without the detour over the covariant formalism. Consider the Lagrangian

$$L=p^{(s)}(q)\dot{q}+h(q), \qquad (49)$$

in which the p's and h are functions of the coordinates and h is Hermitian. In addition we require the p to satisfy the relations

$$p_r{}^{(s)}=\mp p_s{}^{(r)}, \qquad (50)$$

the two signs referring to the scalar and pseudoscalar cases respectively. The $p_r{}^{(s)}$ are defined by $\delta p^{(s)}=p_r{}^{(s)}\delta q_r$ in which are involved the commutation properties of the δq with the q's. Now

$$L_s'[q']-L_s[q]=\lambda_s\delta(t-t_0)-\dot{p}'^{(s)}+\dot{p}^{(s)}\pm p_s{}'^{(r)}\dot{q}_r' \mp p_s{}^{(r)}\dot{q}_r+h_s'-h_s=0. \qquad (51)$$

Integrating over t from t_0-0 to t_0+0 we obtain by using (50)

$$(p-p')^R=\delta p_s{}^R=-\lambda_s/2. \qquad (52)$$

On the other hand

$$\delta p_s{}^R=i[\lambda_r q_r;\ p_s]=i[q_r p_s]_{\mp}\lambda_r, \qquad (53)$$

in the limit $t=t_0\pm 0$. Comparing this with (52) we obtain at once

$$[q_r p_s]_{\mp}=\frac{i}{2}\delta_{rs}. \qquad (54)$$

In the case of the two examples (54) reduces to (42) and (43) respectively.

References

Majorana, E., 1937, *Nuovo Cimento*, **14**, 171.
Peierls, R., 1952, *Proc. Roy. Soc.* A, **214**, 143.
Schwinger, J., 1951, *Phys. Rev.*, **82**, 914.

XVIII. *On the Polarization of High Energy Bremsstrahlung*

By K. Phillips
Metropolitan-Vickers Electrical Co. Ltd., Manchester *

[Received November 10, 1952]

Summary

An attempt has been made to determine whether the bremsstrahlung from a 20 Mev betatron is polarized. The experiment consists essentially of measuring the angular distribution, with respect to the plane of emission of the photons, of photo-protons produced in the photodisintegration of the deuteron. The distribution instead of being purely symmetrical, as would be expected for unpolarized bremsstrahlung, indicates some asymmetry.

§ 1. Introduction

Most investigators using high energy bremsstrahlung tacitly assume that the radiation is unpolarized. This is likely to be of importance in such angular distribution experiments where small effects are measured—for instance the photodisintegration of the deuteron where attempts are made to measure isotropic terms of the order of 0·05. If the incident radiation is polarized a true comparison with present theories will not be valid as the latter are based on purely unpolarized radiation.

From the mechanism of induction acceleration of electrons one might be tempted to believe that the initial beam of electrons is polarized after travelling several hundred kilometers in a magnetic field of maximum value of 3000 gauss. Another possible source of polarization arises in the actual bremsstrahlung process itself, even if the initial beam of electrons is unpolarized. This process has been investigated theoretically in a recent note by May and Wick (1951), and more recently in a longer paper by May (1951). The first publication examines the possibility of polarized bremsstrahlung being emitted from high energy electron accelerators. The polarized photons would have an optimum angle of emission of $\theta=mc^2/E_0$. E_0 being the energy of the incident electron (fig. 1).

The authors consider the bremsstrahlung cross section to be made up of two components, $d\sigma_{\parallel}$ and $d\sigma_{\perp}$, which are defined as the cross section for photons polarized parallel and perpendicular to the plane of emission, i.e. the plane containing the direction of the incident electron and the outgoing photon (plane of OAB, fig. 1). It turns out that the direction of the electric vector tends to lie perpendicular rather than parallel to the plane of emission. The calculations indicate for photon energies equal to half the initial electron energy it is possible to have a ratio

* Communicated by the Author.

of 5 : 1 for the perpendicular to the parallel cross sections. May's later paper gives the results of more detailed examination of the problem, but only for values of $E_0 \gg 137Z^{-1/3}mc^2$. The effect of multiple scattering of the electrons in the target is also considered. From the well-known multiple scattering formula of Williams (1939) for small angles it is easy to show that after passing through a 5 mil. tungsten target the electrons are scattered through an angle of many times that of the optimum polarization. This 'small angle' scattering will obviously have a reducing effect on the detectable polarization, and May finds that for 300 MeV electrons that the percentage polarization is reduced to only a few per cent in some cases.

Fig. 1

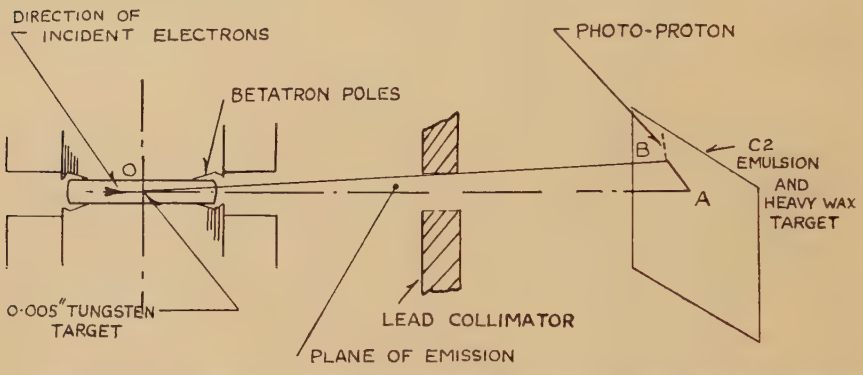

A schematic diagram of the experimental layout. OAB is the plane of emission and OA the direction of the accelerated electrons before striking the tungsten target. OB is the direction of a photon.

§ 2. Experimental Methods

The obvious method to use for the detection of the polarization of high energy bremsstrahlung is by studying the reciprocal process of pair production. This has been treated theoretically by May who concludes that the plane containing the pair and direction of the polarized photon tends to lie parallel to the plane of polarization except for one limiting case. In studying the pair production process one would inevitably use a Wilson cloud chamber with stereoscopic photography. Although a working expansion chamber with accurate stereoscopic cameras was available in the laboratory, other methods were considered as this experiment was likely to be long and tedious. Counting techniques for the detection of the pairs are almost ruled out by the large background in the betatron enclosure.

One of the usual methods of detecting lower energy polarization of x-rays is by measuring the angular distribution of photo-electrons (Kirkpatrick 1931). For the present work it was decided to use the corresponding photo-nuclear disintegration of the deuteron. This method has been used recently by Wilkinson (1952) to investigate the polarization of 5·5 MeV gamma rays in the $^2H(p, \gamma)^3He$ reaction. This author

measured the angular distribution of some 120 photo-protons produced in an Ilford C2 emulsion soaked in heavy water. This technique however presents certain difficulties when used with a continuous x-ray spectrum owing to the large proton background produced in the emulsion. This has been avoided here by using a thin heavy wax target as the source of photo-protons.

Fig. 2

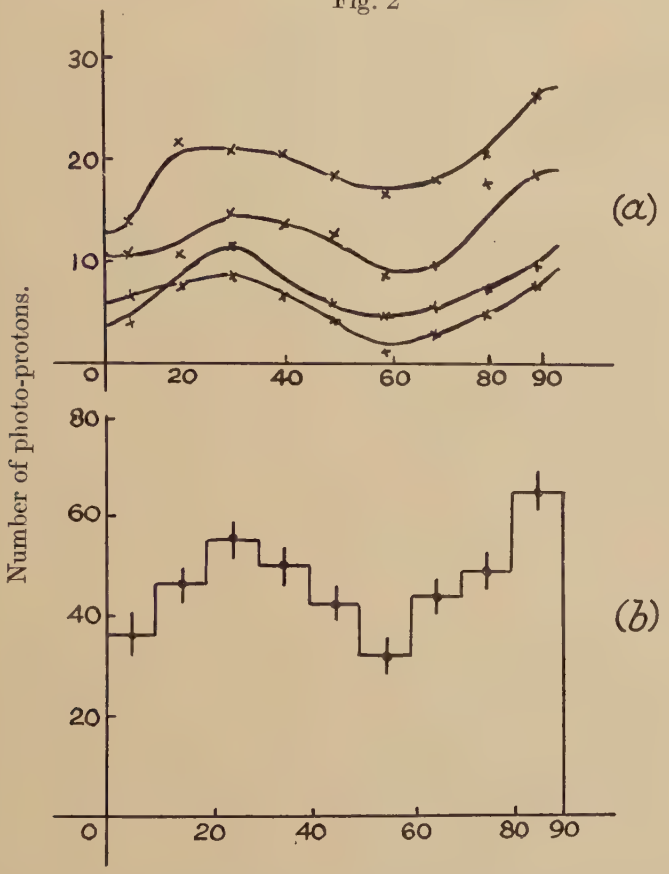

Angle between plane of emission and photo-protons.

(*a*) Angular distribution of the photo-protons of the four separate areas.

(*b*) Angular distribution of all the photo-protons. The errors are taken as $0{\cdot}67\ n^{1/2}$ where n is the number of tracks in each group.

A 10-micron thick heavy wax ($C_n\ D_{2n+2}$) target evaporated on a piece of thin cellophane was placed in front of a 200-micron Ilford C2 emulsion. The plate was exposed, to the collimated radiation from a 20 Mev betatron, in a vertical position such that the maximum half angle subtended at the 0·005 in. thick tungsten was about 3 deg. (see fig. 1). The centre of the x-ray beam was located accurately by photographic methods and a further check was made by measuring the variation of the x-ray blackening of the nuclear emulsion. In order to prevent

undue x-ray blackening of the emulsion the exposure lasted for only one minute with the betatron intensity reduced, the present output of the machine being approximately 100 Röntgens/min at one metre. The nuclear plates were developed in a solution of Azol and 1% potassium bromide. They were scanned by means of a Cooke, Troughton and Simms microscope, type 4005.

§3. Discussion of Results

Four different areas of plate corresponding to different angles AOB (fig. 1) were scanned and some 500 proton tracks corresponding to photon energies between 6 and 15 Mev measured. The position coordinates on the microscope micrometer scales of each track were noted thus enabling the angle between the ejected particle and the plane of emission to be determined accurately. The total angular distribution of all the protons divided into groups of 10 deg. is shown in fig. 2 (*b*); the errors are taken to be $0{\cdot}67n^{1/2}$. The distribution indicates a definite peak at 90 deg., together with a second maximum at about 20 deg. This is further confirmed by examining the distributions of the four separate areas themselves, fig. 2 (*a*), and even though the number of tracks is not large, each curve indicates maxima at about 20 and 90 deg. A maximum at 90 deg. would agree with the previously mentioned theories of May and Wick, as one would normally expect a $\cos^2$ distribution of protons about the electric vector. The other increase is difficult to explain. If was first thought to be spurious and in order to check this a large area of the plate was rescanned. No change in distribution was found.

§4. Conclusions

The asymmetry of the angular distribution of the photo-protons at 90 deg. lends support to the theoretical work of May and Wick indicating that the bremsstrahlung may be polarized perpendicular to the plane of emission. The other maximum at about 20 deg. may be due to another effect which is not covered by the theory.

Acknowledgments

The author wishes to acknowledge the help given by all the members of the betatron team. He also wishes to thank Dr. E. H. S. Burhop of University College, London, for his discussion of the results, and Mr. F. R. Perry for his encouragement and advice, also Dr. C. Dannatt, M.C., O.B.E., Director of Research and Education, and Mr. B. G. Churcher, Manager of the Research Department, Metropolitan-Vickers Electrical Co. Ltd. for permission to publish this paper.

References

Kirkpatrick, 1931, *Phys. Rev.*, **35**, 1139.
May, 1951, *Phys. Rev.*, **84**, 265.
May and Wick, 1951, *Phys. Rev.*, **81**, 628.
Wilkinson, 1952, *Phil. Mag.*, **43**, 659.
Williams, 1939, *Proc. Roy. Soc.*, **169**, 531.

XIX. *The L Spectra of Nickel and Copper* *

By Y. Cauchois
Laboratoire de Chimie Physique, Université de Paris†

[Received July 25, 1952, revised October 12, 1952]

Summary

An experimental investigation has been made of the L spectra of nickel and copper, with a view to obtaining information about the distribution of the 3d, 4s and 4p states in these metals, and also the processes of x-ray emission and absorption. As already known, the L emission bands of nickel and copper show striking differences. The copper band observed is somewhat different from the one reported by Farineau ; it is in good agreement with that to be expected from Mott's views on the behaviour of the electrons in this metal. The L absorption spectra of copper and nickel were obtained for the first time ; they help in interpreting the emission spectra. Some discussions are given of the present results in connection with former experimental and theoretical results from other authors. It is shown that the L spectra here obtained are consistent with the colour of nickel and copper. Mention is made of a similar agreement in the case of silver.

§1. Introduction

The K spectra of nickel and copper, both in emission and absorption, have been extensively studied by many workers (for references see Cauchois 1948). Beeman and Friedman (1939) observed them with the help of a double-crystal spectrometer ; they discussed the experimental curves in connection with Krutter and Slater's theoretical curve for the density of states in the conduction band of copper and found a surprisingly good agreement.

The L emission spectra of these two metals provide a much better resolution for studying the density of states as a function of the energy of the conduction electrons. They give information about transitions to 2p states, and thus about s and particularly d states in the conduction band. The behaviour of d and s electrons in these metals is of great interest (see Mott and Jones 1936, Mott 1952). The L emission spectra have usually been taken from Farineau's (1938) dissertation. The L absorption spectrum of nickel was previously unknown, until measured in this laboratory (Cauchois 1952 a) ; we found an anomalous behaviour

* Preliminary results were given at the Madison Conference, 1950. See Reports Madison Conference : Applications of x-ray spectroscopy to solid state problems.

† Communicated by the Author.

of the L_{III} absorption edge as compared with the emission edge. The L absorption spectrum of copper was also unknown ;* we obtained it by making use of different kinds of absorbing foils, together with the emission spectra either from the same foils or from bulk copper anticathodes of high purity.

The emission spectrum of copper, such as we observe it, shows features which are somewhat different from Farineau's results. They agree better with Saur's (1936) and with Gwinner's (1938) ; but these authors did not try to discuss their experimental curves in the light of any theory. The absorption curves we have now obtained are of help in interpreting the emission curves. We shall accordingly report our results, doing so here more fully for copper than for nickel.

The experimental device was described elsewhere (Cauchois 1945, 1952 b) ; we made use of mica crystals which give a dispersion of 4 ev/mm in the Cu L region and 3·2 ev/mm in the Ni L region ; and (mostly) of gypsum crystals† which give‡ respectively 2 and 1 ev/mm. Emitters were of pure thick copper and thick nickel of different origins ; thin foils on aluminium base were used for comparison of the emission edge with the related absorption edge ; different heavy metals were used as emitters for obtaining the absorption spectra. The window of the x-ray tube was of aluminium, *c.* 0·5 μ thick. Measurements§ were performed with reference to the wavelengths of the maxima of intensity of Ni and Cu Lα and β given by Cauchois and Hulubei (1947), according to Tyrén (1937, 1938) : Cu Lβ, 13.053 ; Cu Lα, 13.330 ; Ni Lβ, 14.279 ; Ni Lα, 14.566 Å.

The excitation was obtained under varied stabilized tensions, between 2 and 10 kv. Figures 1, 2, 3 and 6 give curves of several spectra as obtained with different microphotometers. See also Plates 5 and 6.

---

* Sandström (1935) reported observations which he later attributed himself to some oxidized form of copper (private communication) ; the wave-length of the observed edge certainly does not refer to metallic copper.

† Unfortunately gypsum crystals rather quickly dehydrate in vacuo ; white areas starting from thin scratches appear on the surface of the sheet whose reflecting power then decreases very rapidly, while the SO_4 Ca 2 Aq transforms into amorphous SO_4 Ca $\frac{1}{2}$ Aq and finally into anhydrous SO_4 Ca.

‡ Dispersions given here are as on the photographic plates ; they are increased up to say 50 times on microphotometric registration. Some data in the literature refer to dispersion obtained after enlarging by many times.

§ We did not retain the values given by J. Shearer (1935) for the Ni L maxima of intensity, for the following reasons : This author made use of a bent mica crystal. Reference lines of high order were registered close to Ni L bands in the first order. The Bragg angles were then calculated with the help of wavelengths and grating constants from Siegbahn's ' Spektroskopie der Röntgenstrahlen '. But wave-lengths values have since then been modified ; and moreover mica crystals may have widely different ' constants ', depending on the nature of the mica. This may introduce errors in the final results. We preferred to take Tyrén's values from optical grating measurements and optical standard references, that is in Angström unit, for nickel as for copper.

§ 2. The L_{III} and L_{II} Spectra of Nickel and Copper

The L_{III} and L_{II} emission bands ($L\alpha$ and $L\beta$) from nickel show the shape already known from Farineau's work. The L_{III} band is shown in fig. 1. The L_{III} and L_{II} emission edges respectively are well pronounced.

Fig. 1

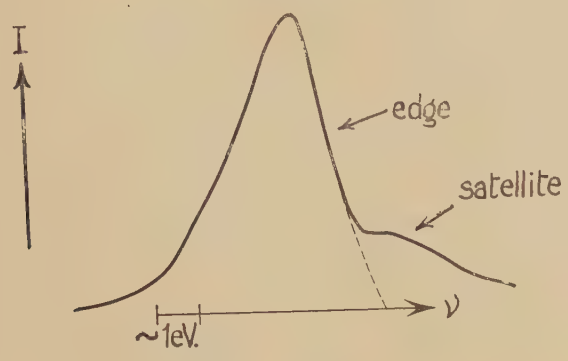

Ni Lα emission.

On their long-wave side is the main band ; the intensity increases from the edge up to a maximum and then decreases steadily. There is no trace of maxima and minima such as could be expected from Beeman and Friedman's measurements agreeing with Krutter and Slater's calculations and from Fletcher and Wohlfarth's (1951) curve. On the short-wave side is the already known ' satellite ' emission whose origin may be found either in multiple ionization or in excitation of singly ionized atoms.

$L\beta$ is much fainter than $L\alpha$. Neither the main band nor the satellites are exactly similar to $L\alpha$ (in contradiction with Farineau's observations). $L\beta$ is much more symmetrical than $L\alpha$.

Some data are given in table 1.

Table 1. L Emission Spectrum of Nickel (in ev)

Breadth* of the main band : $\alpha : 5\pm1$; $\beta : 3\pm1$.
Breadth† of the edge (uncorrected) : α : 0·5 to 1·0 ; β : 1 to 1·7.
Position of the maximum relative to the edge : α and β : $0{\cdot}9\pm0{\cdot}1$.
Satellite emission. Distance from the maxima to the maximum in the normal band : α' : $3{\cdot}_3$; α'' : $5{\cdot}_4$; α''' : $8{\cdot}_5$; β' and β'' appear at practically the same distance from β as α' and α'' from α ; the third maximum is hardly visible.

* From measurements performed on spectra already strong enough to show the satellite emission ; the fall of intensity at the edge being then extrapolated to get rid of it. The breadth is definitely less on short exposures not showing the satellites. It is then of the same order as that of the (less intense) β band.

† The second figure refers to an extrapolation of the fall of intensity which excludes the satellite emission.

Farineau reported a larger breadth of the L_{III} band, that is 6 ± 1 ev and a larger distance from the maximum α to the edge 1·5 ev.

The breadth of the K level was determined by Beeman and Friedman (*loc. cit.*) using the method of Richtmyer, Barnes and Ramberg based upon the theory of Weisskopf and Wigner and using certain hypotheses and approximations ; they found $1{\cdot}9\pm0{\cdot}5$ ev. From this and from the measured breadths of the $K\alpha_1$ and α_2 lines, they obtained the breadths of the L levels : L_{III} : 0·7 ev ; L_{II} : 1·7 ev. Our measurements on the L_{III} and L_{II} emission edges agree with these values. The larger width of the L_{II} level may partly account for differences in shape of the β and α bands. In spite of this, the β band shows a smaller breadth than the α, but this might come from its much lower intensity.

The Lα and Lβ bands of copper are very different from those of nickel. (See figs. 2 and 3 and compare with fig. 4.) They have a complicated structure. Going from low to high frequencies, each shows a strong maximum of intensity which looks as if it were due to a narrow symmetrical band superimposed on a feeble broader band with one and possibly two secondary maxima ; then there is a minimum of intensity followed by several secondary maxima. It is hardly possible to distinguish between the ' main band ' and the ' satellites ' without the help of the absorption spectrum. Farineau looked for the emission edge and concluded that it was unobservable, due to the strong satellite emission which covers it. With the help of the absorption spectrum which we obtained, it is now possible to locate the edge and even to guess the position of the emission edge on such curves as in fig. 2. (See, however, the discussion given below).

We call ' main band ' the part of the band which is of lower frequency than the edge ; ' satellite ', the other one.

The following data were obtained.

Table 2. L Emission Spectrum of Copper (in ev)

Total breadth of the main band (uncorrected) : about 5 ev both for α and β.
Position of the strong maximum d relative to the edge* : $3{\cdot}_0$; breadth (uncorrected) : $2{\cdot}_3$.
Position of the secondary maxima relative to the d maximum : α', $1{\cdot}_7$ and $2{\cdot}_8$; β', $2{\cdot}_2$.
Position of the minimum of intensity : $3{\cdot}_7$ ev from the main d maximum.
Satellites : The first satellite is at $4{\cdot}_5$ to $7{\cdot}_5$, with a maximum at 5 from the main d band ; the second one is at about $8{\cdot}_4$ from the same.

* Saur (1936) measured one secondary maximum which he called K and classified as a satellite, at a distance (recalculated from his paper) of 1·5 ev from the main α maximum.

Gwinner (1938) gives it as double (α' and α''') with the values 1·65 for α' and 2·8 for α'''. In the Lβ band they both observed one secondary maximum, β' at 2·2 (Saur) and 2·8 ev (Gwinner) from the main β maximum. Our measurements agree with Gwinner's.

Fig. 2

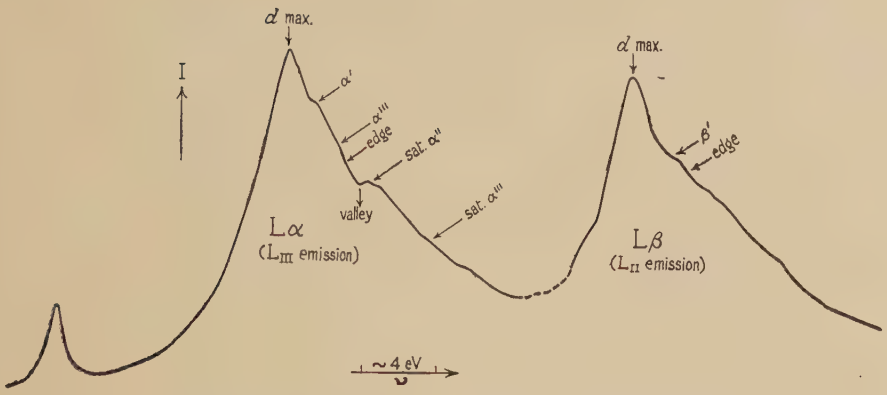

Cu Lα and Lβ emission (Vassy's microphotometer).

Fig. 3

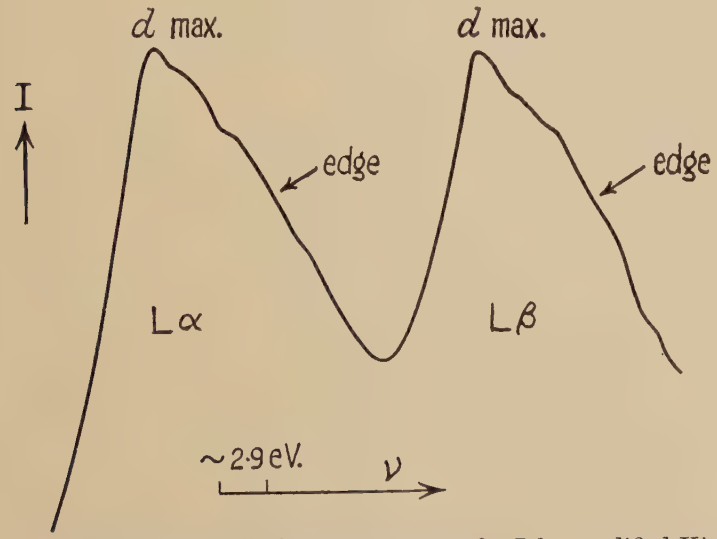

Cu Lα and Lβ emission (Spectrometer set for Lβ; modified Kip microphotometer).

Fig. 4

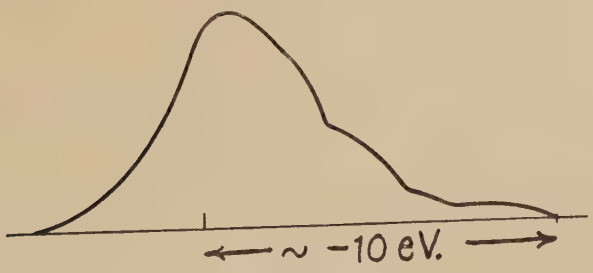

Cu Lα emission, according to Farineau (1938).

The first satellite looks somewhat like the main band with a relatively less strong maximum. The second is more shapeless.

A strong background emission extends from the α to the β band, the origin of which is not clear.

Due to satellite emission, it is impossible to measure the breadth of the emission edges. We give below the breadths of the edges, as measured in absorption. The β band differs somewhat from the α band, but with the precision here obtained, the maxima and minima of intensity are located at practically the same distances from the main maximum. The minimum of intensity between the position of the edge and the first α satellite, looks like a deep valley ; it does not show so markedly between the L_{II} edge and the first β satellite. The maximum called β', which according to us belongs to the main β band, is relatively less intense than α', in the main α band. Some differences between the α and β bands come from the difference in breadth of the L_{III} and L_{II} levels ; this eventually accounts for the fact that α' is resolved in two, whereas β' is not.

According to Beeman and Friedman (1939), taking $K=1{\cdot}3\pm0{\cdot}5$, the $K\alpha$ lines give for the breadths of the levels : $L_{II}=2{\cdot}4$; $L_{III}=1{\cdot}4$ ev, both definitely broader than for nickel.

It is to be noted that both the experimental width, the natural width of L_{III} (or L_{II}) and the natural width of the d band, all contribute to the total uncorrected widths given here ; this means that the total true width of the band is definitely less than 5 ev and that the main part of the d band is of the order of 1·2 ev wide, which is certainly very sharp. We do not know *a priori* whether the d band is located below the conduction band, or whether it is included in the energy range covered by the conduction band ; the x-ray emission spectra of pure copper would answer the question.

It would be difficult to account for the relatively high intensity of $K\beta_5$ on the basis of quadrupole transitions, were the 3d states purely atomic and non-hybridized. We rather expect some hybridization, although the overlap of the corresponding wave functions on neighbouring atoms should be small. However, the difference of energy between the maximum density of d states and the first empty levels which are effective in absorption should be given by the measured distance in L emission between the maximum d and the edge ; it is of the order of 3 ev.

We shall now compare the copper and nickel emission before discussing the absorption spectrum of copper.

Referring to Mott's theory of the transition metals, as given in Mott and Jones (1936, p. 189), we see that the copper main L band agrees with his picture of a narrow 3d band superimposed on a 4s band of low density whose surface gives rise to the edge. Following a suggestion due to Bethe, theoreticians predict a splitting of the d band in two when the atoms are in a face-centred cubic crystal, such as for metallic copper or nickel. (The splitting is to be seen for instance on Krutter and Slater's

curve for copper* and on Fletcher and Wohlfarth's curve (1951) for nickel.) It is not easy to say from our experiments whether the secondary maxima in the main bands correspond to this splitting. Whether they do or not, the experimental curves widely differ from the calculated ones ; the relative intensities and the separation of the maxima are far from those predicted.† The secondary maximum might also come from a higher density of s states. The two maxima on the K emission curve due to Beeman and Friedman might well correspond to the main and secondary L maxima respectively ; then in the latter case, the relative intensity of the high energy L component, close to the edge, is much lower in the L band than in the K band because transitions from p to p states are forbidden and transitions from s to d states much less probable than those from p to d states.

The main copper bands are thus in striking contrast with the main nickel bands which show a broad monotonous s+d distribution, to be explained by the fact that in Ni the d shell is incompletely filled. (Here again we do not observe the predicted splitting of the d band.) As shown by Farineau, his total breadth of 6 ev for the Ni band corresponds to 0·6 conduction electrons per atom (and consequently 0·6 d holes), when put into the Fermi–Sommerfeld formula for free electrons. This was in wonderfully good agreement with the expected value. But the breadth is probably less than 6 ev ; we give 5 ev although it is extremely difficult to give any precision measurement of the breadth of such dissymmetrical bands, when no definition is known of what ought to be measured. On the other hand, the Fermi–Sommerfeld approximation for the breadth of the electron distribution may not be a very good one. Because of this and of recent experiments (Cauchois 1952 a) relating to the L_{III} absorption and emission edges of nickel, we ought not at this stage to give too much meaning to the above result.

Some differences between α and β bands are possibly due to differences in transition probabilities associated with the bound levels which play a part in emission in the sense of Friedel's (1952 a) work. However, some kind of spin–orbit coupling might well exist in such cases, which would explain a different behaviour in L_{III} and L_{II} processes.

The absorption spectrum of copper was measured relative to the α and β emission bands (taking the values from Cauchois and Hulubei (1947) as corresponding to the strong d maxima of emission). The spectrum consists of the L_{III} and L_{II} main edges, each followed by several ' structures of absorption ', that is by minima and maxima of intensity towards high frequencies as shown in the microphotometric curve, Plate 6.

We were not able to observe the L_I edge whose breadth must be much increased by Auger processes.

---

* See Beeman and Friedman (1939), who extended this curve to nickel by simply displacing the Fermi limit towards the bottom of the band.

† No doubling of the full nickel d band is observed with non magnetic Cu–Ni alloys (unpublished results).

The L_{III} and the L_{II} spectra are very similar, though not identical. The (uncorrected) breadths of the absorption edges, 1·2 ev for L_{III} and 1·7 ev for L_{II}, are distinctly smaller than those given by Beeman and Friedman for the levels : 1·4 and 2·4 (see above) ; these thus appear as overestimated.

Table 3 gives numerical features of the spectra. The distance here measured between Lα (d max.) and the L_{III} absorption edge, 3·0 ev, is smaller than the distance between $K\beta_5$ (d max.) and the inflexion point of the K edge according to Beeman and Friedman, 3·4 ev.

The structures of absorption here observed both on the L_{III} and on the L_{II} regions consist of three minima and three maxima of intensity ; they extend a distance of less than 15 ev from the edge. On the K spectrum (see Cauchois and Manescu 1950) this interval of energy includes but the total drop of intensity, made up of the following features : the K edge proper (called K_1), a small minimum of intensity (at 2·7 ev from K_1), then a small maximum immediately followed by the secondary edge called K_2 (at 10·16 ev from K_1) which terminates in the minimum called A (at 14·9 from K_1).

Table 3. Absorption Spectrum of Copper (data in ev)

Breadth of the main edge (uncorrected) : $L_{III} : 1{\cdot}_2 \pm 0{\cdot}_1$; $L_{II} : 1{\cdot}_7 \pm 0{\cdot}_2$
Distance from the main edge to the main maximum of emission (L_{II} and L_{III} regions) : $3{\cdot}_0 \pm 0{\cdot}_4$

Distances from the structures of absorption to the main edge (the data refer to L_{III} ; those for L_{II} are practically the same within the limits of error, that is of the order of ±0·5 ev for the first structures, ±1 ev for the further ones) :

1st min. of intensity	$1{\cdot}_0$
1st max. ,, ,,	$3{\cdot}_5$
2nd min. ,, ,,	$5{\cdot}_0$
2nd max.,, ,,	$7{\cdot}_0$
3rd min. ,, ,,	$9{\cdot}_0$
3rd max. ,, ,,	$12{\cdot}_0$

It is evident that, apart from intrinsic differences coming from different parities of the wave functions in the final states, the K and the L_{II} and L_{III} absorption curves may differ widely because of the much better resolution in the latter case. (See schematic curves, figs. 1 (*b*) and 5 given by Cauchois 1952 c.)

Minima and maxima of absorption may result from several causes, including :

(*a*) variations in the total density of states $N(E)$ as a function of the energy E ;

(*b*) change of character of the wave function as a function of E, which modifies the probabilities ;

(*c*) change of the bound level (in the sense of Friedel) taking part in the absorption process. This later effect would superimpose fluctuations of intensity due to the above two effects, in a rather intricate way.

It is accordingly difficult to isolate effects due to $N(E)$ fluctuations proper and also to compare the K and the L curves. However, the quoted features of both the K and L spectra were taken care of when drawing the approximate diagram proposed in fig. 5 for the density of states in metallic copper.

Fig. 5

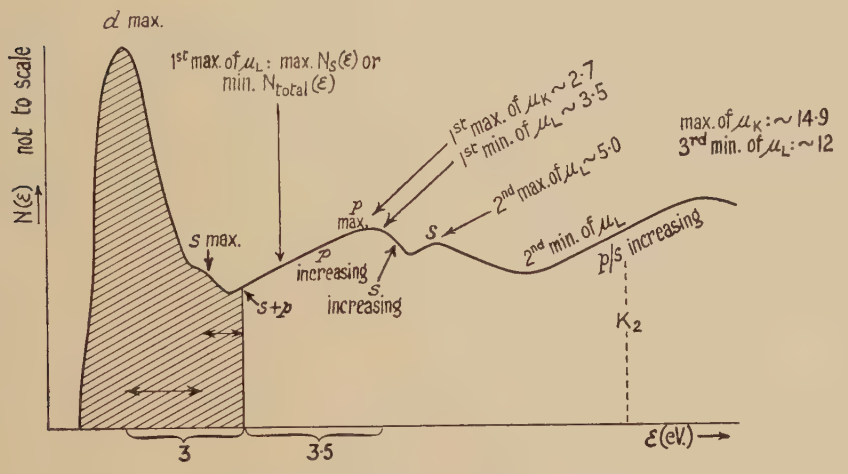

Proposed density of states for Cu.
μ_L=absorption coefficient in the L_{III} region.
μ_K=absorption coefficient in the K region.

The L absorption spectrum of nickel was first obtained with nickel foils thinned by beating. As already reported (Cauchois 1952 a), the L_{III} absorption edge of the metal at room temperature does not coincide with the emission edge* in direct excitation. It is displaced several tenths of an electronvolt towards lower energies. This absorption edge is single. Its (uncorrected) breadth is about 1 ev. It then is of the order of magnitude determined from the K spectrum for the breadth of the L_{III} level (0·7 ev).

It is followed towards high energies by a dissymmetrical absorption band (see fig. 6) whose breadth† is about 2 ev, the minimum of intensity being at about 0·7 ev from the foot of the edge.

Neither L_{II} nor any other structure of absorption has yet been obtained, probably due to the foils being too thick. The ratio of intensities of L_{II}

* No difference was observed between the emission edge from thick pure nickel and the emission edge from pieces of the absorbing foil placed on a copper base.

† If due to empty s states, according to the oversimplified views of a Fermi–Sommerfeld gas, it ought to be considerably broader.

to L_{III} as shown by the ratio $L\beta$ to $L\alpha$ must be low, much lower in nickel than in copper. As explained in a former paper (Cauchois 1952 a) we tentatively connected the anomaly of position of the absorption edge respective to the emission edge with the magnetic behaviour of nickel. This point of view was in apparent agreement with the displacement of the absorption edge towards higher frequencies observed when the absorbing foil was heated above the Curie point ;* in this case, the emission and the absorption edges practically coincided. Later experiments, however, showed that this displacement was partly due to a modification of the crystal when one foil was heated.

However, from this ' anomaly ' in the nickel spectrum arises the question of whether we can safely identify the position of an emission edge—when difficult to locate, as above in the case of copper— with that of the corresponding absorption edge. For copper, we think we are justified in so doing, as the copper *emission* edge is visible on our spectra,† although difficult to locate precisely because of the near-by satellites.

Fuller report on the nickel spectrum will be given later. Other papers will deal with copper and nickel alloys.

Fig. 6

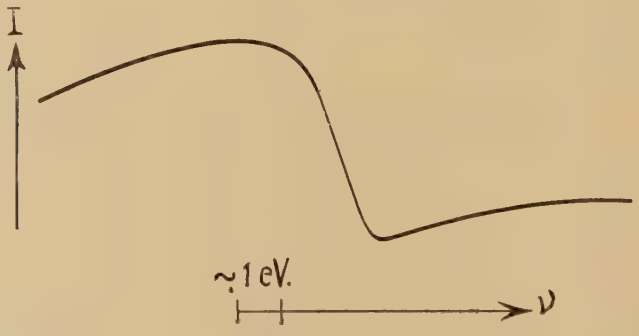

Ni L_{III} absorption.

§ 3. Comparison with Former Results, X-Ray and Optical

(*a*) *Farineau's curves* for Cu Lα, as given by Farineau (1938, 1939) and Morand and Farineau (1938) for pure copper, are flatter than ours. (See fig. 4 from the first of these papers.) Professor Morand was kind enough

* Debye–Scherrer diagrams were taken (*a*) with the ' cold ' absorbing foil, (*b*) with the same sample when cold after it was heaten in vacuo, (*c*) with another piece of the original sample when hot, the temperature being about the same (~400° c) as that of the hot absorbing foil. The diagrams failed to show any anomalous behaviour of the sample. Heating gave rise to an expansion which, if the only effect, would displace the edge towards lower frequencies.

The author wishes to thank Professor S. Goldsztaub and Dr. H. Curien for these diagrams.

† It looks slightly displaced towards small energies, which may be due to expansion of the emitting ' hot ' copper.

to look for documents left by Dr. Farineau in his laboratory in Liège. Curiously enough, they show two types of spectra : one with rather flat bands, as published by Farineau, the other one, which Farineau discarded for some unknown reason, in rather good agreement with our own. Professor Morand and I agree on that differences may come either from differences in purity or from differences in resolving power. Taking into account the changes already observed in the structure of the band which result from alloying, some impurity effect is very unlikely, as a rather high amount of foreign atoms is necessary in order appreciably to modify the L bands. It might be restricted to the surface, but we could hardly detect any change in the spectrum over a wide range of tensions of excitation, that is with varying depth of the excited material.*

Differences in the resolving power may come from differences in the degree of perfection of the analysing crystal. Our gypsum crystals provide a dispersion more than three times that of Farineau's equipment with mica crystals which, also, may well have been more or less perfect ; the resolution in our case is very good. This may explain discrepancies between Farineau's results and ours.

Skinner and Johnston (1937) have observed the M spectra of copper. Farineau and Skinner pointed out a good agreement between L and M emission bands for nickel, copper and zinc. Contrary to their views, the first satellite in each L band of copper has a higher frequency than the main absorption edge ; according to Skinner this is not the case in the M spectrum.

Table 4 shows the good agreement between K, L and M measurements.

Table 4. Comparison of K, L and M Data for the Edges† of Ni and Cu (absorption edges, except for Ni L_{III})

		λÅ	ν/R	ev (exp.)	ev (calc.)
Cu	L_{III}	$13{\cdot}28_7$	$68{\cdot}58_3$	93_3	K abs.—Kα_1 : 93_1
	L_{II}	$13{\cdot}01_2$	$70{\cdot}03_3$	95_3	K abs.—Kα_2 : 95_1
	$M_{II,III}$	165·8	$5{\cdot}49_6$	74·8	M_{III} : K abs.—Kβ_1 : $74{\cdot}_1$
					M_{II} : K abs.—Kβ_3 : $76{\cdot}_6$
Ni	L_{III} (em)	$14{\cdot}56_6$	$62{\cdot}56_1$	85_1	K abs.—Kβ_1 : 85_3
	$M_{II,III}$	188·4	$4{\cdot}83_7$	$65{\cdot}_8$	K abs.—K$\beta_{1,3}$: $66{\cdot}_6$

† K from Cauchois and Hulubei (1947) ; M from Skinner and Johnston (1937) ; L from author's measurements.

(*b*) Mott (see Mott and Jones 1936) interpreted some features of the *optical absorption curve* of a metal as due to transitions of electrons from its conduction band to excitation states in its band scheme ; this effect

* Yet, we observed some influence of the nature of the metal of the cathode. In every case was the structure of the bands more pronounced than on Farineau's published curves.

he calls ' internal photoelectric effect '. This connects the colour of the metal with the x-ray emission bands.

The reddish colour of copper comes from a strong absorption which starts at about 5700 Å (2 ev). There is a maximum of absorption* at about 2·5 to 2·7 ev (4500 to 5000 Å), and there is also another increase in absorption at 5 ev after a minimum at about 4 ev (3100 Å). These features, according to Mott, have to be explained on the basis of an internal photoelectric absorption in which electrons from the d band jump into empty states of the conduction band.

From our emission bands we locate the maximum of density of d states at about 3 ev below the first empty states ; taking into account the breadth of the d band and the breadth of the L_{III} level, we thus expect a strong optical absorption to start at about 2·3 ev and to increase until about 3 ev. This is in good agreement with the quoted optical data.

As for nickel, the small distance between the maximum in the emission band and the edge suggests of a strong absorption in the infra-red, which was in fact observed.

The author has recently observed the 4d and 5(s+p) contributions to the L spectrum of silver (Cauchois 1952 d). The spectrum shows that an energy of about 4 ev would be sufficient to transfer a 4d electron to an empty state in the conduction band of silver. This again is in good agreement with the optical absorption edge at about 3100 Å.

There are no recent precise optical measurements for further comparison with the x-spectra of these metals.

Whether any bound level under the conduction band plays a part in the processes involved (see Friedel 1952 b) does not matter for this direct comparison of experimental data.

§ 4. Conclusion

Summing up our present results for the pure metals, we may draw attention to the following facts :—

The Cu L emission spectrum has a more pronounced structure than shown by Farineau's ' classical ' curve. It shows striking differences from the Ni L spectrum. Both are in good qualitative agreement with Mott's theory for the distribution of electronic states in these metals.

The L_{III} and L_{II} absorption of copper and the L_{III} absorption of nickel are now known ; comparison of absorption or emission curves with theoretical curves for the densities of states shows poor agreement. An approximate diagram is proposed for the density of states in metallic copper (fig. 5).

There is a good agreement between our results and the ' colour ' of nickel and copper. Mention is made of a similar agreement in the case of silver.

---

* These figures are taken from curves given by Seitz (1940) after Minor and Meier.

Acknowledgment

The author wishes to express her best thanks to Professor N. F. Mott for his interest in this work and for very helpful discussions.

Note added October 1952 on the L Spectrum of Copper

The complicated Lα (or Lβ) emission of copper may be thought of as consisting of three bands : namely, the main band, Lα and two satellite bands (Lα″ and Lα‴ according to Gwinner's notation). These fainter bands approximately reproduce the overall features of Lα, more or less blurred as if corresponding to states of shorter half-lives. Such satellites may be—and usually are—attributed to atoms which would be initially ionized both in the 2p states and in another inner level ; such multiple ionization may result from Auger processes.

Alternately, we may consider another process : Friedel (1952 a) has shown that an inner ionization in copper (e.a.), must be screened, either by a heaping up of charge in the conduction band or by an electron from the conduction band falling into a bound level such as the 4s excitation level, which he calls 4s′. Let us think of a 4s′ screening as the most probable. According to these views we may picture the 2p emission in two ways : (*a*) the screening electron is excited, an electron from the conduction, s+p or 3d states falls into the 2p hole ; (*b*) the screening electron falls into the 2p hole. The main band, Lα, is emitted through process (*a*) ; the maximum observed very close to the edge might be due to process (*b*).

Let us now suppose that the screening is obtained from a higher excitation state : 4p′, 5s′, . . . , instead of 4s′. We then expect to observe satellite bands of higher frequency than the main band, but roughly similar in shape, although fainter and less sharp. The separation from the main band may be estimated as follows : the *initial* states (after absorption) differ ; they are somewhat similar to $3d^{10}$ 4s, $3d^{10}$ 4p, $3d^{10}$ 5s . . . . respectively, in Zn^{+} ; whereas the final states are the same.

We then expect separations of the order of Zn^{II} 4s 4p, Zn^{II} 4s 5s, etc. According to Bacher and Goudsmit (1932), we get the following values, to compare with the experimental values for the observed satellites :

Zn^{II} 4s 4p———∼ 6 ev———satellite observed at ∼5·0 ev,
Zn^{II} 4s 5s———∼11 ev———satellite observed at ∼$8{\cdot}_4$ ev.

We thus obtain the very order of magnitude of the observed separations. Corrections due to exchange energies should be calculated. However, the agreement appears to support the above interpretation of the satellites.

Going further, we expect similar excitation processes to show in absorption, where the same differences in energy would refer to *final* states. In fact, the L absorption curves show secondary increases of the absorption coefficient giving rise to the minima of intensity at about 5 and 9 ev. Whether these structures of absorption come from the

above mechanism of from Kronig's or from both, is difficult to say. In case the views expressed in this note are retained, the $N(E)$ curve (fig. 5) should be reconsidered, especially as regards the empty states some 5 ev from the Fermi limit.

References

Bacher, R. F., and Goudsmit, S., 1932, *Atomic Energy States* (New York: McGraw Hill).

Beeman, W. W., and Friedman, H., 1939, *Phys. Rev.*, **56,** 392.

Cauchois, Y., 1945, *Journ. de Phys.*, *S.* VIII, T. VI, 89/96; 1948, *Les spectres de rayons X et la structure électronique de la matière* (Paris); 1952 a, *Phil. Mag.*, **43,** 375; 1952 b, *Acta Crystallogr.*, **5,** 348; 1952 c, *Journ. de Phys.*, **13,** 113; 1952 d, *C.R.*, **235,** 613.

Cauchois, Y., and Hulubei, H., 1947, *Tables de Constantes et données numériques.* Vol. 1.—Constantes sélectionnées. Longueurs d'onde des émissions et des discontinuités d'absorption X (Paris).

Cauchois, Y., and Manescu, I., 1950, *Journ. Chim. Phys.*, **47,** 892.

Cauchois, Y., and Mott, N. F., 1949, *Phil. Mag.*, **40,** 260.

Farineau, J., 1937, *Nature, Lond.*, **140,** 508; 1938, *Ann. de Phys.* S. 11, **10,** 20; 1939, *Journ. de Phys.* S. 7, **10,** 327.

Farineau, J., and Morand, M., 1938, *Journ. de Phys.* S. 7, **9,** 447.

Fletcher, G. C., 1952, *Proc. Phys. Soc.* A, **65,** 192.

Fletcher, G. C., and Wohlfarth, E. P., 1951, *Phil. Mag.*, **42,** 106.

Friedel, J., 1952 a, *Phil. Mag.*, **43,** 153; 1952 b, *Proc. Phys. Soc.* B, **65,** 769.

Gwinner, E., 1938, *Zeits. f. Phys.*, **108,** 523.

Mott, N. F., 1952, *Progr. in Met. Phys.*, **3,** 76.

Mott, N. F., and Jones, H., 1936, *The Theory of the Properties of Metals and Alloys* (Oxford).

Sandström, A., 1935, *Nova Acta Reg. Soc. Sci. Upsala*, 4 S, **9,** nº 11.

Saur, E., 1936, *Zeits. f. Phys.*, **103,** 421.

Seitz, F., 1940, *Modern Theory of Solids* (New York).

Shearer, J., 1935, *Phil. Mag.*, **20,** 504.

Skinner, H. B., and Johnston, J. E., 1937a, *Nature, Lond.*, **140,** 508; 1937 b, *Proc. Roy. Soc.*, **161,** 420.

Tyrén, F., 1937, *Ark. Mat. Astr. Fys.*, **25A,** 32; 1938, *Zeits. f. Phys.*, **98,** 768.

XX. *Note on the Electronic Structure of the Transition Metals*

By N. F. Mott, F.R.S.
H. H. Wills Physical Laboratory, University of Bristol*

[Received January 5, 1953]

Summary

A discussion is given of the Van der Waals forces between the 3d and 4d shells of transition metals, and it is shown that a consideration of their nature may account for the low number of conduction electrons (0·6) in these metals and their alloys.

In 1935 the present author put forward a model (Mott 1935, Mott and Jones 1936) to explain the magnetic and electrical properties of the alloys of nickel, cobalt and palladium with each other and with other metals. This model assumed overlapping s and d bands ; the density of states in the d band was supposed to be high ; and the d band to be so placed that, for energies below its upper limit E_D, there would be about 0·6 states per atom in the broad s (or conduction) band. Thus the number of vacancies in the d band—and hence the magnetic and many electrical properties of these alloys—is determined according to this model by the condition that the number of conduction electrons remains near to 0·6. This must mean that the energy of the lattice, for a wide series of alloys, is a minimum when the number of conduction electrons is 0·6. The purpose of this note is to propose a tentative explanation for this remarkable constancy, and for the occurrence of so low a value as 0·6.

In the first place we shall show that the assumption that the cohesion is due entirely to the conduction electrons cannot explain their small number. If there are n electrons in the conduction band, it will be reasonable to write their contribution to the cohesive energy, apart from a constant term independent of n, as

$$-n(E_0-E_d)+\tfrac{3}{5}n^{5/3}E_F,$$

where E_F is the width of the Fermi band with one electron per atom (as in copper), $-E_0$ the energy of the lowest state calculated by the method of Wigner and Seitz, and $-E_d$ the energy of an electron in the d band referred to the same zero. This has its minimum when

$$n=\{(E_0-E_d)/E_F\}^{3/2}.$$

Since in nickel the state $3d^{10}$ has energy about 1·2 ev above that of the state $3d^94s^1$, it is reasonable to suppose that (in ev)

$$E_0-E_d=E_0-1{\cdot}2.$$

---

* Communicated by the Author.

For E_0 we take the binding energy (81·5 kcal) of copper *plus* the Fermi energy $3E_F/5$. With E_F equal to 7·1 ev this gives for n a value of about 0·9.

The calculation has omitted the correlation energy, which is of the form (Wohlfarth 1949)

$$-\tfrac{3}{4}Ne^2(3N/\pi V)^{1/3},$$

where N is the total number of electrons and V the volume. Since this term is negative and increases with N faster than the first power, its inclusion would give a still higher value of n. Although these calculations are very rough, it seems unlikely that the minimum energy occurs when n is 0·6.

Let us now turn to the collective electron model of the d band and see what it implies. It is consistent with this model to treat nickel, for instance, as a mixture of ions in the states $3d^{10}$ and $3d^9$, with perhaps some in the state $3d^8$. If one does this, the ' holes ', or points in the lattice where the ion is in the state $3d^9$, must be thought of as moving about ; one applies the Fermi–Dirac statistics to them, and the collective electron treatment follows. This way of regarding the metal suggests a way of explaining the value 0·6, which we shall put forward and then dispose of. The shells with configurations $3d^9$ and $3d^{10}$ carry charges 1 and 0 respectively, so that if the conduction electrons were uniformly distributed the respective lattice points would carry considerable charges ; each atom would tend to be surrounded by charges of opposite sign, so that there would be a large electrostatic term in the binding energy. Friedel's recent calculation (1952 a) suggests, however, that the conduction electrons are by no means uniformly smeared out, but, on the contrary, that every atom is practically electrically neutral.* Moreover, if such electrostatic forces were important, we should expect a super-lattice to form in, for instance, $Ni_{0\cdot65}Cu_{0\cdot35}$, which has not been observed.†

We believe the clue to lie in the Van der Waals forces between the ions. Friedel (1952 c) has examined the effect of these forces for copper, and finds that they contribute at least 25 kcal of the total binding energy, compared with *c.* 50 kcal from the conduction electrons. In nickel, containing the neutral $3d^{10}$ shell, the contribution is likely to be bigger and perhaps to exceed that from the conduction electrons. For copper Friedel deduces the magnitude of the Van der Waals force from the strength and frequency of the optical absorption band which gives the metal its colour ; the force depends on the oscillator strengths of the absorption lines due to the ion. The absorption band considered is one in which the d electron jumps into the conduction band just above the limit of the Fermi distribution.

---

* Cf. the author's analogous calculation for β-brass (Mott 1937), where it is shown that the electrostatic contribution to the energy of the super-lattice is small.

† In this alloy there should be 0·25 holes per atom.

Now such a transition will have a finite oscillator strength only owing to the presence of p terms in the wave functions of the unoccupied states in the conduction band. The more states with a p component that are unoccupied, the greater, therefore, will the Van der Waals interaction be. Since we have seen that in transition metals the Van der Waals interaction will be large in any case, it is clear that we have here a reason which can explain a considerable reduction in the number of electrons in the conduction band.

Now, as first shown by Jones, Mott and Skinner (1934) on theoretical grounds, it is possible that on the boundaries of the first Brillouin zone —that with s-symmetry at the centre—the wave functions have purely p-symmetry. Experiment (soft x-ray emission) indicates that this is

Fig. 1

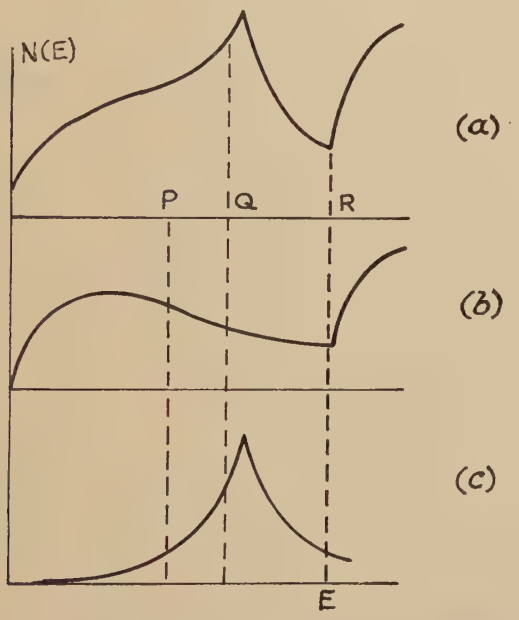

Density of states in nickel or copper. (*a*) Total; (*b*) states of s-symmetry; (*c*) states of p-symmetry. It is suggested that the states are occupied up to P for nickel, Q for copper, and that R is the energy at which the second Brillouin zone begins.

so in magnesium (Mott and Jones, p. 126). The calculations of Howarth and Jones (1952) show that this is not the case in sodium, and certainly Skinner's Li K and Na L_{III} emission bands suggest that the highest occupied states for these metals have mainly s-symmetry. These bands show a maximum well before the short wave limit for Li, where the x-ray level is s, but at the limit for Na, where the x-ray level is p. But for copper, with its comparatively small 4s–4p excitation potential (*c.* 3 ev) and wide Fermi band (7·1 ev), it is probable that the reverse

is the case. There is some evidence that this is so from the x-ray emission spectrum (Cauchois 1953), which will be reviewed below.

The density of p-states would then be as in fig. 1. If so, the Van der Waals forces would increase if the Fermi surfaces were forced down from the level Q to the level P in the figure, but not much if it were forced down still further. Such a model is well capable, then, of explaining the constant value of about 0·6 conduction electrons in a wide variety of alloys.

The x-ray evidence that copper, nickel, etc., resemble Mg in having p-symmetry comes from the L_{III} absorption of copper (Cauchois 1953, plate 6). Here it will be seen that, about 3·5 ev from the main edge, the absorption sharply increases ; the point is marked S in the plate. It is natural to ascribe this to the setting in of absorption into the second Brillouin zone (R in fig. 1), which must thus have s-symmetry at the bottom. But this would imply that, in the first zone at points near the (111) planes, the symmetry was p. This is what we wish to show.

Unfortunately, however, the explanation of the second maximum in terms of a zone structure is not the only possible one ; Friedel (1952 a) has shown that similar subsidiary edges in lithium can be explained by assuming that, after absorbing a quantum, the electron which screens the positive hole in the x-ray level is in an excited state ; in copper he shows (Friedel 1952 c) that such an excited state exists with about the right energy. All we can say with certainty, however, is that the x-ray evidence does not contradict our hypothesis.

References

Cauchois, Y., 1953, *Phil. Mag.* (this issue).
Friedel, J., 1952 a, *Phil. Mag.*, **43,** 153 ; 1952 b, *Ibid.*, **43,** 1115 ; 1952 c, *Proc. Phys. Soc.* B, **45,** 769.
Howarth, D. J., and Jones, H., 1952, *Proc. Phys. Soc.* A, **65,** 555.
Jones, H., Mott, N. F., and Skinner, H. W. B., 1934, *Phys. Rev.*, **45,** 378.
Mott, N. F., 1935, *Proc. Phys. Soc.*, **47,** 571 ; 1937, *Ibid.*, **49,** 257.
Mott, N. F., and Jones, H., *Theory of the Properties of Metals and Alloys*, Oxford, 1936.
Skinner, H. W. B., 1938, *Reports on Progress in Physics*, **5,** 257.
Wohlfarth, E. P., 1949, *Phil. Mag.*, **40,** 703.

XXI. *The Multiple Scattering of Protons in Thin Foils*

By D. M. Skyrme
Atomic Energy Research Establishment, Harwell*

[Received October 30, 1952]

Summary

The multiple scattering of 147 mev protons in thin foils has been investigated using platinum, silver and photographic emulsion as the scattering materials. The projected mean scattering angles, and the shape of the projected angular scattering distributions agree with the multiple scattering theory of Williams as modified by Voyvodic and Pickup.

§ 1. Introduction

When a charged particle passes through a material medium it undergoes elastic scattering in the screened Coulomb fields of the nuclei which it encounters. The mean deflection of the particle from its original path after many such collisions is proportional to $zt^{1/2}/p\beta c$ where t is the thickness of material traversed, p the momentum of the particle, βc its velocity and z its charge, expressed as a multiple of the electronic charge. The ' constant ' of proportionality or ' scattering constant ' is determined mainly by the properties of the scattering medium although, as will be seen later, it depends also to some extent on the values of β and t. It is often inconvenient to measure the total scattering angle, or the distribution in space of the scattered particles. Instead, the quantity observed is the projection of this angle or distribution on a plane at right angles to the initial direction of motion of the particle. In the following discussion the terms ' projected angle ' and ' projected distribution ' will be used to denote these quantities. Measurements of multiple scattering are used to determine the masses and energies of fast ionizing particles occurring in cosmic radiation, the scattering medium employed being the photographic emulsion which records the track of the particle. (See, for example, Fowler (1950), and Goldschmidt-Clermont, King, Muirhead and Ritson (1948).) The appropriate scattering constant can be calculated or, alternatively, it may be obtained experimentally using particles whose charge, mass and momentum are known, in order to calibrate the emulsion.

In the present experiments, the scattering of high energy protons by Ilford G5 nuclear emulsion and also by thin foils of platinum and silver has been examined. The projected mean scattering angles, and the shape of the projected angular scattering distributions obtained are shown to agree with the predictions of the multiple scattering theory of Williams (1939 and 1940) as modified by Voyvodic and Pickup (1952).

* Communicated by the Author.

§ 2. Experimental Arrangements for Obtaining Distribution Curves

A collimated beam of protons, with energy (147 ± 1) Mev can be obtained from the Harwell 110 in. cyclotron (Cassels, Pickavance and Stafford 1952). These particles, after passing through the scattering foil, entered the emulsion of a photographic plate, and their distribution was investigated by examining the processed plate under a microscope. Figure 1 shows a plan of the experimental arrangements. Protons travelling along the evacuated tube T reached the brass block B, whose length (5 cm) was greater than the range of these protons in brass. Along the axis of the block was milled a rectangular slit S, 8 mm wide in the plane of the diagram and 25 mm long at right angles to this plane. The reasons for having so wide a slit, and the modifications of the simple

Fig. 1

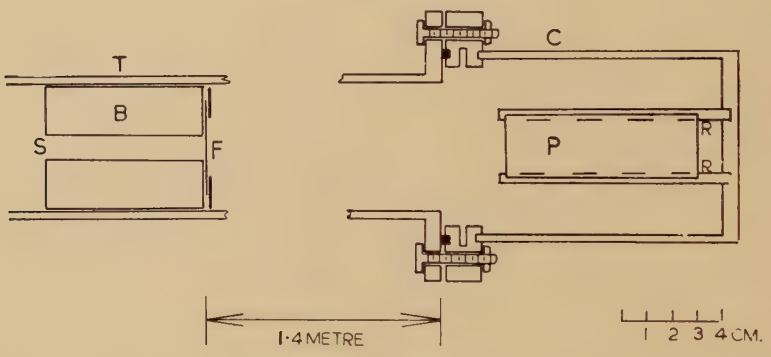

Plan of apparatus.

multiple scattering theory which its use necessitates, are discussed in § 4. The scattering foil F was clamped across the face of the block remote from the cyclotron. The thickness of the silver and platinum foils were 26·2 and 27·3 milligrams per square cm respectively. The scattering in photographic emulsion was investigated by using as the scattering foil a piece of unbacked G5 emulsion 98·6 μ thick. The energy lost by the protons in passing through the foils was much less than the spread in energy of the incident particles.

The camera C containing the recording photographic plate P was bolted to the end of the proton tube about 140 cm beyond B. This distance was chosen, in conjunction with the thickness of the scattering foils, to produce a convenient linear spread in the scattered proton beam reaching the plate. For the theory of multiple scattering to be applicable it is necessary that the final deflection of a particle from its initial path be less than about 10°, and that the number of collisions, M, made by the particle in traversing the scattering medium be much greater than

unity ; the formulae are reliable if $M > 10$. With the present arrangements protons could not reach the recording plate if they had been scattered through a resultant angle of more than 0·5°, and the values of M, calculated from the formula given by Voyvodic and Pickup, were 167·3 for emulsion, 110·5 for silver and 63·9 for platinum.

Preliminary experiments showed that a convenient track density on the recording plate was obtained by exposure of ten or twenty seconds. This plate, which was supported on the axis of the beam by the brass rods R, was inclined at 15° to the horizontal so that the protons made dipping tracks in the emulsion. After processing, the plate was examined under a microscope to determine the distribution, in a direction perpendicular to the axis of the proton beam, of particles passing through a plane parallel to the surface of the emulsion. Each point on the distribution curve was obtained by scanning parallel to the length of the tracks, rather than at right angles to this direction, so that it was unnecessary to decide exactly where each track came into focus. If the line across which the plate was examined were not strictly perpendicular to the axis of the beam, but instead made an angle θ with this perpendicular, the width of the observed projected distribution would be wider than the true one by a factor $1/\cos\theta$. By locating the centre of the distribution at different positions along the plate it was found that θ was in all cases less than 1° ; the correction involved was therefore negligibly small. Figure 4 shows the results obtained for the projected distributions, and their interpretation is discussed in § 4. The errors shown are standard deviations, statistical errors in track counting only being considered.

§ 3. Theories of Multiple Scattering

Theories of multiple scattering differ from each other mainly in their treatment of the effect on the impinging particle of the partial shielding of the nuclear field by that of the orbital electrons ; that is, they involve different expressions for the fundamental single scattering cross-section. The theory of Snyder and Scott (1949) is valid only for fast particles in thin foils. Molière (1947, 1948) obtains an expression for the single scattering cross-section which is exact for $\gamma \ll 1$ and $\gamma \gg 1$, and which holds with sufficient accuracy in the intervening region. ($\gamma = Zz/137\beta$ where Z is the charge in the scattering nucleus, expressed as a multiple of the electronic charge.) In the original theory of Williams (1940) two expressions are derived for the single scattering cross-section, and hence for the mean angle of scattering, one being appropriate for $\gamma \ll 1$ and the other for $\gamma \gg 1$. The difference between the two arises because the effect of the orbital electrons, regarded as a Thomas–Fermi distribution, can be treated by Born approximation when $\gamma \ll 1$, whereas the classical theory of orbits is appropriate for $\gamma \gg 1$. When scattering in a mixed medium such as photographic emulsion is considered, it may be essential to have a unified theory to cover the wide range of γ values encountered.

Goldschmidt-Clermont (1950) and Voyvodic and Pickup (1952) have now shown that by incorporating a correction term which they call the 'Molière factor' (see eqn. (3)) into Williams' calculation, an expression for the mean scattering angle applicable over the whole range of γ values can be obtained, while still retaining the convenient form in which Williams expressed his results. Voyvodic and Pickup have calculated the mean projected angle by this modified Williams theory, for singly charged particles scattered in G5 emulsion; the values obtained agree to within 1% with those derived from Molière's theory over a wide range of values of t and β. Values of the mean projected angle of scattering in silver and platinum calculated for conditions appropriate to the present experiments show agreement between the Molière and modified Williams theories which is better than 2% for platinum and 1% for silver.

The expression obtained by Williams for the actual distribution in angle of the scattered particles is only an approximation, but it is simple, and often more convenient to use than the more exact distribution calculated by Molière. In particular it is very easy, with Williams' formulation, to estimate the importance in any experiment of single scattering compared with multiple scattering and to decide in what circumstances the finite size of the nucleus imposes an upper limit on the possible scattering angle. Goldschmidt-Clermont (1950) gives curves comparing the projected distributions of Williams, Snyder and Scott, and Molière for a special case, and shows that they are very nearly the same up to angles of three times the mean value, by which time the number of particles has fallen to about 1/20 of its value at the origin. Beyond this angle the Williams curve lies somewhat below the other two. It appears, therefore, that the modified Williams theory should give essentially correct results except, perhaps, for the detailed form of the scattered distribution at large angles.

When an infinitely narrow beam of incident particles passes through a foil, the mean angle of the complete projected distribution of particles after scattering is given by $\bar{\theta}$ where :—

$$\bar{\theta}=\frac{2ze^2(NZ^2)^{1/2}\,.\,t^{1/2}}{p\beta c}\,.\,\bar{\alpha}=\delta\bar{\alpha}, \qquad (1)$$

N being the number of scattering nuclei with charge Ze per unit volume.

The dimensionless quantity δ is the same in all theories and is a convenient unit of angle in which to measure deflections. The various treatments of nuclear screening result in slightly different values of $\bar{\alpha}$. According to Williams

$$\bar{\alpha}=0{\cdot}80(\log_e M)^{1/2}+1{\cdot}45, \qquad (2)$$

where M is the average number of collisions made by a particle in going through the foil. Voyvodic and Pickup write :—

$$M=M_B\Big/\left(1+\frac{\gamma^2}{0{\cdot}31}\right), \qquad (3)$$

where $M_B=0{\cdot}64\pi NtzZ^{4/3}\beta^{-2}(\hbar/mc)^2$, and is the original expression derived by Williams for the limiting case $\gamma \ll 1$. The so-called 'Molière factor', $(1+\gamma^2/0{\cdot}31)$, extends the range of validity of (3) to all γ values.

Williams treats the shape of the projected angular distribution as the sum of a gaussian, $g(\alpha)$, representing the effect of multiple scattering, and a term $s(\alpha)$ which takes into account any large angle scattering. The values of these two terms are :—

$$g(\alpha)=(1-\pi/2\phi_2{}^2)\,.\,\frac{2}{\pi\alpha_m}\exp\left(-\frac{\alpha^2}{\pi\alpha_m{}^2}\right)=k\exp\left(-\frac{\alpha^2}{\pi\alpha_m{}^2}\right)$$

and

$$s(\alpha)=0 \text{ for } \alpha\leqslant\phi_2$$

$$=\frac{\pi}{\alpha^3}\text{for } \alpha\geqslant\phi_2.$$

The angle ϕ_2 at which single scattering begins to contribute to the distribution is :—

$$\phi_2=5{\cdot}1(\log_e M)^{1/2}-4{\cdot}0.$$

In the conditions where the finite size of the nucleus limits the maximum scattering angles obtainable, the single scattering tail may be suppressed ; but in the present experiments the momentum of the particles was insufficient to produce this effect.

α_m, the arithmetic mean of the gaussian part of the distribution is given by

$$\alpha_m=\frac{\bar{\alpha}-(\pi/\phi_2)}{[1-(\pi/2\phi_2{}^2)]}.$$

All angles are measured in terms of δ.

§ 4. Interpretation of Results

In order to calculate the projected distributions to be expected with the present experimental arrangements, we have to apply the modified Williams theory to the case of a slit of finite width, traversed by a divergent beam of particles, the incident beam intensity being constant over the centre region of the slit, but falling off at the edges due to collisions between the particles and the walls of the brass collimator. Figure 2 shows the results obtained by scanning a plate exposed to the proton beam without a scattering foil over the slit. Uniform beam intensity is obtained over 7·95 mm on the plate, corresponding to a uniformly 'illuminated' slit width of 7·95 d/D mm, where d and D are the effective distances of the source of protons from the slit and plate respectively. The effective total width of the slit, given by linear extrapolation of the falling-off part of the curve is 8·80 d/D mm.

The experimental arrangements are shown schematically in fig. 3. The number of particles reaching a point P on the plate as a result of

multiple scattering through a resultant angle between α and $(\alpha+d\alpha)$ in an element dx of the foil is :—

$$g(\psi)\,d\psi=n(x)\,.\,k\,.\,\exp\,(-\alpha^2/\pi\alpha_m{}^2)\,d\alpha,$$

Fig. 2

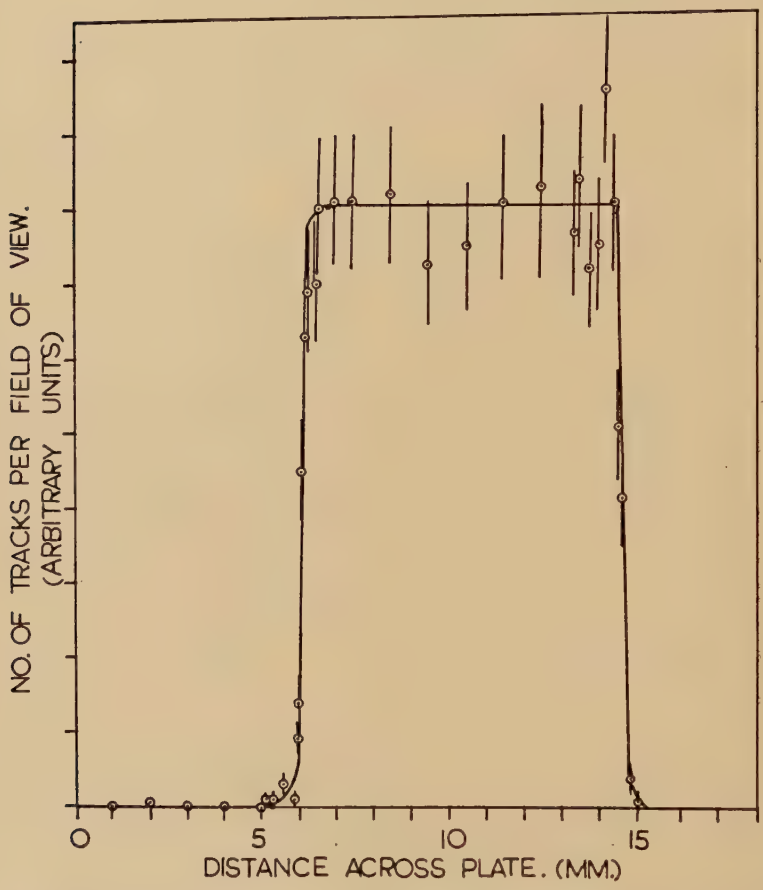

Results of a typical scan across a plate exposed with the slit uncovered.

where $n(x)$ is the number of particles incident per unit width of the foil at x. Integrating across the entire slit, the total number of particles reaching P can be shown to be given by :—

$$G(\psi)=k\sqrt{\pi}\alpha_m\left[\int_{[\psi+(D/d)\Gamma_2]/\sqrt{\pi}\alpha_m}^{[\psi+(D/d)\Gamma_1]/\sqrt{\pi}\alpha_m} n(x)\,e^{-p^2}\,.\,dp+n(0)\int_{[\psi-(D/d)\Gamma_1]/\sqrt{\pi}\alpha_m}^{[\psi+(D/d)\Gamma_1]/\sqrt{\pi}\alpha_m} e^{-p^2}\,.\,dp\right.$$
$$\left.+\int_{[\psi-(D/d)\Gamma_2]/\sqrt{\pi}\alpha_m}^{[\psi-(D/d)\Gamma_1]/\sqrt{\pi}\alpha_m} n(x)e^{-p^2}\,dp\right],$$

where

$$p=\frac{\alpha}{\sqrt{\pi\alpha_m}}=\frac{\psi-(D/d)\Gamma}{\sqrt{\pi\alpha_m}}.$$

$2\Gamma_1$=angular width of the uniformly 'illuminated' central portion of the slit.

$2\Gamma_2$=effective angular width of the whole slit.

$n(0)$=number of particles incident on unit width of the foil over the uniformly illuminated region.

The first and last terms express the contribution of the non-uniformly illuminated edges, each of angular width $(\Gamma_2-\Gamma_1)$; together they amount to about 3% of the total at the centre of the distribution and 10% at the extremes. In evaluating the contribution due to edge effects we shall take the average value of $n(x)$ as $n(0)/2$; further, since e^{-p^2} changes by only about 10% over the integration involved, we shall take it as constant, and equate it to its value at the midpoint of the range. With these approximations we obtain :—

$$G(\psi)=n(0)k\sqrt{\pi\alpha_m}\left[\int_{[\psi-(D/d)\Gamma_1]\sqrt{\pi\alpha_m}}^{[\psi+(D/d)\Gamma_1]\sqrt{\pi\alpha_m}} e^{-p^2}\,dp + \frac{\Gamma_2{}^1-\Gamma_1{}^1}{\sqrt{\pi\alpha_m}}\exp\left[-(\psi^2+\overline{\Gamma^1}^2)/\pi\alpha_m{}^2\right]\cosh\left(\frac{2\psi\overline{\Gamma^1}}{\pi\alpha_m{}^2}\right)\right]. \quad . \quad . \quad . \quad (4)$$

where $\Gamma^1=(D/d)\Gamma$ and $\overline{\Gamma}=(\Gamma_1{}^1+\Gamma_2{}^1)/2$. $\Gamma^1\delta$ can be calculated directly using the data obtained from the trace of the uncovered slit (fig. 3) and the measured distance between the scattering foil and the line of scanning on the plate.

It can be seen that the effect of beam divergence is to increase the effective slit width by a factor D/d.

Preliminary experiments with a narrow slit showed that the scattering of particles by the collimator walls produced a broadened and somewhat ill-defined beam. This could not be regarded as infinitely narrow, and neither could the treatment used above be applied, since $n(x)$ varied across the entire slit and no convenient analytical expression could be found to describe it. It was for this reason that a wide slit was used in the final arrangement.

We consider now the single scattering of particles in the foil; this does not affect the observed distribution for very small angles of scattering. At the extreme ends of the curve obtained with a G5 scattering foil single scattering accounts for 30% of the scattered particles, and in the cases of the silver and platinum foils, where the scattered distribution was not followed out to such a large angle, the contribution is still smaller. It is therefore sufficient to regard the single scattering as arising from a uniformly illuminated foil, of effective angular width $2\overline{\Gamma}$. As in the derivation of Williams' expression for $s(\alpha)$, the effect of 'plural' scattering is neglected, a sharp discontinuity between the multiple and single scattering processes

being assumed to exist. Integrating Williams' expression for $s(\alpha)$ over the relevant portions of the slit we obtain for the number of particles reaching P as a result of large angle scattering,

$$S(\psi)=0 \text{ for } \psi\leqslant(\phi_2-\bar{\Gamma}), \quad \ldots\ldots\ldots\ldots\ldots\ldots 5\,(a)$$

$$S(\psi)=n(0)\frac{\pi}{2}\left[\frac{1}{\phi_2{}^2}-\frac{1}{(\psi+\bar{\Gamma})^2}\right] \text{ for } (\phi_2-\bar{\Gamma})\leqslant\psi\leqslant(\phi_2+\bar{\Gamma}), \quad \ldots\ldots 5\,(b)$$

$$S(\psi)=n(0)\frac{\pi}{2}\left[\frac{4\psi\bar{\Gamma}}{\{(\psi-\bar{\Gamma})(\psi+\bar{\Gamma})\}^2}\right] \text{ for } \psi\geqslant(\phi_2+\bar{\Gamma}). \quad \ldots\ldots 5\,(c)$$

Fig. 3

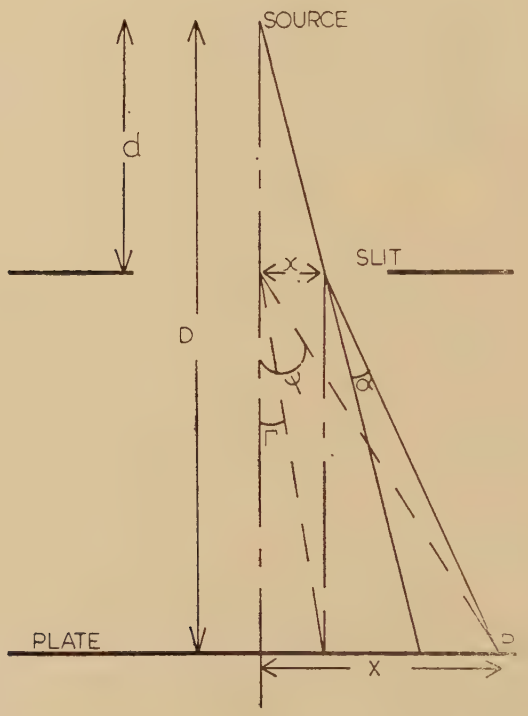

Schematic diagram of experimental arrangements (not drawn to scale).

The values of δ, α_m and ϕ_2 were calculated for the three scattering foils, the data supplied by Voyvodic and Pickup being used in the case of the G5 foil. Theoretical curves showing $[G(\psi)+S(\psi)]$ as a function of ψ are given in fig. 4. They are normalized for comparison with the experimental points $N(\psi)$ by using $\Sigma N(\psi)=A\Sigma[G(\psi)+S(\psi)]$ where the summation extends over all the observations. The agreement between theory and experiment is very satisfactory except perhaps near the centre of the distributions, where the observed track densities are slightly less than the theoretical values. It is believed that this apparent flattening of the curve is due to the presence of a systematic error, arising from the

possibility of failing to count all the tracks in the densely populated central region of the plate. In other parts, where the number of tracks per field of view was small, the observer was unlikely to have missed any of them.

The value of P obtained by applying the χ^2 test to the data is shown in the figure. This quantity P gives the percentage of trials in which a

Fig. 4

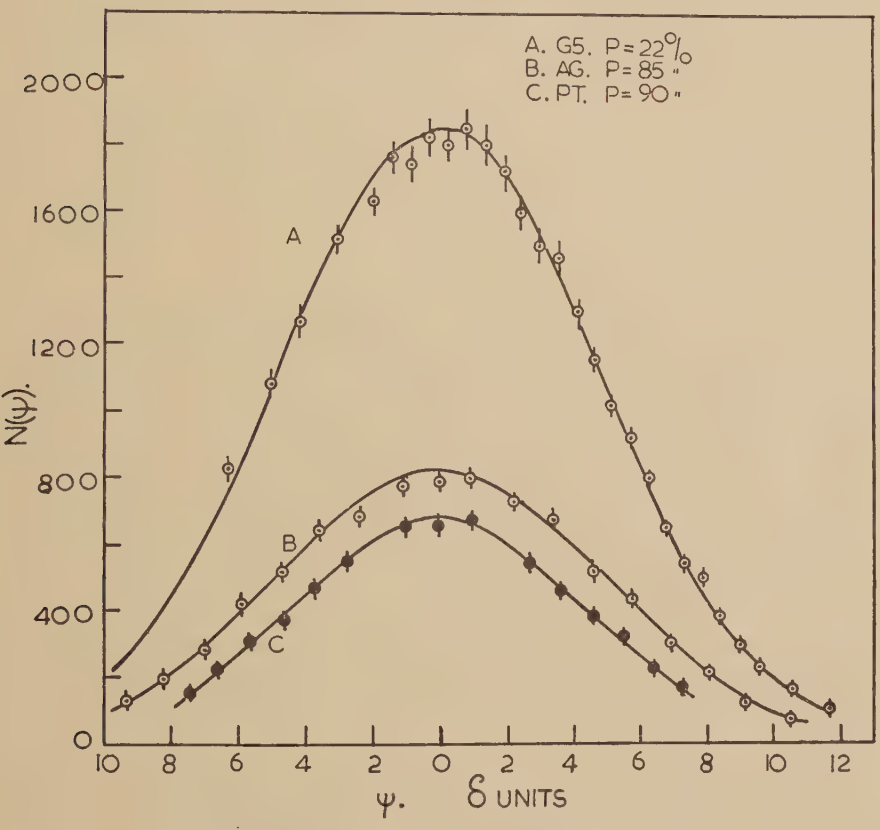

Projected distributions of protons scattered by

(A) G5 emulsion,
(B) silver foil and,
(C) platinum foil.

discrepancy greater than that actually obtained between theory and experiment would occur if the theoretical expression were in fact correct. Since $P \geqslant 5\%$ is usually accepted as representing a reasonable correlation, it is clear that the distribution curves obtained in this experiment do not differ significantly from the calculated ones. A more detailed analysis of the results has been made by adjusting $\bar{\alpha}$ so as to obtain a minimum

value of χ^2 when the corresponding values of α_m and ϕ_2 are inserted in the expression for the wide slit distribution function (see eqns. 4 and 5). These ' best-fit ' values of $\bar{\alpha}$ are shown in column 4 of the table and, as would be expected on account of the systematic error in track counting, are all slightly greater than the theoretical values given in column 3. The errors stated are for 95% confidence. The best-fit value of $\bar{\alpha}$ obtained for photographic emulsion was used in calculating the scattering constant, as explained in the next section.

Foil	δ (deg.)	$\bar{\alpha}$ (δ units) Theory	Experiment	γ
G5	$3{\cdot}65\times10^{-2}$	3·26	$3{\cdot}38\pm0{\cdot}16$	0·59*
Silver	$3{\cdot}38\times10^{-2}$	3·19	$3{\cdot}26\pm0{\cdot}16$	0·68
Platinum	$4{\cdot}27\times10^{-1}$	3·08	$3{\cdot}22\pm0{\cdot}30$	1·13

* Assuming effective $Z=41$.

§ 5. Comparison with Previous Results

The scattering of heavy particles in substance other than G5 emulsion has not been extensively investigated, and such results as do exist are rather contradictory. Code (1941) and Wilson (1940) observed in a cloud chamber the scattering of μ-mesons with energies in the range 100 to 1000 Mev and obtained distribution curves in agreement with Williams' prediction for a shielded nucleus of finite size. Code used tungsten as his scattering material, whereas Wilson investigated gold, copper and lead. Sinha (1945), on the other hand, found a mean scattering angle for μ-mesons in lead which was only 47% of the predicted value. The particles in this experiment had energies between 55 and 155 Mev. Crewe (1951), using μ-mesons whose energies were better defined, (184 ± 12 Mev), found that the scattering in lead was 65% of the predicted value.

Williams (1940) points out that the experiments of Geiger (1910) and of Mayer (1913) on the scattering of α-particles in metallic foils indicate no systematic departure from theory ; but recent work by Ashmore and Crewe (1952) on the scattering of 8 Mev deuterons in seven elements ranging from aluminium to gold shows that the mean projected angles of the Gaussian portions of the scattered distribution are about 10% smaller than those predicted by Williams' theory with classical treatment of screening and 14% smaller than the values calculated from the Molière theory. The present work does not reveal the existence of any such anomaly for high energy protons scattered by silver and platinum.

In the case of scattering in photographic emulsion, it is customary to express the results in terms of a so-called ' scattering constant '. Equation (1) can be written :—

$$\bar{\theta}=Kt^{1/2}/p\beta, \quad . \quad . \quad . \quad . \quad . \quad . \quad . \quad . \quad . \quad (6)$$

where the scattering constant K depends mainly on the properties of the scattering medium for particles of a given charge; but since K involves $\bar{\alpha}$ it will vary also according to the particle velocity and the thickness of the medium. In the co-ordinate method of Fowler (1950) which is often used for measuring the scattering of charged particles in photographic emulsions, the displacement of the track of the particle from an arbitrary straight line is measured at equal intervals (cell lengths) along this line. From these measurements the mean angle $\bar{\theta}_{\text{chord}}$ between successive chords drawn along the track may be calculated. It can be shown that if the number of measurements is sufficiently large

$$\bar{\theta}_{\text{chord}}=(\tfrac{2}{3})^{1/2}\bar{\theta}.$$

Hence a new scattering constant K_0, appropriate to chord angles can be defined by

$$\bar{\theta}_{\text{chord}}=K_0 t^{1/2}/p\beta,$$

where

$$K_0=(\tfrac{2}{3})^{1/2}K.$$

In the present experiments, projected scattering angles greater than about four times the mean value were not observed. Nevertheless, a value for the scattering constant, independent of this experimental cut off, was obtained by putting $\bar{\theta}=\bar{\alpha}\delta$ (eqn. 6), where $\bar{\alpha}$ is the 'best-fit' value of the mean angle of the complete projected Williams distribution. This procedure gives $K_0=(27{\cdot}7\pm1{\cdot}3)$ deg. MeV $(100\,\mu)^{-1/2}$ for 147 MeV protons scattered in $98{\cdot}6\,\mu$ of G5 emulsion.

The curves in fig. 5 show K_0 for protons scattered in G5 emulsion as a function of β^2. The upper curve refers to a cell length of $1000\,\mu$ and the lower to $100\,\mu$. The units of K_0 are deg. MeV $(100\,\mu)^{-1/2}$. Over the range of particle velocity and cell length used here, the data supplied by Gottstein *et al.* (1951) based on the Molière theory, give results identical with those obtained by Voyvodic and Pickup from the modified Williams theory. The points show the results of experimental determinations of K_0, the numbers beside each point giving the cell length in microns. Because of the possible inclusion of too many single-scattering events it is to be expected that the experimental values of K_0 obtained in previous experiments will exceed the calculated ones. In the present experiments the statistics were sufficiently good to avoid this source of error, but the value obtained should still lie above the theoretical curve for the reasons discussed in the previous section.

The values of K_0 reported by Berger (1952), and also those obtained by Bosley and Muirhead (1952) with 47 MeV protons ($\beta^2=0{\cdot}09$) seem rather small when compared either with the theoretical curve or with the present results. But on the whole the results of the present investigation are in accordance with those of previous work, and fit the general trend which K_0 should show when cell-length and particle velocity are changed.

Finally, it should be pointed out that the γ values for the three materials used in the conditions of this investigation are all in the neighbourhood

of unity (see table, column 5). Since neither of Williams' original expressions for the mean projected scattering angle is valid here, it is very satisfactory to find that the modification introduced by Voyvodic and Pickup gives values which agree so well with an experimental determination.

Fig. 5

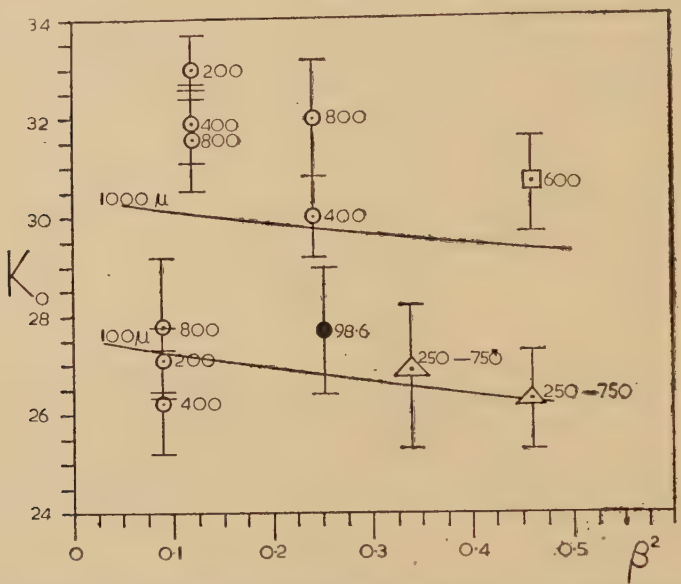

Comparison of experimental determinations of K_0 for G5 emulsion with calculated values.

- ⊙ Bosley and Muirhead, 1952.
- △ Berger 1952.
- ⊡ Gottstein *et al.* 1951.
- ● Present work.

Acknowledgments

I should like to thank Drs. J. M. Cassels, T. G. Pickavance and T. H. R. Skyrme for helpful discussions during the course of these experiments, and the cyclotron crew for their co-operation. I am grateful also to Dr. J. Howlett and the computing group for help with the numerical work. The unbacked specimen of G5 emulsion was kindly supplied by Messrs. Ilford Ltd. This paper is published by permission of the Director, Atomic Energy Research Establishment, Harwell.

References

Ashmore, A., and Crewe, A. V., 1952 (to be published).
Berger, M. J., 1952, *Bull. Amer. Phys. Soc.*, **27**, 62.
Bosley, W., and Muirhead, H., 1952, *Phil. Mag.*, **43**, 63.
Cassels, J. M., Pickavance, T. G., and Stafford, G. H., 1952, *Proc. Roy. Soc.* A, **214**, 262.

Code, F. L., 1941, *Phys. Rev.*, **59,** 229.
Crewe, A. V., 1951, *Proc. Phys. Soc.* A, **64,** 660.
Fowler, P. H., 1950, *Phil. Mag.*, **41,** 169.
Geiger, H., 1910, *Proc. Roy. Soc.* A, **83,** 492.
Goldschmidt-Clermont, Y., 1950, *Nuovo Cimento*, **7,** 331.
Goldschmidt-Clermont, Y., King, D. T., Muirhead, H., and Ritson, D. M., 1948, *Proc. Phys. Soc.*, **61,** 183.
Gottstein, K., Menon, M. G. K., Mulvey, J. H., O'Ceallaigh, C., and Rochat, O., 1951, *Phil. Mag.*, **42,** 708.
Mayer, F., 1913, *Ann. der Physik*, **41,** 931.
Molière, G., 1947, *Z. für Naturforschung*, **2** (a), 133 ; 1948, *Ibid.*, **3** (a), 78.
Sinha, M. S., 1945, *Phys. Rev.*, **68,** 153.
Snyder, H. S., and Scott, W. T., 1949, *Phys. Rev.*, **76,** 220.
Voyvodic, L., and Pickup, E., 1952, *Phys. Rev.*, **85,** 91.
Williams, E. J., 1939, *Proc. Roy. Soc.* A, **169,** 531 ; 1940, *Phys. Rev.*, **58,** 292.
Wilson, J. G., 1940, *Proc. Roy. Soc.* A, **174,** 73.

XXII. *The Ionic State of* LiH

By J. M. Bijvoet
University of Utrecht
and
K. Lonsdale, F.R.S.
University of London*

[Received November 19, 1952]

Summary

Several workers have independently measured the x-ray diffraction effects from LiH, and have obtained consistent intensity data. Such measurements, contrary to previous claims, cannot be used to determine the state of ionization of the atoms in the crystal.

In principle it would appear that since x-rays are scattered by the electrons it should be possible to determine the state of ionization in any compound by means of x-ray diffraction measurements. A light-atom compound such as LiH in which the valency electrons constitute a considerable fraction of the total number of electrons seems to suit this purpose best. This compound has been measured and interpreted by different authors (Ahmed 1951, Zintl and Harder 1931, Bijvoet and Frederikse 1929). These investigations have led to differing conclusions. In Bijvoet and Frederikse (1929) the presence of ions is deduced; in Ahmed (1951) 25% ionic character is regarded as more probable.

We have re-examined the data together, and have come to the conclusions: firstly, that the experimental data are consistent (see table 1), and secondly, that *no certain conclusion about the state of ionization is possible in this case.*

It may be elucidating first to apply and discuss the method by which Debye and Scherrer in 1918 tried to deduce that the atoms in LiF must be ionized. LiH, like LiF, crystallizes with the rock-salt-type structure, and one measures (f_A+f_B) and (f_A-f_B) for the reflexions of ' all even ' and ' all odd ' indices respectively. Because of the decline in scattering power with increasing indices it is only the value of f extrapolated to $\Sigma h^2=0$ which gives direct information about the number of electrons in the scattering particles. Debye and Scherrer plotted the ratio $(f_F+f_{Li})/(f_F-f_{Li})$ as a function of Σh^2. In the figure the corresponding graph for $(f_{Li}-f_H)/(f_{Li}+f_H)$ is shown. It has been deduced from the curves for $(f_{Li}+f_H)$ and $(f_{Li}-f_H)$ as given by the mean values of table 1.

---

* Communicated by the Authors.

The experimental data have all been placed on an absolute scale by making $(f_{Li}+f_H)_{002}=2{\cdot}0$, which is the value for atoms deduced from the *International Tables for Crystal Structure Determination* (1935).

One expects the extrapolated ratio of $(f_{Li}-f_H)/(f_{Li}+f_H)$ to assume the value zero in the case of ions, the value 2/4 in the case of atoms. The graph of the figure appears to extrapolate to about 1/4.

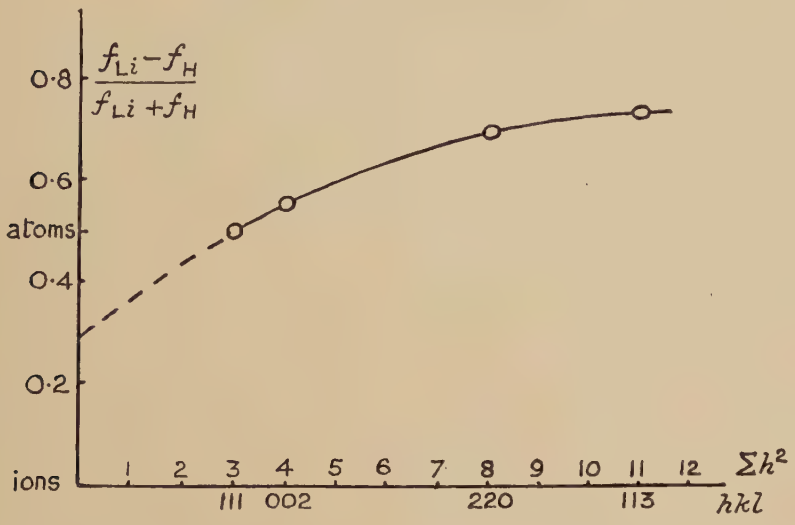

Table 1. Experimental Values of the Scattering Factors (all normalized to the value $(f_{Li}+f_H)_{002}=2{\cdot}0$)

hkl	Ahmed (1951)	Zintl and Harder (1931)	Bijvoet and Frederikse (1929)	Mean *f*	$\frac{\sin\theta}{\lambda}$
000	—	—	—	4	0
111	1·0	1·1	1·1	1·1	0·21
002	2·0	2·0	2·0	2·0	$0{\cdot}24_5$
220	$1{\cdot}6_5$	$1{\cdot}5_5$	1·5	$1{\cdot}5_5$	$0{\cdot}34_5$
113	1·0	1·1	$1{\cdot}0_5$	$1{\cdot}0_5$	$0{\cdot}40_5$
222	1·2	1·4	$1{\cdot}2_5$	1·3	$0{\cdot}42_5$
004	$1{\cdot}0_5$	1·1	—	1·1	0·49
331	$0{\cdot}6_5$	0·8	0·7	0·7	$0{\cdot}53_5$
420	—	$0{\cdot}8_5$	—	$0{\cdot}8_5$	0·55
224	0·7	—	—	0·7	0·60
115, 333	0·5	—	$0{\cdot}5_5$	$0{\cdot}5_5$	$0{\cdot}63_5$

The reasoning just given, however, is unsound. The radius of the valency electron orbit around a cation is such as to reduce the scattering factor of the electron to a negligible value (cf. *International Tables*)

even in the region where Σh^2 is small. On the other hand in the extrapolation to $\theta=0$ this electron introduces a dominating term. The same applies, to a less extent, to the valency electron of the anion. The shape of the graph in the experimental domain, therefore, gives very little information about the correct way of extrapolation, the dominating factor arising for the greater part in the very domain of extrapolation.

In spite of the relative importance of the valency electrons in the case of LiH the circumstances prove to be unfavourable. The criterium whether a decision will be possible as to the state of ionization is whether there is a perceptible difference in scattering power to be expected between ion and atom at the diffraction angles corresponding to Σh^2 small. In the case of LiH the doubling of the number of electrons in H^- as compared with H turns out to be almost exactly compensated by the increase in radius involved, as shown in table 2.

Table 2. Comparison of f_H and f_{H^-}*

hkl	$\frac{\sin\theta}{\lambda}$	f_H	$f_{H^-}\left(\frac{\sin\theta}{\lambda}\right)=2f_H\left(\frac{16}{11}\cdot\frac{\sin\theta}{\lambda}\right)$
111 (LiH)	0·21	0·45	0·49
200	$0{\cdot}24_5$	0·36	0·36
220	$0{\cdot}34_5$	0·19	0·14

Accordingly it appears to be possible to extrapolate the scattering curves for Li and H determined by the above authors either to the atomic or to the ionic scattering factor values at zero angle.† The placing on the absolute scale of table 1 by making $(f_{Li}+f_H)_{002}=2{\cdot}0$ thus appears to be valid irrespective as to the state of ionization.§

Our conclusion is in full accordance with the statement of R. W. James (1948) "that any attempt to determine the state of ionization of atoms in a crystal by means of measurement of the atomic scattering factor is likely to fail since the curves will differ appreciably only at angles for which no spectra exist".

Finally let us consider the matter from the Fourier point of view. With radiation of short wavelength an exact electron distribution can be determined. If the scattering of the valency electrons has practically vanished even for reflections of lowest Σh^2 the dimensions of the outer electron cloud is of the order of the cell dimension. This involves considerable overlapping of the outer electron clouds (R. Brill *et al.*

* The effective nuclear charge in H^- is taken to be $1-5/16=11/16$.

† The model consisting of atoms with undisturbed outer electron clouds is, of course, highly improbable.

§ Figure 1 of Ahmed (1951) is not consistent with the value $(f_{Li}+f_H)_{002}=2{\cdot}0$ and must certainly, therefore, be incorrect.

1939)* and the impossibility of an unequivocal counting of the number of electrons around each lattice point.

It appears, therefore, that the x-ray method cannot give reliable information about the ionic condition of LiH. This conclusion would not be invalidated even if absolute measurements were made at very low temperatures, or with other possible x-radiations.

References

Ahmed, M. S., 1951, *Phil. Mag.* [7], **42,** 997.

Bijvoet, J. M., and Frederikse, W. A., 1929, *Rec. Trav. Chim.*, **48,** 1041 (figures deduced from curve shown in fig. 4).

Brill, R., Grimm, H. G., Hermann, C., and Peters, C., 1939, *Ann. der Physik*, **5,** 34, 393.

Debye, P., and Scherrer, P., 1918, *Phys. Z.*, **19,** 474.

James, R. W., 1948, *The Crystalline State*, II, p. 304.

Zintl, E., and Harder, A., 1931, *Z. Phys. Chemie* B, **14,** 265 ; 1932, *Ibid.* B, **15,** 416.

* The valency electron to be localized, if practically smeared out over a considerable part of the cell, will give a background electron density which is very small. In the case of a rocksalt structure of about $(4\text{Å})^3$ a homogeneous density of the valency electron would amount to 4/64 el/Å^3 or 4/16 el/Å^2 in projection (cf. the min. values of 0·23 el/Å^2 in the [1 1 0] projections of NaCl).

XXIII. CORRESPONDENCE

The Spectrum of the Radiation emitted during μ-Meson Capture by Carbon

By F. D. S. Butement
Atomic Energy Research Establishment, Harwell, Berks.

[Received November 20, 1952]

The process of negative μ-meson capture by atoms, whereby transitions of the meson between Bohr orbits should lead to the emission of characteristic electromagnetic radiations, has been discussed theoretically by various authors, including Wheeler (1949). Evidence for the emission of electromagnetic radiation during μ-meson capture has been obtained by Chang (1949) and Fafarman and Shamos (1952), although their experiments did not determine the energy of the radiation, nor decide whether it arose from orbital transitions or as a consequence of nuclear capture of the meson. In the somewhat analogous case of π-meson capture, evidence for radiative transitions has very recently been obtained by Camac, McGuire, Platt and Schulte (1952) although nuclear capture from the outer orbits is the predominant process.

This letter describes the measurement of the spectrum of the radiation emitted during the capture of cosmic-ray μ-mesons in carbon. The apparatus (fig. 1) consisted of two scintillation counters. The upper counter (I) was a cylindrical brass tank, lined with very thin aluminium foil as a reflector, and filled with a solution of *p*-terphenyl in toluene (8 g per litre). A photomultiplier tube dipping into the toluene was sealed in position with a rubber ring. The base of the tank was made of thin (0·1 mm) brass foil, and another scintillation counter (II) with a NaI–Tl crystal was placed as shown in the figure. The whole apparatus was surrounded with 15 cm of lead.

Pulses from counter I were amplified and fed through a discriminator which eliminated any pulses smaller than those produced by an ionizing particle losing 0·5 Mev energy in traversing the toluene. The residual pulse counting rate was 140 per minute, and the pulses were fed into a delayed coincidence circuit which gave an output pulse (C) only if any pulse (A) was followed by another pulse (B) in an interval of 0·5–6·0 microseconds. The counting rate for (C) was 18·7 pulses per hour, due mainly to μ-mesons of either sign which stopped in the toluene, and a few positive μ-mesons which stopped in the walls of the tank, in cases where both the meson and the decay electron traversed the toluene. The calculated spurious counting rate due to random delayed coincidences was only

0·11 per hour. The number of negative μ-mesons stopped in the toluene cannot be calculated precisely, but would have been approximately 7 per hour.

Pulses (D) from counter II were amplified and used to operate a conventional type of γ-scintillation spectrometer, the pulses being displayed on a cathode-ray tube. The peak of the pulses was reached 10 microseconds after the moment of initiation. The pulses (D) were also fed through a fast amplifier into a multiple coincidence circuit, which gave an output pulse for the coincidence (AD, followed by C), but not for (BD followed by C). This output was used to brighten the cathode-ray tube spot, which was otherwise permanently blacked out. The traces so

Fig. 1

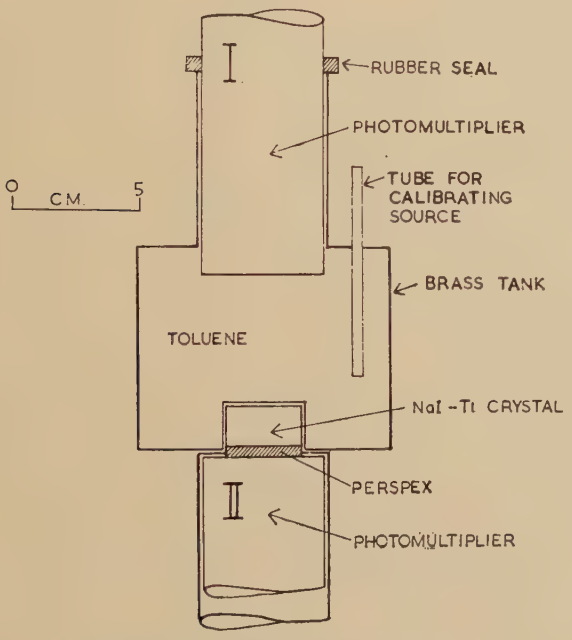

Arrangement of scintillation counters.

obtained were photographed by a continuous exposure. Thus only the electromagnetic radiation coincident with the capture of μ-mesons by carbon atoms in the toluene was recorded. Neither γ-rays due to subsequent nuclear capture of some of the mesons, nor bremsstrahlung produced by the decay electrons would have been recorded.

The experiment ran for 953 hours, during which about 6700 negative μ-meson captures occurred. The number of pulses (less than 300 kev) photographed on the scintillation spectrometer was 127. There was also a group of very large pulses over 1 Mev. These may be attributed to some of the positive mesons which stop and decay in the crystal.

The spectrometer was calibrated by temporarily inserting radioactive sources into a tube projecting into the tank, using the 84 kev γ-ray of ^{170}Tm, and, with a known change in amplification, the 661 kev γ-ray of ^{137}Cs. The spectrum of the ^{170}Tm γ-ray, corrected for the small amount of Yb K x-rays, is shown in fig. 2. The sharp rise below 30 kev is due to noise pulses.

Fig. 2

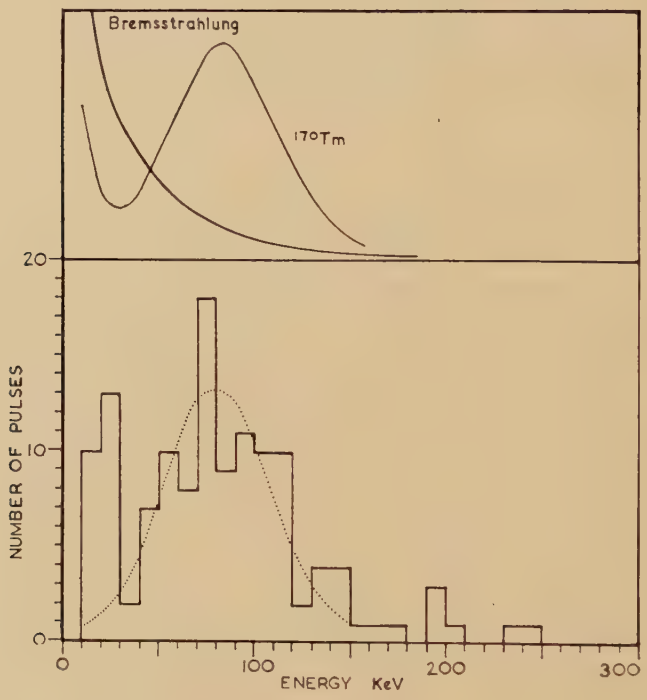

Above: Spectra of bremsstrahlung and ^{170}Tm γ-ray.
Below: Histogram of meson capture radiation.

The histogram for the meson capture radiation (fig. 2), apart from the effect of random coincident noise pulses below 30 kev, shows a single peak with a maximum at about 80 kev. By suitably modifying the electronic circuit, the spectrum of the bremsstrahlung emitted by single cosmic-ray particles traversing the toluene was determined (fig. 2). It is evident that bremsstrahlung do not make any appreciable contribution to the observed meson capture spectrum.

The calculated energy for the 2p–1s transition of a μ-meson in carbon is 77 kev, but it is to be expected that the observed peak would appear to be slightly above this energy owing to weaker unresolved contributions from the transitions 3p-1s at 91 kev, 4p–1s at 96 kev etc. up to the series limit at 102 kev.

The number of pulses comprising the peak was about 100, or about one sixty-seventh of the observed number of mesons captured. This fraction is approximately equal to the calculated efficiency of counter II for radiation from the toluene, so that it is concluded that approximately one radiative transition terminating in the 1s level occurs for each meson captured.

I wish to thank Mr. I. A. D. Lewis for advice on one of the coincidence circuits.

References

Camac, M., McGuire, A. D., Platt, J. B., and Schulte, H. J., 1952, *Phys. Rev.*, **88,** 134.
Chang, W. Y., 1949, *Rev. Mod. Phys.*, **21,** 166.
Fafarman, A., and Shamos, M. H., 1952, *Phys. Rev.*, **87,** 219.
Wheeler, J. A., 1949, *Rev. Mod. Phys.*, **21,** 133.

The Range Energy Relation for Protons of Intermediate Energy in Air

By W. E. Burcham
University of Birmingham

[Received November 28, 1952]

The extension of the range–energy relation for protons in air to energies above 2 Mev (Livingston and Bethe 1937) is based on the theoretical formula for the rate of loss of energy of a charged particle in passing through matter. Predictions of stopping power are uncertain for proton energies of less than 2 Mev and fixed points from nuclear reaction energies are helpful in correcting the range–energy relation in this region (Bethe 1950). Although there is little reason to doubt the validity of the stopping power formula for proton velocities for which capture and loss of electrons by the moving particle is negligible, it is of interest to see to what extent the higher energy part of the range–energy curve receives experimental verification. This may be done by comparing the ranges of groups of protons observed in (dp) reactions with the values predicted from the accepted range–energy curve, using energies calculated from accurately determined Q-values.

The results of such a comparison are shown in fig. 1. The Q-values for the (dp) reactions were taken from recent experiments on the magnetic analysis of disintegration products, and have a precision of 0·2% or better. The range measurements selected for comparison were taken from work in which conditions were sufficiently well defined to allow all necessary corrections for the reduction of observations to mean ranges to be made ; they fall into two groups. In the first group are experiments with deuterons of less than 1 Mev energy for which the ranges of protons

emitted in the (*dp*) reactions were generally found by absorption directly in air or in mica. The second group includes work with deuteron energies up to 4 MeV for which proton ranges were found by absorption in aluminium.* In both groups correction for the variation of the stopping power of absorbers with particle energy was made where necessary by use of fig. 34 of the article by Livingston and Bethe (1937); the general experimental accuracy of the range measurements is about 1%.

Figure 1 shows that the range–energy relation given by Livingston and Bethe (1937) is fairly well verified. If a least squares line is drawn through the distribution of deviations of observed ranges from the curve,

Fig. 1

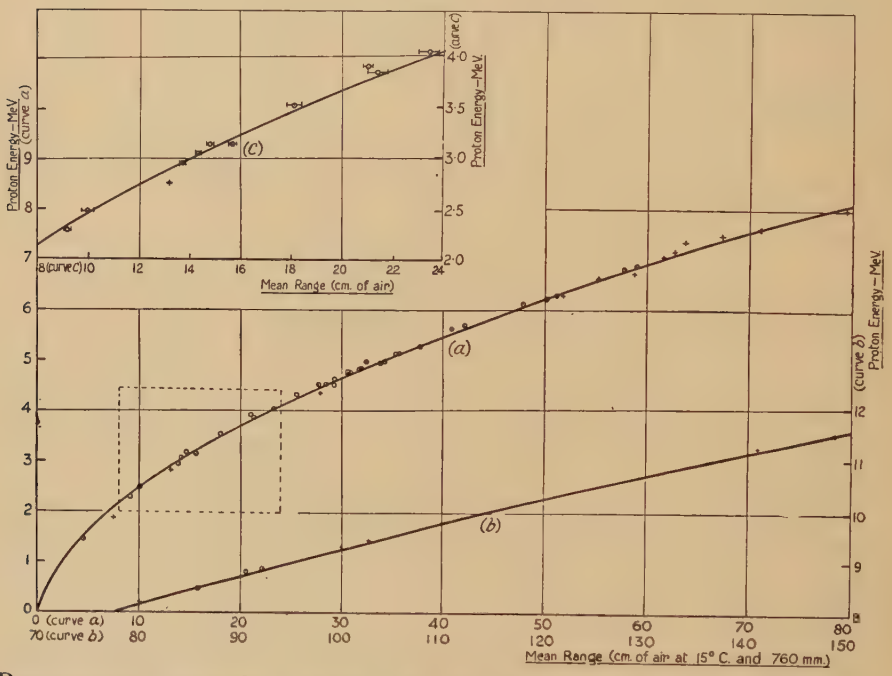

Range–energy curve for protons in air (at 15° c and 760 mm). The full curve is given by Livingston and Bethe (1937); points marked ⊙ are for ranges obtained by absorption in air or mica; points marked + are for ranges obtained by absorption in aluminium.

it is found that for the points taken with mica absorbers the curve overestimates the measured range by about 0·3 cm for energies between 2 and 8 MeV. This difference is about equal to the accuracy of most of the range determinations and is only twice that claimed for the range–energy relation. If the points taken with aluminium absorbers are included,

* In the case of published work in which *Q*-values only are given, proton ranges have been obtained for the present purpose from calculated proton energies by making use of the range–energy relation given by Livingston and Bethe (1937).

the deviation given by the least squares line increases with mean range and is about 1·3% of the mean range for ranges between 50 and 150 cm.

There is no obvious reason in the experimental material examined for measured proton ranges to be generally a few mm too short, although in some experiments the deposition of carbon films on the targets may not have been detected. However, the points which lie most off the curve are those for which the experimental uncertainty is greatest and further accurate measurements of range or of stopping power for protons of energy up to 4 MeV would be desirable. The inset to fig. 1 shows the spread and experimental errors in the existing information for energies between 2 and 4 MeV ; at higher energies the accuracy of existing range determinations is worse because of increasingly large corrections for the variation of stopping powers of absorbers with proton velocity.

References

Bethe, H. A., 1950, *Rev. Mod. Phys.*, **22,** 213.

Livingston, M. S., and Bethe, H. A., 1937, *Rev. Mod. Phys.*, **9,** 245.

References for Q-value determinations

Buechner, W. W., and others, 1949, *Phys. Rev.*, **76,** 1543 ; 1950, *Ibid.*, **80,** 771 ; 1951 a, *Ibid.*, **81,** 747 ; 1951 b, *Ibid*, **82,** 248 ; 1952 a, *Ibid.*, **85,** 142 ; 1952 b, *Ibid.*, **86,** 518 ; 1952 c, *Ibid.*, **87,** 51.

Collins, E. R., McKenzie, C. D., and Ramm, C. A., *Proc. Roy. Soc.* A, in course of publication.

Keller, K. K., 1951, *Phys. Rev.*, **84,** 884.

Klema, E. D., and Phillips, G. C., 1952, *Phys. Rev.*, **86,** 951.

Li, C. W., and Whaling, W., 1951, *Phys. Rev.*, **82,** 122.

Tollestrup, A. W., Jenkins, F. A., Fowler, W. A., and Lauritsen, T., 1949, *Phys. Rev.*, **75,** 1947.

References for range determinations (air and mica)

Allan, H. R., 1949, *Thesis*, Cambridge.

Allan, H. R., and Wilkinson, C. A., 1948, *Proc. Roy. Soc.* A, **194,** 131.

Allan, H. R., Burcham, W. E., Curling, C. D., and Wilkinson, C. A., 1949, *Nature, Lond.*, **163,** 210.

Bower, J. C., and Burcham, W. E., 1939, *Proc. Roy. Soc.* A, **173,** 379.

Cockcroft, J. D., and Lewis, W. B., 1936, *Proc. Roy. Soc.* A, **154,** 246.

Holloway, M. G., and Moore, B. L., 1940, *Phys. Rev.*, **58,** 847.

Jelley, J. V., 1949, *Thesis*, Cambridge.

Murrell, E. B. M., and Smith, C. L., 1939, *Proc. Roy. Soc.* A, **173,** 410.

Oliphant, M. L. E., Kempton, A. E., and Rutherford, Lord, 1935, *Proc. Roy. Soc.* A, **149,** 406.

Rumbaugh, L. H., Roberts, R. B., and Hafstad, L. R., 1938, *Phys. Rev.*, **54,** 657.

Williams, J. H., Haxby, R. O., and Shepherd, W. G., 1937, *Phys. Rev.*, **52,** 1031.

References for range determinations (aluminium)

Allen, R. C., and Rall, W., 1951, *Phys: Rev.*, **81,** 60.

Bateson, W. O., 1950, *Phys. Rev.*, **80,** 982.

Heydenburg, N. P., and Inglis, D. R., 1948, *Phys. Rev.*, **73,** 230.

Heydenburg, N. P., Inglis, D. R., Whitehead, W. D., and Hafner, E. M., 1949, *Phys. Rev.*, **75,** 1147.

Motz, H. T., and Humphreys, R. F., 1951, *Phys. Rev.*, **80,** 595.

Whitehead, W. D., and Heydenburg, N. P., 1950, *Phys. Rev.*, **79,** 99.

Visual Observations of the Formation of Bulk Liquid from the Helium II Film

By A. C. Ham and L. C. Jackson
H. H. Wills Physical Laboratory, University of Bristol

[Received December 20, 1952]

It has been shown that when liquid helium II is transferred through flow of the film from a vessel containing it, bulk liquid is formed from the film whenever the latter runs on to a periphery, below the level of the liquid in the vessel, which is smaller than that controlling the rate of transfer. Daunt and Mendelssohn (1939), Mendelssohn (1951) and Chandrasekhar (1952) have inferred this indirectly from their observations of the formation of drops of liquid from the film, but Jackson and Henshaw (1953), using the optical method of Burge and Jackson (1951), observed the formation of bulk liquid directly but were unable to observe the initial stages of the process owing to the shape of their beaker.

To make it possible to observe the process in all its stages a conical beaker has been constructed, again of stainless steel (fig. 1), 4 cm long and 1 mm wall thickness, the inner and outer diameters being respectively 7 mm and 9 mm at the top and 3 mm and 5 mm at the bottom, with a 2·5 mm wide strip of plane mirror ground and polished on the outside of the beaker along its length. The beaker was supported, with its axis vertical, inside a radiation shield and was provided with a glass sight-tube to indicate the level of the liquid in the beaker as shown in fig. 1 of Jackson and Henshaw (1950). The beaker was filled with liquid helium II at 1·59°K and was raised until only the lower end was immersed in the outer liquid.

From the earlier observations it would be expected that, by reflecting polarized light from the mirror, the latter would initially be found to be covered by the helium II film from the upper rim to a point B where the outside periphery is equal to the inside periphery at the level of the liquid in the beaker. Immediately below B the first signs of bulk liquid should appear and, as the outer periphery continues to decrease as one proceeds further down the beaker, bulk liquid should be ejected from the film in greater and greater amounts as one approaches the outer liquid level. In the course of time the inner level falls, and the outer level, at which bulk liquid first appears, should correspondingly fall. When the inner liquid level has fallen below B only the film should be observed.

The observations confirmed these expectations satisfactorily. Bulk liquid was observed in the form of discrete drops, with diameters ranging from about 0·1 mm to 0·5 mm, which moved down the mirror with apparently constant velocities up to about 2 cm/sec, according to their size. The upper part of the mirror was initially free from drops. The position at which the drops were first observed was rather ill-defined, but

certainly in the neighbourhood of the middle of the mirror, and the clear portion above increased in length as the inner liquid level fell, the whole of the mirror being clear when the beaker was less than half full.

Continued visual observation gave a clear impression of the number of drops increasing progressively towards the bottom of the mirror. Instantaneous photographs do not, however, show this convincingly on account of the statistical fluctuations in the production of the drops.

Fig. 1

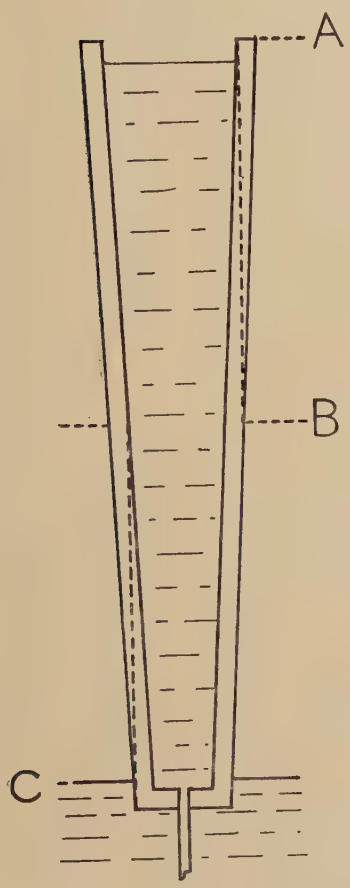

Fig. 2

Photograph showing drops of bulk liquid. Images of drops are foreshortened laterally by a factor of about 2 due to tilt of mirror, and extended longitudinally by about the same amount on account of the velocity down the mirror. Overall magnification $4\frac{1}{2}$ times.

Figure 2 is a photograph, taken with an exposure of 1/40 sec, 4 minutes after raising the beaker and covering the mirror from close to B to just above C. The number of drops entering the liquid at C per sec decreased continuously with time, becoming zero when the inner liquid level was at B.

The drops gave very strikingly the impression of being squeezed out of the film. They then fell like raindrops on a window, presumably sliding down the solid surface, either under the very much thinner helium II film or displacing the latter locally. Their behaviour is in reasonable agreement with the theory of Frenkel (1948) of liquid drops on the surface of a solid which is wetted by the liquid. Thus Frenkel calculates that the drop should leave a trail behind it (observed in some of the helium II drops) and should only roll down the vertical solid surface if the radius of the undeformed drop is greater than $(3\sigma/\pi\rho g)^{1/2}$ where σ=surface tension and ρ=density of the liquid. Inserting the values for helium II at 1·59°K gives R=0·5 mm, which agrees as regards order of magnitude with the observed drops. Drops smaller than this should not run, and the smallest drops were indeed seen to be stationary. The discrete drops were observed only if conditions were clean, i.e. the surface of the mirror was free from condensed gaseous impurities. If this was not the case the bulk liquid could just be observed as a stream of liquid of uneven thickness flowing on an irregular substrate.

References

Burge, E. J., and Jackson, L. C., 1951, *Proc. Roy. Soc.* A, **205**, 270.
Chandrasekhar, B. S., 1952, *Thesis, Oxford.*
Daunt, J. G., and Mendelssohn, K., 1939, *Proc. Roy. Soc.* A, **170**, 423.
Frenkel, Y. I., 1948, *Journ. Expt. Theor. Phys.*, **18**, 659.
Jackson, L. C., and Henshaw, D. G., 1950, *Phil. Mag.*, **41**, 1081 ; 1953, *Ibid.*, **44**, 14.
Mendelssohn, K., 1951, *Proc. Internat. Conf. on Low Temperature Physics, Oxford*, p. 66.

Nuclear Polarization of Cobalt 60

By E. Ambler, M. A. Grace, H. Halban, N. Kurti, H. Durand, C. E. Johnson and H. R. Lemmer
Clarendon Laboratory, Oxford

[Received January 2, 1953]

Gorter (1948) and Rose (1949) have independently suggested that nuclei of paramagnetic ions may be polarized at sufficiently low temperatures through the magnetic hyperfine structure coupling, provided the electron spins are polarized by an external field. Bleaney

(1951) has pointed out that in salts having anisotropic hyperfine structure ($A \neq B$ in the spin Hamiltonian) nuclear alignment may be produced under certain circumstances in zero external field (Daniels, Grace and Robinson 1951), while application of an external field will in general result in a reduction in the degree of alignment. The difference between nuclear polarization and alignment has been discussed by Bleaney (1951) and by Simon, Rose and Jauch (1951). Where the hyperfine structure is isotropic (i.e. $A=B$) there is no alignment in zero field, and we have a favourable case for producing directional effects in radioactive emission solely by nuclear polarization. Recent measurements by Trenam (1953) have shown that in certain salts of the composition $3Co(NO_3)_2.2M(NO_3)_3.24H_2O$, where M is a trivalent ion, $A=B$ for probably two-thirds of the Co ions, while for the remaining one-third $A \gg B$.

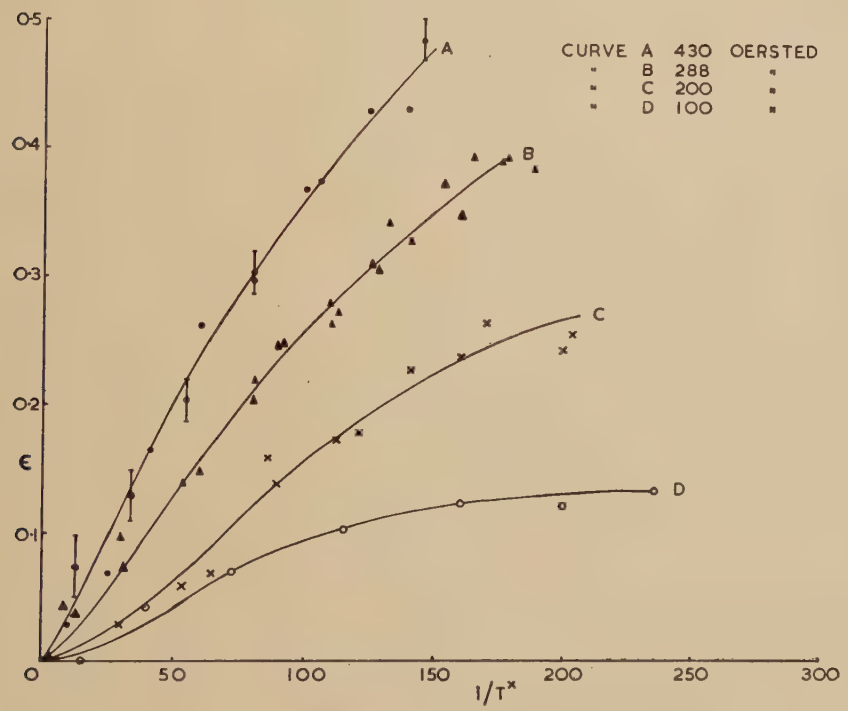

The variation with $1/T^*$ of the anisotropy (ϵ) of γ-radiation from polarized cobalt 60 nuclei for different values of the polarizing field.

We have carried out experiments to try to polarize cobalt nuclei in such salts. We first used powdered magnesium lanthanum nitrate in which 5% of the magnesium was replaced by cobalt containing 100 μ Curie of ^{60}Co. This was mixed with the cooling agent, chromium potassium alum, and pressed to form a bonded pill. The specimen was

demagnetized from 30 kø at 1° K to a final field of 250 ø. Under these conditions a significant polarization should have been set up in the cobalt nuclei of the ions for which $A=B$. No spatial anisotropy of the γ-emission was detected however.

The absence of an appreciable nuclear polarization could be ascribed to one or several of the following causes : (*a*) decomposition of the double nitrate through chemical reaction in the pill ; (*b*) bad thermal contact between the grains of the double nitrate and of the alum ; (*c*) insufficient cooling in the partial demagnetization to 250 ø.

All these difficulties were overcome by incorporating as cooling agent cerium in the same crystal as the cobalt. Apart from the proven superiority of this technique (Daniels *et al.* 1951), the substance used, namely $3[0{\cdot}5\%\mathrm{Co}, 99{\cdot}5\%\mathrm{Mg(NO_3)_2}].2\mathrm{Ce(NO_3)_3}.24\mathrm{H_2O}$ containing 50 μ Curie of ^{60}Co, had the following additional advantages. Along one crystallographic axis the g-value of the cerium ion is very small, so that when, after demagnetization, a polarizing field is applied in this direction the resulting temperature rise is small (Cooke, Duffus and Wolf 1953). Furthermore, very low temperatures 0·004° K can be reached by demagnetizing from moderate values of H/T (Daniels and Robinson 1953).

The sample used consisted of twelve single crystals (total weight 4 g) mounted with their crystallographic axes parallel. They were magnetized in 25 kø at 1° K along a direction in which cerium has a large g-value. After demagnetization the polarizing field was applied, and while the crystals warmed up to 1° K (this took about 10 minutes) the γ-ray intensity in the direction of the polarizing field $I(0)$ and perpendicular to it $I(\pi/2)$ was measured by means of G–M counters. Values of the anisotropy $\epsilon=[I(\pi/2)-I(0)/I(\pi/2)]$ of up to 50% have been observed. The figure shows ϵ as a function of the reciprocal of the magnetic temperature T^* for various values of the polarizing field. Further measurements are in progress to determine the contribution to ϵ from the ^{60}Co nuclei of ions with $A \gg B$ and also to obtain a correlation between T^* and T° K in the polarizing fields used.

As always, we are greatly indebted to Professor F. E. Simon for his stimulating interest.

References

Bleaney, B., 1951, *Phil. Mag.*, **42**, 441.
Cooke, A. H., Duffus, J., and Wolf, W. P., 1953, to be published.
Daniels, J. M., Grace, M. A., and Robinson, F. N. H., 1951, *Nature, Lond.*, **168**, 780.
Daniels, J. M., and Robinson, F. N. H., 1953, to be published.
Gorter, C. J., 1948, *Physica*, **14**, 504.
Rose, M. E., 1949, *Phys. Rev.*, **75**, 213.
Simon, A., Rose, M. E., and Jauch, J. M., 1951, *Phys. Rev.*, **84**, 1155.
Trenam, R. S., 1953, *Proc. Phys. Soc.* A, **66**, 118.

The Use of Stripped Emulsions for Recording the Tracks of Charged Particles *

By C. F. Powell, F.R.S.
H. H. Wills Physical Laboratory, University of Bristol

[Received December 26, 1952]

It is well known that one of the limitations of the photographic method, as commonly employed for recording the tracks of charged particles, is due to the restricted depth of the emulsion. An emulsion 500 μ thick is equivalent in stopping-power to about 1 metre of air at N.T.P. In general, therefore, a large proportion of the charged particles, emitted from nuclear disintegrations occurring in the emulsion, with energy greater than $\sim$15 Mev, escape from one of the surfaces. Only rarely is a particle of greater energy brought to rest in the emulsion so that any secondary effects occurring at the end of its range can be observed.

Secondary effects at the end of the range of charged particles are frequently of decisive importance for identifying their nature, and several different methods have been employed to increase the effective thickness of the emulsion. Thus Dilworth, Occhialini and Vermasen (1950) have successfully processed emulsions 1 200 μ thick, and Yagoda (1950) has poured emulsions in special cells with a thickness of 2 mm. The difficulties of processing plates without introducing distortion mount rapidly, however, as the emulsion thickness is increased. Further, the microscopic examination of the plates becomes increasingly arduous, because of the absorption and scattering of the light in traversing the emulsion ; and difficulties begin to appear because of the limited working distance of conventional objectives. Emulsions of thicknesses greater than 1 200 μ have therefore rarely been employed.

As an alternative approach to the problem, many investigators have employed stacks of plates with pairs of emulsions face to face, so that the tracks of individual particles can be traced from one to another of two facing emulsions. Further, it has been shown by Peters that (*a*) the individual tracks of heavy nuclei, and (*b*) the narrow ' jets ' of secondary fast particles, produced by the nuclear interaction of protons with an

---

* This letter describes a technical development to which many members of the Laboratory have contributed. The idea of using stripped emulsions is well known, but the method has been rarely employed because of technical difficulties, particularly those met in processing the emulsions and mounting them for microscopic examination without introducing distortion. These difficulties have now been overcome. A brief report appeared desirable in order to give an account of the new technical developments, to emphasize the importance of employing the method widely in nuclear physics, and to point out the many problems of great contemporary interest to which it can be applied.

energy greater than 10^{13} ev, can be traced through the plates of a stack in spite of the wide gaps associated with the passage of the particles through the glass. For individual particles with the electronic charge, however, this procedure can rarely be employed because of the difficulty of recognizing the track of an individual particle in the separate emulsions. This method also suffers because nothing is known of any processes which may have occurred in the glass.

It appeared that, in relation to present problems, there would be very great advantages to be gained if the technical difficulties of employing thick, stripped emulsions could be successfully overcome. During manufacture, such emulsions are poured on to glass in the usual way, and then stripped off so that they can be packed together to form, in effect, a solid, sensitive mass.

The idea is not new and members of several laboratories have employed the method; see, for example, Demers (1952), and Shapiro (private communication). There have, however, been serious technical difficulties associated with the problem of processing such emulsions so that they are free from distortion, and applications have been very limited. It appeared that if these difficulties could be overcome, the method would find a wide field of application and would allow a considerable increase in the weight of the attack on several problems of great contemporary interest in the physics of elementary particles. Among these problems are the following:

(*a*) Accurate determinations of the mass of heavy mesons. It has been shown that about one in fifteen of the fast particles ($\beta \sim 0{\cdot}6$ c) emitted from stars are heavy mesons. If the tracks of such particles could be traced through, say, ten emulsions, mass measurements could be made in each, and the mass of the individual particles more accurately determined. Further, in some cases, it should be possible to trace such heavy mesons to the end of their range and to study the characteristics of their transformations.

(*b*) When the track of a heavy meson has been identified by mass measurements in one emulsion, the additional lengths of track available for inspection in others would greatly facilitate the observations necessary to determine the mean length of path in the emulsion of such a particle before making a nuclear interaction, and its proper time of flight before suffering decay could be measured.

(*c*) In the case of the τ-meson, it is of great interest to determine the sign of the charge. Apart from magnetic deflection experiments, the sign could be determined by the behaviour of the three π-particles at the end of their range. The average value of the ranges of these mesons is, however, about 1 cm, and they commonly all escape from the emulsion. In an extended stack of stripped emulsions they could all be arrested, the positive and negative particles readily distinguished, and the observed ranges of the three particles would give an accurate value of the total energy released. Decisive evidence for the nature of the charged

decay particle, and its energy, could also be obtained in the case of other types of heavy mesons.

(*d*) The π-particles brought to rest in the emulsion, could be traced to their point of origin. In this way, one might find τ or V_0 particles decaying in the stack.

(*e*) Similar advantages would be present if stripped emulsions could be employed in magnetic deflection experiments. In addition to making available a much greater length of track from which to determine the magnetic deflection, the ' dead space ' represented by the glass would, in effect, be replaced by emulsion.

Because of these and other possible advantages, a stack of 50 stripped emulsions, 6 in. $\times$ 4 in., 600 μ thick, was exposed to the cosmic radiation. They were packed separately, with thin tissue paper between them (0·1 mg per cm^2) and were exposed for about 25 hours at an altitude between 30 000 and 40 000 ft. in a Comet aircraft on a flight from London to Singapore and back.

After the exposure, the plates were exposed to a narrow beam of x-rays to provide a number of marks on the four edges of all the plates to facilitate registration of any one emulsion against its neighbours. Each of the individual emulsions was then made to adhere to a specially treated glass plate, provided by the manufacturers, by dipping it in a 1% solution of glycerine for 30 sec, placing it while under the solution on the glass plate, and then passing the assembly between the rubber-lined rollers of an ordinary domestic mangle. After allowing the plates to dry, they were processed in the usual way. The success of this operation appears to depend rather critically on the pressure between the rollers and it is therefore best to use a mangle in which this pressure can be varied.

The most serious problem met in securing plates free from distortion is to avoid the formation of blisters in the gelatine during fixation. These commonly appear if very small air bubbles are trapped between the emulsion and the supporting plate. To avoid them, it seems to be important to boil the glycerine solution and cool it to room temperature immediately before the mounting operation ; and to brush the glass and the surface of the emulsion which is to adhere to the glass with a broad, soft camel-hair brush while the emulsion is in the solution.

In processing ordinary plates with Amidol-bisulphite developer, it has been found in this laboratory that emulsions with very small distortion can be produced if the temperature in the ' hot stage ' is kept to a minimum ; temperatures of about 10° c are therefore commonly employed in this laboratory (see also Herz 1953). In the case of the stripped emulsions, however, it appears that it is easier to avoid bubbles if a higher temperature in the ' hot stage ', $\sim$25° c, is employed. We do not understand the reason for this effect and it is possible that the same result would be obtained by raising the plates to 25° c during the ' pre-soaking ' of the emulsion and using the favourable lower temperatures during development.

After processing, the plates are placed in turn on a base-plate inscribed with lines against which the x-ray marks are registered. The base plate is provided with hinged pieces which then allow the plate to be marked with a diamond glass cutter so that the cut edges of the final plate are in a standard relation to the x-ray markings. The registration of one plate against another can then be made from the edges of the plate and further reference to the x-ray marks is unnecessary.

In following a track out of the top of one emulsion into the bottom of the next, the plates are placed in turn in a standard position against the stops on the microscope stage. With the procedure described above, the continuation of a steeply dipping track then appears in the same field of view, when using a total magnification of about 100. If the track is inclined at a small angle to the surface of the emulsion, there is a displacement corresponding to the traversal of the tissue paper, but the continuation of the track is usually easily found, since the line of motion of the particle is defined. In practice, it is usually possible to follow the track of a particle through ten emulsions in about 20 minutes.

The method of cutting the plates introduces small errors because the fracture is not a true plane. When a higher precision of registration is desirable it can be secured by lightly grinding the edges of the plate to a standard shape with a grinding wheel. For most purposes, however, this appears to be unnecessary.

Because of the great advantages of the method, and the fact that the processed plates are of comparable quality with those obtained by conventional procedures, it seems reasonable to suggest that stripped emulsions should be widely employed in experiments with the cosmic radiation in place of ordinary plates. There is much to gain and little or nothing to lose. Similar advantages should also be present in experiments with artificially generated protons and mesons so that the method promises to be of very general application.

My colleagues and I are greatly indebted to Mr. C. Waller and other members of the staff of Ilford Limited, who supplied the stripped emulsions and who gave us valuable advice on the best methods for securing the adhesion of the emulsion to the glass.

References

Demers, P., 1952, *P. Sc. Ind. Phot.*, **23**, 1.

Dilworth, C. C., Occhialini, G. P. S., and Vermaessen, L., 1950, *Bulletin du Centre de Physique Nucleaire de l'Universite Libre de Bruxelles*, No. 13a, February.

Herz, A. J., and Edgar, M., 1953, *Proc. Phys. Soc.* A, **66**, 115.

Yagoda, H., 1950, *Phys. Rev.*, **79**, 207 ; *Ibid.*, **80**, 753.

The Observation of Polyhedral Sub-Structures in Crystals of Silver Bromide

By J. M. Hedges and J. W. Mitchell
H. H. Wills Physical Laboratory, University of Bristol

[Received December 29, 1952]

The purpose of this note is to report a series of observations on the separation of photolytic silver under illumination in boundaries between adjacent elements of a polyhedral sub-structure in large transparent single crystals of silver bromide. It is thought that in this experimental work, dislocation lines have been made visible for the first time by the separation of photolytic silver along them. The observations were made in the course of an investigation of the formation of the internal photographic latent image in strained and polygonized crystals of silver bromide (Hedges and Mitchell, to be published).

The crystals used for the experiments were produced by slowly cooling a disc of molten silver bromide between two optically polished flats of Pyrex glass. Because of the differential contraction between silver bromide and Pyrex glass, the crystals are initially heavily strained, as may be observed with the polarizing microscope. Their separation from the plates is accompanied by the release of part of the strain, but some plastic strain is retained. The separated sheets were systematically annealed in bromine vapour at a pressure of two atmospheres for different times over a wide range of temperatures. At the end of an anneal, the pressure of bromine was reduced near to that in equilibrium with solid silver bromide at the annealing temperature and, after a further period, the system was cooled rapidly and the specimens were removed. They were then exposed to filtered radiation with wavelengths at the long wave edge of the absorption band of silver bromide. This caused silver to print-out internally both in strained crystals and in crystals which had been annealed at temperatures below 350° c. In specimens which had been annealed over a critical range of temperatures, exposure to light revealed the presence of a well developed polyhedral sub-structure through the separation of photolytic silver in the boundaries between adjacent elements. The regular patterns of particles of photolytic silver which have been observed appear to correspond remarkably well with current descriptions of the structure of mosaic boundaries in terms of dislocations. Three types of structure have been noted :

(1) Boundaries of the type shown in fig. 1 (figs. 1–3, Plate 7), in which the photolytic silver separates as parallel rows of discrete particles.

(2) Boundaries in which the photolytic silver separates to form hexagonal networks as illustrated in fig. 2.

(3) Three dimensional networks of lines outlined by particles of photolytic silver as in fig. 3.

The magnification of all the illustrations is $\times 1200$.

The observations are consistent with the hypothesis that the photolytic silver separates in the components of the systems of dislocations which form the boundaries between adjacent elements of the polyhedral structure. Boundaries with the structure of type (1) would be formed by the rotation of adjacent elements of the crystal about a line lying in the boundary while those of type (2) would, in the simplest case, be formed by rotation about a line perpendicular to the boundary.

Further evidence that dislocations are involved in these phenomena is provided by the observation that, when the crystals are plastically deformed before exposure to light, the dislocations move away from the boundaries and the regular arrays are rapidly destroyed. That this has occurred can, of course, only be observed after the separation of photolytic silver under illumination. Figures 4, 5 and 6 (Plate 8) illustrate three stages in the plastic deformation of the crystals.

It should be remarked that no trace of dislocations or of a polyhedral sub-structure has yet been observed in crystals which have been annealed for long periods within 20° C of the melting point of silver bromide, either before or after plastic deformation. It is possible that the transformations occurring during polygonization make the dislocations more ready to accept photolytic silver through the introduction of a high density of jogs.

Evidence for the Direct Production of κ-Mesons

By N. Isachsen, V. Vangen and S. O. Sörensen
Fysisk Institute, University of Oslo, Norway

[Received December 12, 1952]

During the last few years experiments with photographic plates exposed to the cosmic radiation have established the existence of heavy mesons with masses in the region 900–1500 m_e. Apart from the τ-meson of mass $\sim 980\, m_e$ which decays into three charged π-mesons, a number of examples have been reported of heavy mesons decaying into one charged particle and, presumably, one or more neutral particles. These mesons are usually referred to as κ- and χ-particles (O'Ceallaigh 1951, Menon 1952, Powell 1952, Crussard *et al.* 1952, and Levi-Setti and Tomasini 1952). The origin of these particles, their masses and modes of decay are still under discussion. In what follows it will be convenient to employ the term ' heavy meson ' to denote the κ- and χ-particles, not including

the τ-particles. These particles are almost certainly identical with the charged V- and S-particles discovered in experiments with Wilson chambers ; see Rochester and Butler (1947) and Bridge and Annis (1951).

An event bearing on the problem of the mode of origin of heavy mesons, which appears to be closely similar to two others observed independently by Levi-Setti and Tomasini (1952), has recently been observed in this laboratory. It was recorded in an Ilford G5 emulsion, 400 μ thick, exposed by means of free balloons for four hours at an altitude of 90 000 feet. Photo-micrographs of the event are shown in Plate 9. A particle with a total range of 14 mm was ejected from a nuclear disintegration. It came to rest in the emulsion and transformed with the emission of a single charged particle with a velocity closely approaching that of light. Attention was directed to the event by the fact that the momentum of the secondary particle, which produced a track of length 2·5 mm in the emulsion, was of the order of 180 MeV/c, a value considerably greater than the maximum momentum of the electrons formed by the decay of μ-mesons. A study of the variation of the grain-density and scattering along the track of the meson showed that the particle was several times more massive than a μ-meson, and there appears little doubt that it was a κ- or χ-particle. Final measurements of the mass have not yet been completed, but the preliminary observations are as follows :

The Heavy Meson

The nuclear disintegration which gave rise to the ejected meson was of type 16+3p in the nomenclature of Brown *et al.* (1949). The probable energy of the primary proton was $\sim$6 BeV (Camerini *et al.* 1951). None of the other tracks in the star are long enough to allow the particles which produced them to be identified.

The heavy meson was ejected ' backwards ' and made an angle of $\sim$123° with the direction of motion of the parent particle, presumably a proton, which produced the star. The appearance of the end of the track is that of a particle which came to rest before decaying, and it was certainly near the end of its range when it transformed. Since the total range of the particle was 14 mm in a single emulsion, the track provides very favourable conditions for mass determination.

The mass of the ejected meson was determined by observing the multiple scattering as a function of residual range. Using the range vs. scattering method described by Menon and Rochat (1951) and measuring the entire length of the track, a value of (950$\pm$140) m_e was obtained.* The nuclear disintegration occurred very near the processed edge of the plate, and the first half of the track of the heavy meson is very near the surface of the emulsion. It is possible that these factors may have lead to ' spurious ' scattering on this part of the trajectory. These objections

* The authors would like to express their sincere thanks to Mr. M. G. K. Menon for assistance in connection with these measurements.

do not apply to the second half of the track, and we therefore regard the mass value, determined from observations on this part of the track by the scattering method, as more reliable. The result is $(1020\pm200)\,m_e$. Slightly higher values will result ($\sim100\,m_e$) when the variation of the scattering constant with velocity is taken into account.

The range vs. scattering method described by Goldschmidt–Clermont *et al.* (1948) and Holtebekk (1951) was employed on the second part of the track. The mass value obtained was $(1090\pm180)\,m_e$ in good agreement with the estimate given above.

The Secondary Particle

The secondary particle traversed a distance of $2500\,\mu$ before entering the glass backing of the emulsion. The measured grain density, normalized to the 'plateau' value (Voyvodic 1951, and Daniel *et al.* 1952 a) was $g^*=1{\cdot}05\pm0{\cdot}03$. The mean deviation $\bar{\alpha}$ due to multiple scattering, was carefully determined by several observers. A mean value of $\bar{\alpha}_{100\,\mu}=0{\cdot}190\pm0{\cdot}032$ was thus obtained, corresponding to a value of $p\beta=126\pm21$ MeV/c. This is more than twice the maximum theoretical value of $p\beta$ for electrons arising from the decay at rest of μ-mesons.

The observed grain density, $g^*=1{\cdot}05$ corresponds to $p\beta$ values of ~ 190 MeV/c and ~140 MeV/c for π- and μ-mesons respectively. The observations correspond to a mass of $\sim 200\,m_e$ for the secondary particle, thus indicating that it was a μ-meson. The observed grain density of the track is so near that of the 'plateau' value that the possibility that the secondary particle was an electron cannot be excluded, but there appears to be no positive evidence from experiments with emulsions and Wilson chambers that heavy mesons decay in such a mode. It is very improbable that the secondary particle is as massive as a π-meson.

Discussion

Daniel and Perkins (1952 b) have shown by measurements of grain density and multiple scattering on tracks of fast particles emitted from 'stars', that heavy mesons are ejected in considerable numbers from nuclear disintegrations produced by protons with energies as low as ~ 5 BeV. The present observation appears to provide direct information for the existence of such processes.

Evidence is growing which suggests that the secondaries formed by the decay of heavy mesons are in some cases π- and in other μ-mesons (Bridge and Annis 1951, Menon 1952, Menon and O'Ceallaigh 1952). The latter investigators have suggested that two types of heavy mesons exist which transform according to the equations

$$\chi \longrightarrow \pi + ?^\circ$$
$$\kappa \longrightarrow \mu + ?^\circ + ?^\circ$$

The ejected heavy meson in the present event may therefore be classified tentatively as a kappa particle.

The best estimate for the mass of the kappa particle (Menon and O'Ceallaigh 1952) is $\sim 1100\ m_e$. The value of mass obtained for heavy mesons emitted in nuclear disintegrations (Daniel and Perkins 1952) is $\sim 1200\ m_e$. The direct mass measurements on the ejected heavy meson we have described above, i.e. $\sim 1000\ m_e$ are in good agreement with the above values.

An account of more detailed measurements will be given in due course.

Acknowledgments

The authors would like to express their gratitude to Professor C. F. Powell, F.R.S., of the University of Bristol and to Professor J. Holtsmark and Professor R. Tangen of the University of Oslo for providing laboratory facilities. We are indebted to Norges Teknisk Naturvitenskapelige Forskningsraad for financial support.

References

Bridge and Annis, 1951, *Phys. Rev.*, **82,** 445.
Brown, Camerini, Fowler, Heitler, King and Powell, 1949, *Phil. Mag.*, **40,** 862.
Camerini, Davies, Fowler, Franzinetti, Muirhead, Lock, Perkins and Yekutieli, 1951, *Phil. Mag.*, **42,** 1241.
Crussard, Mabboux, Morellet, Trembley and Orkin-Lecourtois, 1952, *C.R. Acad. Sci., Paris,* **234,** 84.
Daniel, Davies, Mulvey and Perkins, 1952 a, *Phil. Mag.*, **43,** 753.
Daniel and Perkins, 1952 b, private communication.
Goldschmidt-Clermont, King, Muirhead and Ritson, 1948, *Proc. Phys. Soc.* A, **61,** 183.
Holtebekk, 1951, *Hovedoppgave i fysikk*, University of Oslo.
Levi-Setti and Tomasini, 1952, *Nuovo. Cim.*, Vol. IX, 1244.
Menon, 1952, *Thesis*, University of Bristol.
Menon and Rochat, 1951, *Phil. Mag.*, **42,** 1232.
Menon and O'Ceallaigh, 1952, private communication.
O'Ceallaigh, 1951, *Phil. Mag.*, **42,** 1032.
Powell, 1952, Copenhagen Conference.
Rochester and Butler, 1947, *Nature, Lond.*, **160,** 885.
Voyvodic, 1952 (in course of publication).

Comments on Planetary Convection as applied to the Earth

By Harold C. Urey
University of Chicago

[Received December 15, 1952]

Vening Meinesz (1951) has pointed out that the first five spherical harmonics derived from Prey's discussion (1922) of the surface of the earth are able to describe its continental and sea areas and has ascribed the origin of the small second and the third, fourth, and fifth order

harmonics to convection in the earth's mantle, but explains the first order harmonic by the escape of the moon from the earth. Chandrasekhar (1952) has studied the theory of convection in a sphere and has shown that the first order spherical harmonic can be explained as due to convection in a sphere without a core or with a liquid core having a radius not larger than 18% of the radius of the sphere, and has shown that these orders of harmonics would appear in a convective sphere in increasing order as the core of the earth increased in size. It is the purpose of this paper to show that if this single cell convection, i.e. along an axis through the sphere and back along the surface, is responsible for the land areas of the earth, then the earth must have been formed in a highly viscous condition, and that the core of the earth has been formed during an appreciable fraction or the whole of the time since the earth was formed.

In order to account for the continents lying in one hemisphere by the convection described by Chandrasekhar, it is necessary that this convection should be possible in a completely formed earth with a less dense floating surface suitable for continent formation, and such convection would not be possible if the radius of any core was greater than 0·18 of the earth's radius. This means that the metallic iron-nickel and iron sulphide did not sink to form a core during the collection of the substance of the earth. Rapid convection would not appear to be a likely mechanism for maintaining a suspension of metallic iron phase in a silicate melt of low viscosity in a body as large as the earth. In addition the energy of the accumulation of the earth as a sphere of uniform composition has been estimated to be approximately $-2{\cdot}23 \times 10^{39}$ ergs while the radioactive energy generated throughout the last 3×10^9 years is only 3·5% of this amount (Urey 1952) and the amount generated in the short time during which the earth may have been formed would be much less than this. Hence radioactive heating could not have been effective in producing rapid convection during the time that the earth was formed since much larger heat sources existed on the surface than in the interior and hence a core should have been formed continuously as the earth grew if the earth had low viscosity at this time. The single convective cell could not have been established at the end of the process and hence this cell could not account for the continents' being predominently in one hemisphere. There seems to be no escape from the conclusion that the earth was so highly viscous that the dense iron core could not collect in a time comparable with the time of accumulation of the earth.

There seems to be no very obvious reason for supposing that the subsequent formation of the core was a rapid process, and in fact the author's assumption that the core has been forming throughout geologic time seems quite natural. This postulate met its greatest difficulty in accounting for the large generation of heat due to the formation of a core, estimated as about $1{\cdot}67 \times 10^{38}$ ergs, as compared with a heat loss through the surface during all geologic time of a seventh of this amount,

assuming a heat loss of about 50 ergs $cm^{-2}\,sec^{-1}$ (or $1{\cdot}2 \times 10^{-6}$ cal $cm^{-2}\,sec^{-1}$). The problem of disposal or storage of this heat as well as additional radioactive heat exists on the basis of Chandrasekhar's interpretation of Vening Meinesz' proposals.

If we assume a rapid organization of the earth's surface during its early history according to their suggestions, and only minor modifications since then, the problem of disposing of this gravitational energy becomes acute and leads to contradictions. If we assume that this occurred in 3×10^8 years, i.e. about one tenth of geologic time, it is necessary to dispose of much of this gravitational energy by storage or conduction through the surface. If storage is assumed, the earth was formed at a low temperature, and it is very difficult to assume rapid movement of the iron to the core. If conduction to the surface is postulated it is necessary to assume a very high temperature gradient at the surface, say about 70 times the present value or 2000° per kilometre, and this means a melted earth only one kilometre below the surface. It would thus appear that the early organization of continental areas assumed would be destroyed when the core was formed, and once it was formed no reorganization according to the Vening Meinesz–Chandrasekhar ideas would be possible. A much longer time must be postulated and indeed only a time of about 3×10^9 years with possibly some storage of energy and an average heat loss somewhat larger than the present observed value permit a consistent description along these lines.

A somewhat greater average heat loss does not seem unreasonable since the sialic crust and continents have grown during geologic time and hence their insulating effects have increased since they do not take part in convection. Also, differentiation of the outer mantle some hundreds of kilometres thick may represent chemical differentiation, i.e. loss of metallic iron and iron sulphide, and hence again another layer growing with time and preventing convection. Storage of heat again does not seem unreasonable since cooling of a body as large as the earth should not be a highly efficient process. These assumptions seem to the writer to be so much less extreme than other assumptions which have been made, e.g. the escape of the moon from the earth with all its quite obvious difficulties. Perhaps the claim can be timidly suggested at least that in the present approach we are attempting to face some difficulties instead of relegating all these problems to an initial assumed high temperature period during which all of them are assumed to be solved before scientific investigators attempt to take over any elucidation of the problem at all. In fact, the general assumption of a very hot, rapidly changing earth during a short time of formation, followed by an earth which has changed only in a minor way since then, is not plausible to the writer and may be only deceptively simple and convenient.

The writer agrees with Vening Meinesz in his view that tl e prominence of the first five orders and the lesser prominence of the higher spherical harmonics constitute ' a remarkable feature of the earth's topography '.

However, he believes that the similarity in magnitude of the first five orders is so great that they can all be regarded as having a similar origin. These orders are given as having amplitudes of 1·055, 0·822, 0·931, 0·850, and 0·751 km. Considering that erosion has modified all of them extensively, the small value of the second does not appear to be significant. The writer believes that the loss of the moon from the earth is a most improbable explanation of the first order harmonic, and that the first order convection is a more probable explanation. The requirement that the earth was formed in a highly viscous state and that its core grew during geologic time agrees with the conclusions of the present writer, which were based on quite different arguments. However, these statements should not be interpreted to mean that this writer regards them as having that high degree of certainty which we desire to establish in the great body of science.

The writer is indebted to Dr. Chandrasekhar for his informative and critical discussions of this problem.

References

Chandrasekhar, S., 1952, *Phil. Mag.*, **43,** 1317, and a second article in press.

Prey, A., 1922, *Abh. Ges. d. Wiss., Göttingen, Math. Phys. Kl. N.F.*, **11,** 1.

Urey, H. C., 1952, *The Planets* (Yale University Press). Chap. 5. See p. 176 especially. The values are approximate since they depend on unknown factors, but no modification of the conclusion drawn is possible.

Vening Meinesz, F. A., 1951, *Proc. K. Ned. Akad. V. Wetenschappen*, **54,** 212–228.

XXIV. *Notices of New Books and Periodicals received*

Journal of the Mechanics and Physics of Solids. Edited by R. Hill and W. M. Baldwin. Vol. I, No. 1, October 1952. (London: Pergamon Press Ltd.) To appear quarterly at £4 10*s.* 0*d.* per volume of 4 numbers.

According to the publisher's advance leaflet the subjects with which this new journal will deal include: Creep; Fatigue; Elastic and plastic properties of engineering metals; Stress analyses of structures and continua; Significance of material tests; Rationale of technological forming processes. Although it is implied that this list is not exhaustive, but is to give an indication of the scope of the journal, it is apparent that it casts its net in certain circumscribed waters in the wide sea defined by its title. In fact, all six papers in this first issue have to do with plasticity, and the solids with which they deal are either metals, or unspecified materials conforming (for example) to the Mises–Hencky yield condition. Three papers are on mathematical plasticity, the other three summarize mechanical properties of some real materials (rheological properties of certain alloys at elevated temperatures; the time laws of creep; the yield phenomenon in mild steel). Briefly, physics appears as the handmaid of mechanics. The reviewer is inclined to think that a truer indication of the valuable purpose which this journal is likely to serve would have been given by omitting physics from the title.

The issue concludes with a friendly announcement of the forthcoming international journal *Acta Metallurgica*, which intends to concentrate on the physics of metals (and non-metals, so far as they throw light on the metals). We can accept the implication that the two new journals will scarcely overlap in function.

A journal devoted chiefly to the engineering mathematics of solids, but not ignoring the physical facts from which that mathematical structure depends; one extracting for the benefit of the engineer the remarkable and sometimes unforeseen implications of those facts: to such a journal we may extend a welcome. It has a rightful place to occupy. This welcome is not lightly given at a time when there are undoubtedly too many journals. F. C. F.

Nuclear Stability Rules. By N. Feather. [Pp. 162.] (Cambridge Monographs on Physics: Cambridge University Press, 1952.) Price 20*s.*

This book, by one of the editors of the series, deals systematically with the stability of known and possible types of nucleus. Professor Feather has taken the experimental facts, as far as they were available in December 1951, and has attempted to marshal them in such a way that significant regularities are apparent. He has considered empirically, in great detail, the factors which appear to make a nucleus liable to α-disintegration, β-disintegration or spontaneous fission. He has succeeded in obtaining, from an enormous amount of uncoordinated information on individual nuclear species, a number of more general facts, which must be explained in any satisfactory theory of nuclear structure.

Professor Feather has not attempted to formulate such a theory himself, but rather to present the facts in such a way that a theorist may be inspired by their regularities, not dismayed by their number. His success will best be measured by the success of those theorists to whom the book is addressed, but one cannot doubt that they will find his work most helpful.

The reader who does not wish to study the subject in great detail must inevitably find a book of this type complicated and somewhat confusing, but this particular book is not therefore useless to him. As a source of information about the ground states of individual nuclei, and of references to the literature, it is as complete as can be expected in a field which is developing so rapidly.

W. M. G.

A Selection of Tables for use in Calculations of Compressible Flow. By L. Rosenhead and others. [Pp. 143 + viii.] (Oxford University Press.) Price 40*s.*

This book, which has been prepared on behalf of the Aeronautical Research Council, contains a selection of tables for use in calculations of isentropic flow, in the method of characteristics, and in the determination of flow conditions behind shock waves and from wind tunnel measurements. There are also some useful miscellaneous tables. In the computations it has been assumed uniformly that γ, the ratio of the specific heats $=1{\cdot}4$ but the derivatives of some funtions with respect to γ have also been given. K. S.

Wind-Tunnel Technique. By R. C. Pankhurst and D. W. Holder. First Edition. (Sir Isaac Pitmann and Sons, Ltd.) Price 57*s.* 6*d.*

There has been in the past a serious lack of any comprehensive book on wind-tunnels. The appearance of the volume under review remedies, and more than remedies, this situation; for the authors have extended the scope of their study further than their title implies, to include the subject of tunnel design. The whole subject is extremely large and the authors have done it justice in a long volume, but without circumlocution; for the writing is precise, and the volume as a whole a pleasure to read.

The volume is divided into twelve chapters, each of which deals with a particular aspect of wind-tunnel work, in general starting with low air speeds which increase as the chapter proceeds. The first chapter outlines the terms and the parts of the theory which are required in later chapters. Here many standard results are quoted, references to their derivation being given, and it should be mentioned that the references here and in later chapters are so full and complete that, published by themselves, they would form a very acceptable book of reference. The second chapter deals with the subject of wind-tunnel design; in almost one hundred pages the authors discuss each aspect in turn, with many illustrations from wind-tunnels in this country. It is true that occasional ideas of the present day are omitted, but this is almost certainly due to the fact that, according to the preface, the manuscript was completed five years ago and only references have been added since; but these omissions are few and far between. The next chapters discuss in detail all measurements made in wind-tunnels, with separate chapters on wind-tunnel interference and reduction of results. In all these it is clear that the authors are writing on a subject in which they are immersed; only long acquaintance with wind-tunnels would allow them to pick so unerringly the right points for comment. A chapter on special measurements includes many techniques to deal with particular problems concerning aircraft, boundary layers and propellers. As every reader will have different views on the items for inclusion in this chapter, some will feel that this chapter could be extended, but on the whole the authors' choice is a good one, though the reviewer regrets that cascade tunnels should only receive six lines.

To summarize, this is not a textbook, but a detailed account of wind tunnels in their design and operation, their auxiliary equipment, and the points to be borne in mind when discussing results obtained from them. It is pleasantly written and a book which can be recommended wholeheartedly. The printing and publication have been carefully done, and the illustrations are well reproduced. T. V. L.

[*The Editors do not hold themselves responsible for the views expressed by their correspondents.*]

Fig. 1 (*a*), (*b*), (*c*), (*e*). Examples of reactions.

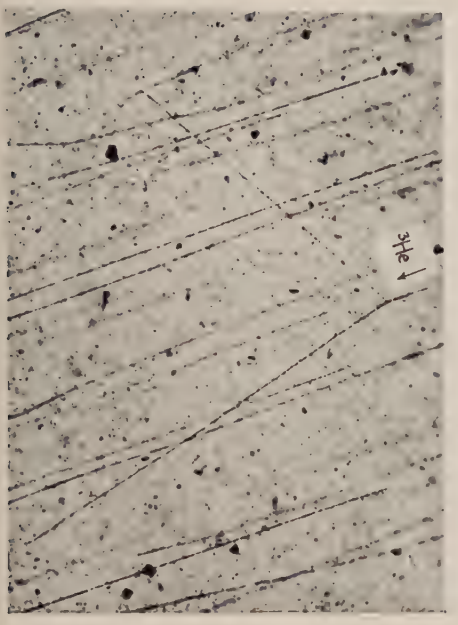

(*a*)

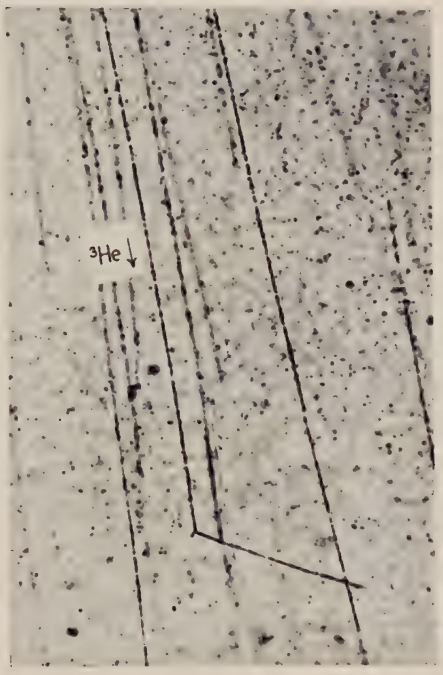

(*b*)

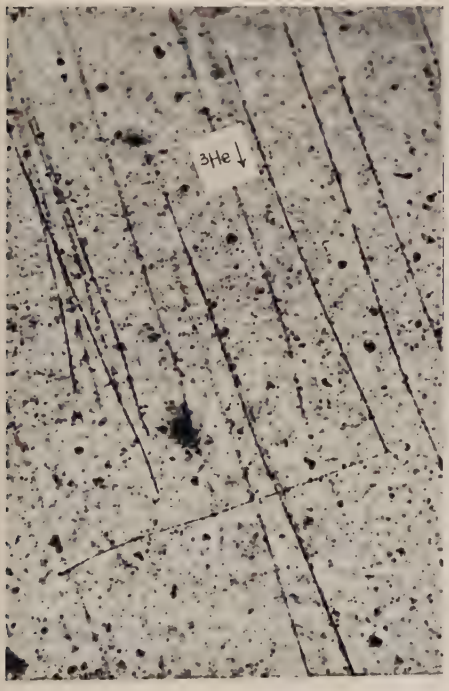

(*c*)

(*e*)

(*a*) Collision between ^{3}He and a hydrogen nucleus. (Reaction 130.) See § 5.3. (*b*) Scattering of ^{3}He by ^{12}C. (Reaction 16.) See § 5.4. (*c*) (^{3}He, p*x*n) with a heavy nucleus. (Reaction 168.) See § 5.5.1. (*e*) (^{3}He, 2p) with a light nucleus. (Reaction 75.) See § 5.8.2.

Fig. 1 (*d*), (*f*), (*g*). Examples of reactions.

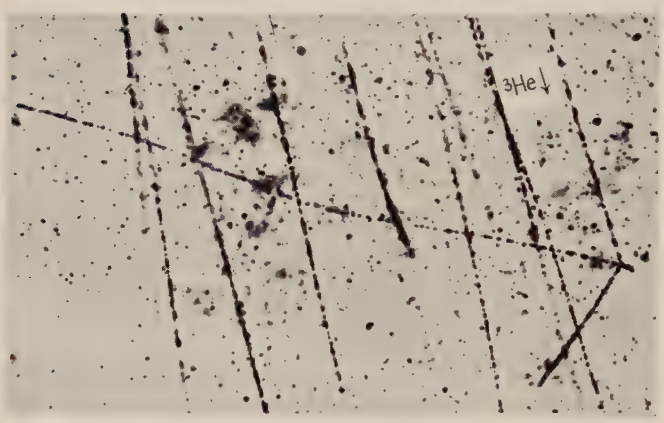

(*d*) (^{3}He, αp) with a light nucleus. (Reaction 102.) See § 5.8.1.

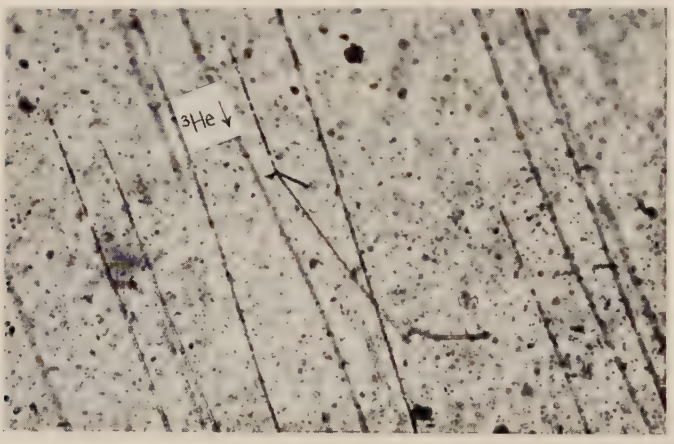

(*f*) Four-pronged star. (Reaction 159.) See § 5.9.

(*g*) ^{14}N (^{3}He, 4α)p. (Reaction 264.) See § 5.10.

Part of one irrelevant ^{3}He track which lay nearly above the event has been erased to avoid confusion.

Vertical momentum before	=2·42
Total vertical momentum after	=2·07
Horizontal momentum along ^{3}He track, before	=8·30
Total horizontal momentum along ^{3}He track, after	=8·23
Total horizontal momentum perpendicular to ^{3}He track, after	=5·43—5·09 =0·34

Cu L emission (overexposed to show satellites)

Cu L absorption and emission (superimposed)

Cu L absorption

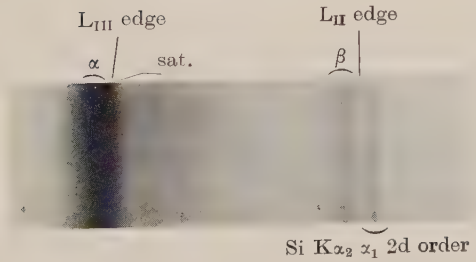

Ni L emission

Cu L absorption, some emission superimposed (original microphotometer curve).

Fig. 1

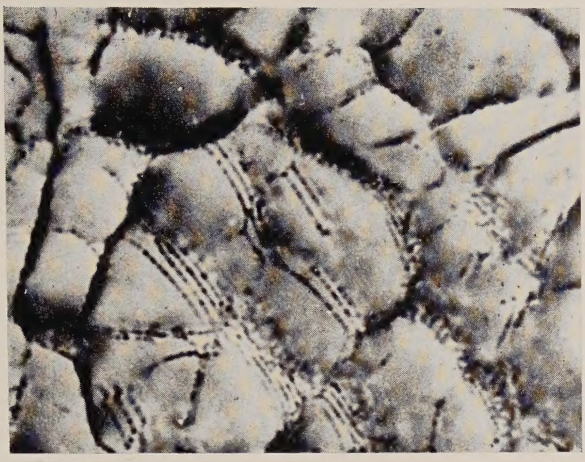

Fig. 2

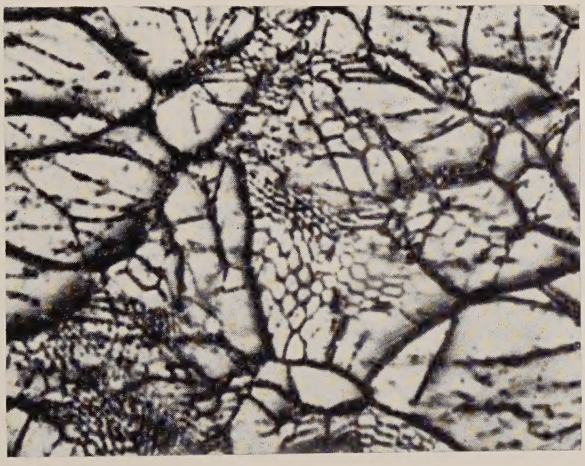

Fig. 3

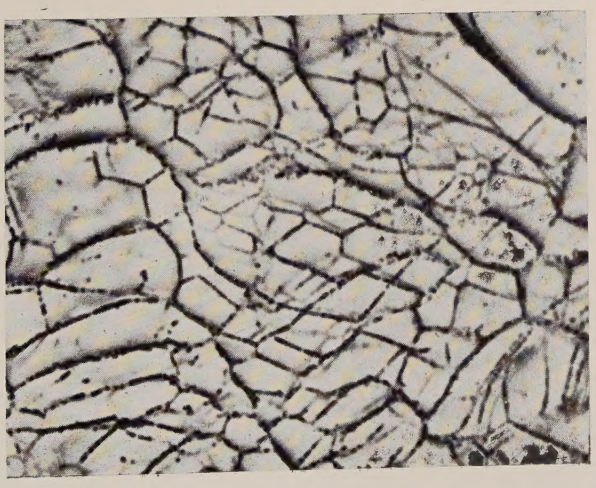

Fig. 4

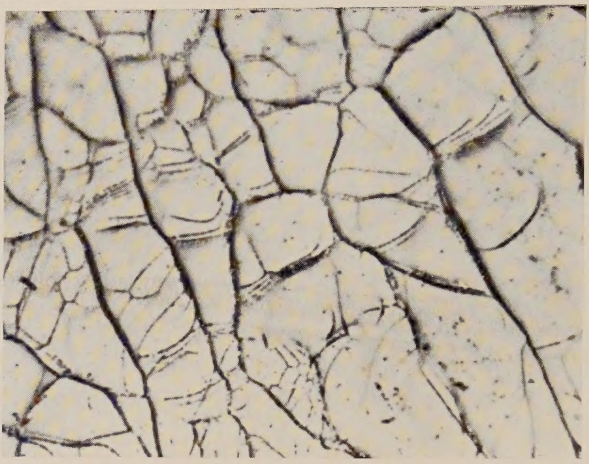

Fig. 5

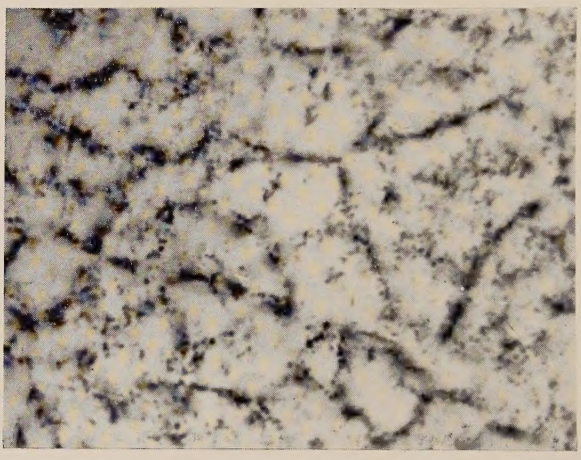

Fig. 6

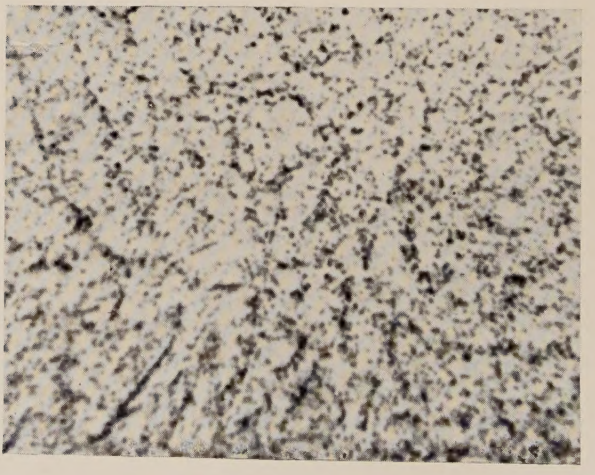

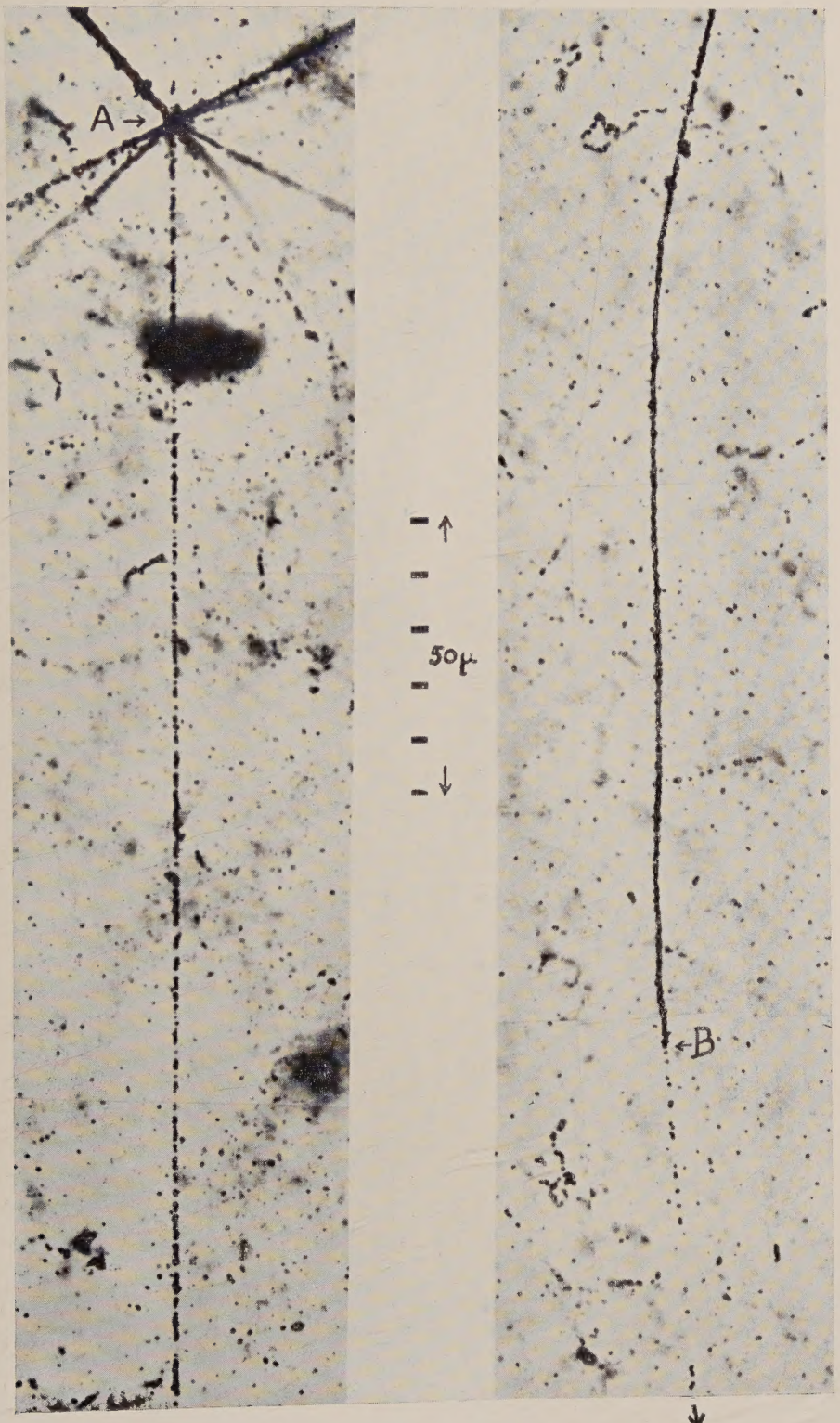

A heavy meson, ejected from the nuclear disintegration at A, produces a track of length 14 mm and comes to rest at B where it decays.